Year: 2011

Effects of new rehabilitation techniques on the human brain using functional magnetic resonance imaging

Blickenstorfer, Armin

Abstract: Summary The human brain has the remarkable capability to adapt its functional and anatomical organization after damage to the central nervous system. Whether it is a stroke or a traumatic event such as spinal cord injury (SCI), the brain finds a way of handling the situation after such an incident. This is also referred to as neural plasticity. Neural plasticity is not only a process that starts after a pathology, it is actually a healthy process that runs all day long, encompassing learning. Whether it be in school or on the playground, learning a language or how to play an instrument – representations on the subcortical and cortical level change. After a stroke, SCI or other incidents affecting the nervous system, patients spend a lot of time in neural recovery, including among other physical therapy interventions when the trauma is motor function related. The relationship between neural plasticity and physical interventions have been poorly investigated up to now, especially when it comes to newer interventions such as functional electrical stimulation (FES) and robot-assisted physical therapy. In this thesis, we investigate neural plasticity and its adaptation to FES (Study 1 2). FES is a well-known technique used in physical therapy. Besides this, its application is found in sports which enhances muscle force and endurance training. Its principle is simple: electrodes are placed above the relevant muscle and bursts of electrical impulses lead to a muscle contraction. In regards to robot-assisted physical therapy, we reference another subject of this thesis, which involved the development of a MR-compatible robotic device in cooperation with Dr. Ningbo Yu of ETH, who engineered the device. This cooperation enabled us to create a manipulandum based on hydrodynamic and pneumatic actuation (Study 3) This prototype may be the basis for future devices to monitor the effects of robot-assisted physical therapy on the subcortical and cortical level, i.e. relating changes within the brain's activation patterns to behavioral outcomes in stroke and spinal cord injured patients. In all three studies, we use functional magnetic resonance imaging (fMRI) as the means to assess changes in the cortical activation patterns. When it comes to the additional application of other devices, the MR-environment is challenging due to its strong magnetic field and limited space. Therefore, we first conducted studies (1 3), for both FES and manipulandum feasibility which demonstrate safe application of both methods in the MR-scanner. No method-related image artifacts were observed. In both studies, we used passive and active tasks. In the former, subjects muscles were activated by FES or the manipulandum; whereas in the latter subjects have used their own force. Passive movements are used in physical therapy when the affected limb cannot be moved voluntarily due to weakness or disability. During the ongoing therapy, use of active V and self-contained movements is the desired goal. Monitoring cortical changes related to an ongoing intervention such as physical therapy requires, at best, a long-term study design. Consequently before conducting a FES-intervention paired with an MR-based monitoring on patients, we established a training study (Study 2) with healthy subjects in order to form a basis for future studies. Up until now, only a few studies investigated the effect of long-term motor training on cortical changes. Our goal was to investigate the impact of a 4-week FES training on muscular output (force) and its respective correlates on cerebral activation patterns. In short, this doctoral thesis provides insights on how to use fMRI in monitoring FES-related changes in the human brain as a result of ongoing medical intervention. Moreover, the development of the MR-compatible manipulandum forms a basis for future studies that implement robotics in physical therapy, in relationship to their effect on neural plasticity. VI Zusammenfassung Das menschliche Gehirn

hat die erstaunliche Fähigkeit seine funktionelle wie auch anatomische Organisation nach einer Schädigung des zentralen Nervensystems anzupassen. Sei es nach einem Schlaganfall oder einem traumatischen Ereignis wie einer Verletzung des Rückenmarks: Das Hirn findet einen Weg mit der neuen Situation umzugehen. Diese Fähigkeit nennt man auch neuronale Plastizität. Der Prozess der neuronalen Plastizität setzt nicht erst nach einer Verletzung ein. Es handelt sich viel mehr ein gesundes Phänomen, das immer aktiv ist. Beispielsweise gehört das alltägliche Lernen - sei es in der Schule oder auf dem Sportplatz - oder das Erlernen eines Musikinstrumentes dazu. In der Folge verändern sich die Repräsentationen auf subkortikaler und kortikaler Ebene. Nach einem Schlaganfall, Schädigung des Rückenmarks oder anderen Ereignissen, die das zentrale Nervensystems betreffen, verbringen Patienten viel Zeit in der Rehabilitation bspw. in der Physiotherapie, wenn die Schädigung das motorische System betrifft. Der Zusammenhang zwischen neuronalen Plastizität und Physiotherapie wurde bislang nur wenig untersucht. Insbesondere wenn es sich dabei um neuere Interventionen wie funktionelle elektrische Stimulation (FES) oder Roboter unterstützende Physiotherapie handelt. In dieser Arbeit wurde die neuronale Plastizität und ihre Adaptionsfähigkeit auf FES (Studie 1 2) untersucht. FES ist innerhalb der Physiotherapie eine bekannte Methode. Daneben findet sie ihre Anwendung auch im Sport, bspw. im Muskelaufbau- und Muskelkonditionstraining. Das Prinzip ist einfach: Oberflächenelektroden werden oberhalb der relevanten Muskelgruppen plaziert und nach einer Serie von elektrischen Stromimpulsen resultiert eine Muskelkontraktion. Bezüglich der Roboter-unterstützten Physiotherapie war die Entwicklung eines Magnetresonanz- kompatiblen Gerätes ein weiteres Thema dieser Arbeit. In Zusammenarbeit mit Dr. Ningbo Yu von der ETH Zürich wurde ein Manipulandum auf der Basis eines hydrodynamischem und pneumatischem Antriebs entwickelt (Studie 3). Dieser Prototyp könnte der Grundstein für die Entwicklung weiterer Geräte sein, mithilfe derer die Effekte der Roboter-unterstützten Physiotherapie in der subkortikalen sowie kortikalen Ebene untersucht werden können. Das heisst, Veränderungen in Hirnaktivierungsmuster können mit den Verhaltensänderungen bzw. den Therapiefortschritten der entsprechenden Patienten in einen Zusammenhang gebracht werden. In allen drei Studien wurde die funktionelle Magnetresonanztomographie (fMRI) als Methode zur Ermittlung der kortikalen Aktivierungsmuster angewandt. Werden zusätzlich weitere Geräte verwendet, ist die MR-Umgebung aufgrund des starken Magnetfeldes und stark limitierten Raumangebotes per se eine Herausforderung. Aus diesem Grund wurden sowohl VII für FES (Studie 1) als auch für das Manipulandum (Studie 3) Machbarkeitsstudien durchgeführt. Dabei zeigte sich, dass beide Methoden sicher im MR-Scanner angewandt werden konnten und keine Methoden-bezogene Bildartefakte beobachtet wurden. In beiden Studien wurden sowohl passive wie auch aktive Bewegungen verwendet, d.h. einerseits wurden die Muskeln durch FES oder das Manipulandum aktiviert und andererseits aktivierten die Versuchsperson (aktiv) ihre Muskelgruppen. Passive Bewegungen werden in der Physiotherapie angewandt, wenn sich die betroffenen Gliedmassen aufgrund von Schwäche oder Lähmung nicht freiwillig bewegen lassen. Im Laufe der Therapie ist das erwünschte Ziel die Anwendung einer aktiven und selbstbestimmten Bewegung. Um die kortikalen Veränderungen beobachten und mit dem Verlauf einer physiotherapeutischen Massnahme in Beziehung setzen zu können, bedarf es optimalerweise einer Längsschnittstudie. Bevor eine FES-Therapie kombiniert mit MR-Untersuchungen an Patienten geplant wurde, wurde eine Trainingsstudie (Studie 2) mit gesunden Probanden durchgeführt, um eine Basis für zukünftige Studien aufzubauen. Bislang bestehen nur wenige Langzeitstudien, die den Effekt eines längerfristigen motorischen Trainings auf die kortikalen Veränderungen untersuchen. Das Ziel der vorliegenden Studie war die Erhebung des Effektes eines vierwöchigen FES- Trainings auf die Muskelkraft und deren Korrelate im cerebralen Aktivierungsmuster. Zusammengefasst gibt diese Doktorarbeit Einsichten über die Verwendung von fMRI als Mittel zur Erfassung von FES-bezogenen Veränderungen im menschlichen Hirn im Verlauf einer Therapie. Und die Entwicklung des MR-kompatiblen Manipulandum stellt ein Grundstein für zukünftige Studien dar, die die Anwendung von Robotern in der Physiotherapie und deren Effekt auf die neuronale Plastizität untersuchen wollen. VIII

EFFECTS OF NEW REHABILITATION TECHNIQUES ON THE HUMAN BRAIN USING FUNCTIONAL MAGNETIC RESONANCE IMAGING

Thesis

presented to the Faculty of Arts

of the

University of Zurich

for the degree of Doctor of Philosophy

by

Armin Blickenstorfer

of Stallikon (ZH)

Accepted in the fall semester 2008

on the recommendation of

Prof. Dr. rer. nat. Lutz Jäncke

Prof. Dr. med. Spyros Kollias

Zurich, 2011

Acknowledgements

First I want to thank my wife Snezana for her much needed love and support as well as enduring patience during the completion of my studies for my PhD.

Prof. Lutz Jäncke had become a role model for me and was the reason why I've chosen to enter the neuroscience community. His enthusiastic and inspiring kindness has led me to pursue this underlying thesis. I thank Lutz for his support and open mindedness in offering me the opportunity to work at the University Hospital in Zurich under the direct supervision of Prof. Spyros Kollias.

I am also grateful to have had the opportunity to work with Prof. Spyros Kollias, who has led me into the world of MRI brain anatomy. I am indebted to his very useful input regarding my projects and exceedingly grateful for his clear and concise corrections in my papers and presentations.
I want to thank Dr. Raimund Kleiser who supported me in my first publication and my introduction to Brain Voyager Software.

Thanks to Dr. Martin Meyer who offered his great experience, direction and encouragement during the difficult times of balancing studies, work and family life. I will especially treasure his fruitful insights from one father to another.

A special note goes to Dr. Birgit Keisker who shared the up and downs in our office. She was always helpful with putting into perspective the different aspects of our common and emotional PhD time.

I am indebted to the "crew" of the motor sensory systems (SMS) lab at the Federal Institute of Technology Zurich (ETH) under the leadership of Prof. Robert Riener, who also was the manager of one of the NCCR sub-projects that funded my work.

Dr. Ningbo Yu needs to be especially mentioned here as we started our PhD thesis together by developing an MR-compatible robotic device. I will never forget the many hours we spent together in the MR-facilities testing the devices and the NCCR conferences presenting our proceedings.

I want to express my gratitude to Dr. Thierry Keller and Dr. Mark Lawrence of the Institute for Automatic Control of the ETH for introducing me to functional electrical stimulation, including its programming and application within the MR-environment.

Thanks also goes to Martin Lang, with whom I worked closely on the training study.

Undoubtedly, I am very much obliged to Dr. Kai Lutz and my old friend Mike Brügger, who both greatly supported me in SPM and my study design.

Last but not least, thanks to Barbara and Beat Urfer for sacrificing their time to proofread my work, which must have been a challenge to understand from their perspective.

Contents

Summary

The human brain has the remarkable capability to adapt its functional and anatomical organization after damage to the central nervous system. Whether it is a stroke or a traumatic event such as spinal cord injury (SCI), the brain finds a way of handling the situation after such an incident. This is also referred to as neural plasticity. Neural plasticity is not only a process that starts after a pathology, it is actually a healthy process that runs all day long, encompassing learning. Whether it be in school or on the playground, learning a language or how to play an instrument – representations on the subcortical and cortical level change.

After a stroke, SCI or other incidents affecting the nervous system, patients spend a lot of time in neural recovery, including among other physical therapy interventions when the trauma is motor function related. The relationship between neural plasticity and physical interventions have been poorly investigated up to now, especially when it comes to newer interventions such as functional electrical stimulation (FES) and robot-assisted physical therapy. In this thesis, we investigate neural plasticity and its adaptation to FES (Study 1 & 2). FES is a well-known technique used in physical therapy. Besides this, its application is found in sports which enhances muscle force and endurance training. Its principle is simple: electrodes are placed above the relevant muscle and bursts of electrical impulses lead to a muscle contraction. In regards to robot-assisted physical therapy, we reference another subject of this thesis, which involved the development of a MR-compatible robotic device in cooperation with Dr. Ningbo Yu of ETH, who engineered the device. This cooperation enabled us to create a manipulandum based on hydrodynamic and pneumatic actuation (Study 3) This prototype may be the basis for future devices to monitor the effects of robot-assisted physical therapy on the subcortical and cortical level, i.e. relating changes within the brain's activation patterns to behavioral outcomes in stroke and spinal cord injured patients.

In all three studies, we use functional magnetic resonance imaging (fMRI) as the means to assess changes in the cortical activation patterns. When it comes to the additional application of other devices, the MR-environment is challenging due to its strong magnetic field and limited space. Therefore, we first conducted studies (1 & 3), for both FES and manipulandum feasibility which demonstrate safe application of both methods in the MR-scanner. No method-related image artifacts were observed.

In both studies, we used passive and active tasks. In the former, subjects muscles were activated by FES or the manipulandum; whereas in the latter subjects have used their own force. Passive movements are used in physical therapy when the affected limb cannot be moved voluntarily due to weakness or disability. During the ongoing therapy, use of active

and self-contained movements is the desired goal. Monitoring cortical changes related to an ongoing intervention such as physical therapy requires, at best, a long-term study design. Consequently before conducting a FES-intervention paired with an MR-based monitoring on patients, we established a training study (Study 2) with healthy subjects in order to form a basis for future studies. Up until now, only a few studies investigated the effect of long-term motor training on cortical changes. Our goal was to investigate the impact of a 4-week FES training on muscular output (force) and its respective correlates on cerebral activation patterns.

In short, this doctoral thesis provides insights on how to use fMRI in monitoring FES-related changes in the human brain as a result of ongoing medical intervention. Moreover, the development of the MR-compatible manipulandum forms a basis for future studies that implement robotics in physical therapy, in relationship to their effect on neural plasticity.

Zusammenfassung

Das menschliche Gehirn hat die erstaunliche Fähigkeit seine funktionelle wie auch anatomische Organisation nach einer Schädigung des zentralen Nervensystems anzupassen. Sei es nach einem Schlaganfall oder einem traumatischen Ereignis wie einer Verletzung des Rückenmarks: Das Hirn findet einen Weg mit der neuen Situation umzugehen. Diese Fähigkeit nennt man auch neuronale Plastizität. Der Prozess der neuronalen Plastizität setzt nicht erst nach einer Verletzung ein. Es handelt sich viel mehr ein gesundes Phänomen, das immer aktiv ist. Beispielsweise gehört das alltägliche Lernen - sei es in der Schule oder auf dem Sportplatz - oder das Erlernen eines Musikinstrumentes dazu. In der Folge verändern sich die Repräsentationen auf subkortikaler und kortikaler Ebene. Nach einem Schlaganfall, Schädigung des Rückenmarks oder anderen Ereignissen, die das zentrale Nervensystems betreffen, verbringen Patienten viel Zeit in der Rehabilitation bspw. in der Physiotherapie, wenn die Schädigung das motorische System betrifft. Der Zusammenhang zwischen neuronalen Plastizität und Physiotherapie wurde bislang nur wenig untersucht. Insbesondere wenn es sich dabei um neuere Interventionen wie funktionelle elektrische Stimulation (FES) oder Roboter unterstützende Physiotherapie handelt. In dieser Arbeit wurde die neuronale Plastizität und ihre Adaptionsfähigkeit auf FES (Studie 1 & 2) untersucht. FES ist innerhalb der Physiotherapie eine bekannte Methode. Daneben findet sie ihre Anwendung auch im Sport, bspw. im Muskelaufbau- und Muskelkonditionstraining. Das Prinzip ist einfach: Oberflächenelektroden werden oberhalb der relevanten Muskelgruppen plaziert und nach einer Serie von elektrischen Stromimpulsen resultiert eine Muskelkontraktion. Bezüglich der Roboter-unterstützten Physiotherapie war die Entwicklung eines Magnetresonanz-kompatiblen Gerätes ein weiteres Thema dieser Arbeit. In Zusammenarbeit mit Dr. Ningbo Yu von der ETH Zürich wurde ein Manipulandum auf der Basis eines hydrodynamischem und pneumatischem Antriebs entwickelt (Studie 3). Dieser Prototyp könnte der Grundstein für die Entwicklung weiterer Geräte sein, mithilfe derer die Effekte der Roboter-unterstützten Physiotherapie in der subkortikalen sowie kortikalen Ebene untersucht werden können. Das heisst, Veränderungen in Hirnaktivierungsmuster können mit den Verhaltensänderungen bzw. den Therapiefortschritten der entsprechenden Patienten in einen Zusammenhang gebracht werden.

In allen drei Studien wurde die funktionelle Magnetresonanztomographie (fMRI) als Methode zur Ermittlung der kortikalen Aktivierungsmuster angewandt. Werden zusätzlich weitere Geräte verwendet, ist die MR-Umgebung aufgrund des starken Magnetfeldes und stark limitierten Raumangebotes per se eine Herausforderung. Aus diesem Grund wurden sowohl

für FES (Studie 1) als auch für das Manipulandum (Studie 3) Machbarkeitsstudien durchgeführt. Dabei zeigte sich, dass beide Methoden sicher im MR-Scanner angewandt werden konnten und keine Methoden-bezogene Bildartefakte beobachtet wurden. In beiden Studien wurden sowohl passive wie auch aktive Bewegungen verwendet, d.h. einerseits wurden die Muskeln durch FES oder das Manipulandum aktiviert und andererseits aktivierten die Versuchsperson (aktiv) ihre Muskelgruppen. Passive Bewegungen werden in der Physiotherapie angewandt, wenn sich die betroffenen Gliedmassen aufgrund von Schwäche oder Lähmung nicht freiwillig bewegen lassen. Im Laufe der Therapie ist das erwünschte Ziel die Anwendung einer aktiven und selbstbestimmten Bewegung. Um die kortikalen Veränderungen beobachten und mit dem Verlauf einer physiotherapeutischen Massnahme in Beziehung setzen zu können, bedarf es optimalerweise einer Längsschnittstudie. Bevor eine FES-Therapie kombiniert mit MR-Untersuchungen an Patienten geplant wurde, wurde eine Trainingsstudie (Studie 2) mit gesunden Probanden durchgeführt, um eine Basis für zukünftige Studien aufzubauen. Bislang bestehen nur wenige Langzeitstudien, die den Effekt eines längerfristigen motorischen Trainings auf die kortikalen Veränderungen untersuchen. Das Ziel der vorliegenden Studie war die Erhebung des Effektes eines vierwöchigen FES-Trainings auf die Muskelkraft und deren Korrelate im cerebralen Aktivierungsmuster.

Zusammengefasst gibt diese Doktorarbeit Einsichten über die Verwendung von fMRI als Mittel zur Erfassung von FES-bezogenen Veränderungen im menschlichen Hirn im Verlauf einer Therapie. Und die Entwicklung des MR-kompatiblen Manipulandum stellt ein Grundstein für zukünftige Studien dar, die die Anwendung von Robotern in der Physiotherapie und deren Effekt auf die neuronale Plastizität untersuchen wollen.

I. Introduction

The coordination of motor movement requires a finely tuned nervous system. Most of the movements such as walking, riding a bike and so on are processed unconsciously. We experience the relevance of our motor system when we have to learn new actions as in sports or, more dramatically, when an injury occurs. A stroke or spinal cord injury (SCI) causes the nervous system to adapt to the new situation. This may result e.g. in the lack of coordination in limb movements as the residual motoric units try to compensate for the injury induced handicap. Recovery from stroke induced neurological deficits may take weeks, months or even years; and this process is often related to the so-called neuronal plasticity of the brain(Ward, et al. 2003). After lesions in the motoric centers within the spinal cord, development of a spastic syndrome is a typical pattern of neuronal reorganization. The patient experiences a disturbance or a complete loss of functional movements such as walking (Dietz 2002).

The application of physiotherapy in stroke or SCI patients is an important procedure after the initial emergency treatment in the hospital. One goal of the rehabilitation treatment is to improve and, if possible, restore the body functions lost as a result of SCI or brain disease / trauma and to help the patients become as self-sufficient and independent as possible (Popovic, et al. 2001b). The effects of physiotherapy on rehabilitation are clinically well investigated; whereas its central correlates and its potential short and long term effects on cortical reorganization have been rarely explored, especially with functional magnetic resonance imaging (fMRI). One advantage of using fMRI is that the relationship between neural plasticity and rehabilitative therapy can be directly and non-invasively assessed and its resulting changes in the cerebral blood flow can be followed (e.g.Dobkin 2004).

In this thesis, new rehabilitative therapeutic strategies will be investigated using fMRI in regard to their effect on cortical reorganization and its behavioral correlate. The two main therapeutic approaches are functional electrical stimulation (FES) and robot-assisted movement therapy. Before going into greater details, I will first give a short explanation on the neural representation of the motor system and then turn towards the applied methods of FES and fMRI.

The human motor system

The human motor system can be described by a two-pronged organization principle. On one hand, there is the somatotopic organization; and on the other hand,the hierarchical multilevel organization exists.

Somatotopic organization

Somatotopic organization refers to the topographical correspondence between cortical regions and their assigned body parts with respect to motor and somatosensory processes. It goes back to the early studies of Wilder Penfield and Herbert Jasper (1954), who mapped the motosensory cortex using intracortical stimulation in epileptic patients before undergoing brain surgery. This organization is also known as homunculus. Moreover, there is a relation between the size of cortical representation and the functional significance of a body part. For instance, fingers and lips cover larger areas on the cortical surface compared to the trunk. This is due to the control of fine muscle structures needed for precise motor control. Figure 1 illustrates the motor and somatosensory homunculus.

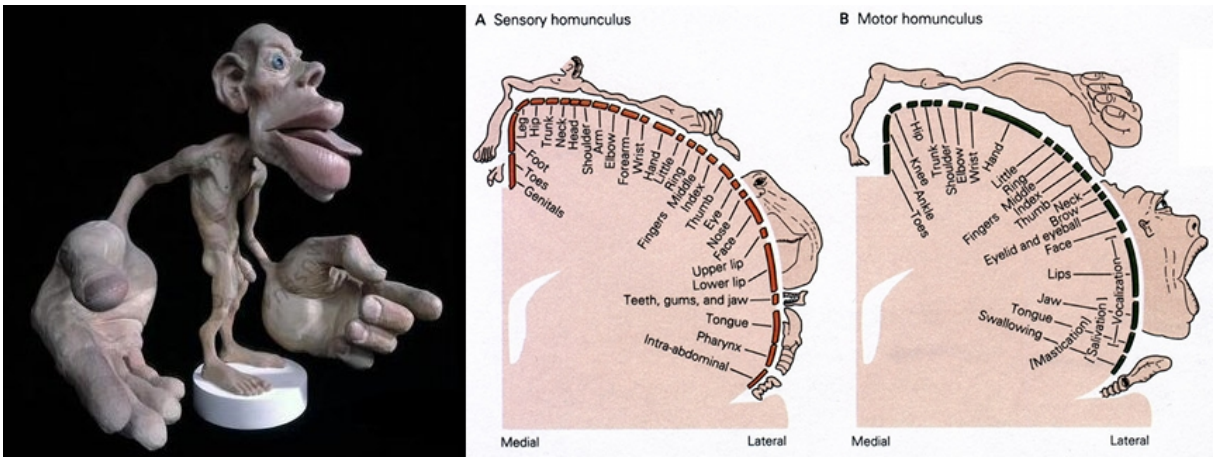

Figure I-1 Human homunculs. Within the motor homunculus (B) cortical regions related to the functional significance of a body part are well represented whereas, regions assigned to processing and distinction of fine external stimuli are larger within the sensory homunculus (A).

A large scale somatotopy of the contralateral primary motor cortex (MI) with distinct subregions controlling the foot, arm and tongue has been demonstrated by means of fMRI (Alkadhi, et al. 2002a). The area controlling the foot is situated on the vertex of the brain, i.e. on the dorsolateral surface at the interhemispheric fissure. Elbow, wrist, hand and finger movements are found on the lateral convexity in this order from superior to inferior. However, there exists a considerable overlap within the representation (Fig. 2). Lastly, tongue

representation is located laterally and close to the Sylvian fissure. Furthermore, the ipsilateral primary motor cortex is also similarly somatopically organized (Alkadhi, et al. 2002b), although its activation depends more on the activation level of other motor related areas.

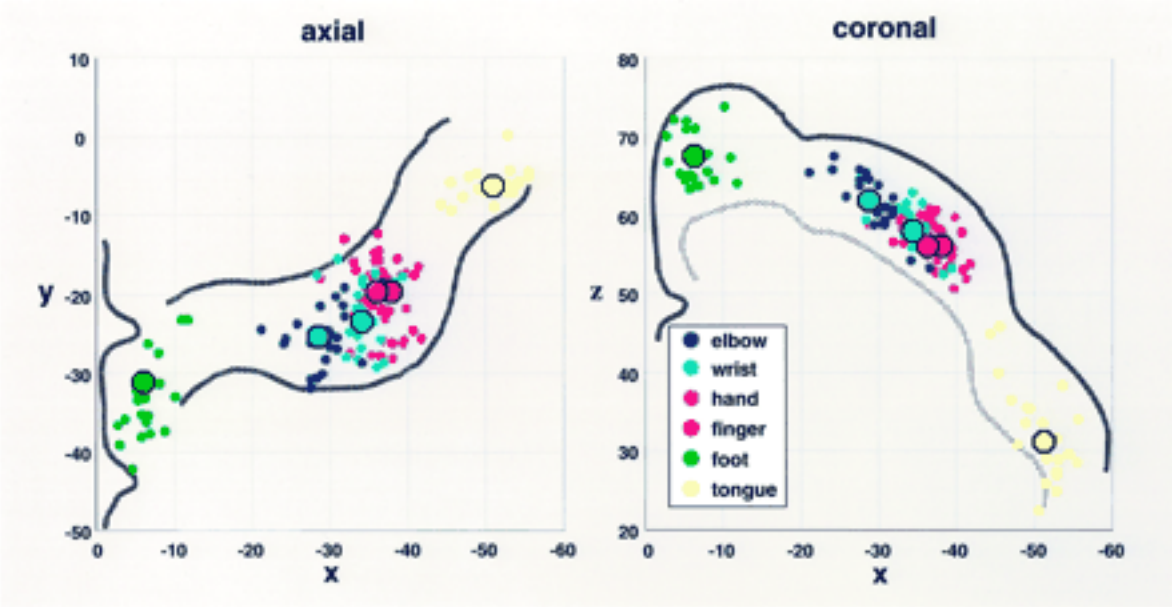

Figure I-2 Two-dimensional scatter plots of the center of gravity (COG) in 12 subjects in the contralateral M1(Alkadhi, et al. 2002a). *Small dots* represent individual COGs, and *large dots* indicate the mean COGs. Note the separate subdivisions for the foot, arm, and tongue and the clear somatotopic gradients within the arm representations in both the axial and coronal planes. The *x*, *y*, and *z* coordinates correspond to those in Talairach space (Talairach and Tournoux 1988) *Left,* Axial plane with approximate contour of the precentral gyrus. *Right,* Coronal plane with the cortical surface and limited to the white matter.

Besides primary motor and somatosensory cortex, a less refined somatotopic organization has been found in the supplementary motor area (Arienzo, et al. 2006; Chainay, et al. 2004; Mayer, et al. 2001), premotor cortex (Buccino, et al. 2001), anterior cingulate (Arienzo, et al. 2006; Mayer, et al. 2001), secondary somatosensory cortex (Eickhoff, et al. 2007; Ferretti, et al. 2004), superior parietal areas (Buccino, et al. 2001) basal ganglia (Gerardin, et al. 2003; Lehericy, et al. 1998; Maillard, et al. 2000; Scholz, et al. 2000) and cerebellum (Bushara, et al. 2001; Grodd, et al. 2001). In short, all major structures involved within the motor network are somatotopically organized. According to this, the arm region within primary motor cortex receives input from premotor areas that control arm movements; and these regions are again connected with descending tracts within the brainstem (Kandel, et al. 1996).

Hierarchical organization

The second organizational principle is a hierarchical multilevel control organization (Fig. 3). Starting from the bottom up, the spinal cord is the first or lowest level of this hierarchy (Gazzaniga, et al. 2002). It can also be thought of as the interface between central and

peripheral nervous system. At this level, simple mono- and poly-synaptic reflexes are controlled. Premotor and association areas are at the highest level (Gazzaniga, et al. 2002). Primary motor cortex, premotor areas and supplementary motor areas project directly via corticospinal tract and indirectly via motor systems within the brain stem to the spinal cord. Additionally, premotor and supplementary motor areas project to the primary motor cortex and receive information from prefrontal and posterior parietal regions in order to coordinate and plan complex movements based on actual, previous, desired or imagined sensory information (Kandel, et al. 1996). The motor cortex - together with basal ganglia, brainstem and cerebellum - translate these higher (motor related) cognitions into actual behavior (Gazzaniga, et al. 2002). Figure 3 illustrates how the control of motor action is distributed over several systems. Each system contributes to the final motor output but not every system deals with the details of a movement. As discussed above, higher levels deal rather with planning an action whereas lower structures execute the intended motor behavior.

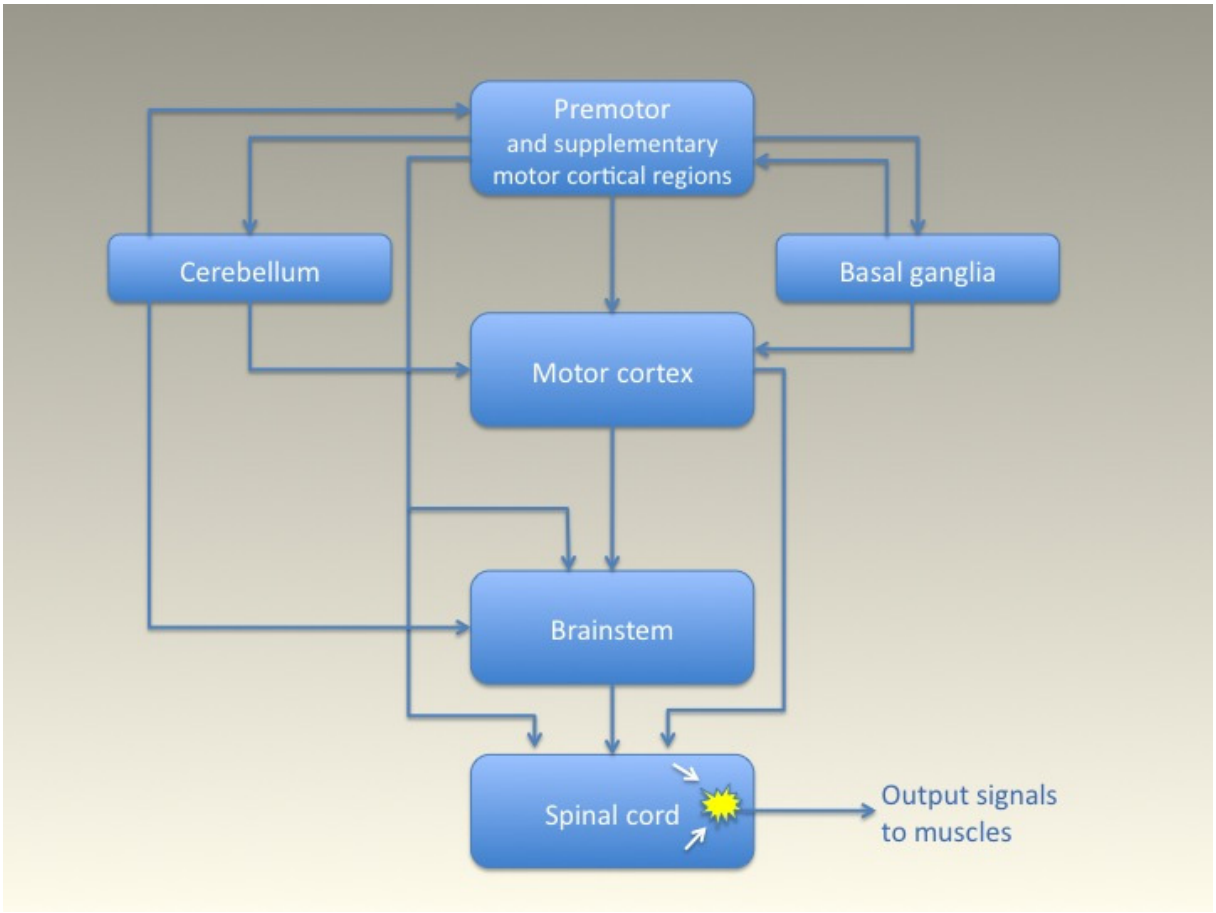

Figure I-3 The motor hierarchy. All signals to the limbs converge within the spinal cord. These signals are influenced and modulated by different systems within the brain (adapted after Gazzaniga, et al. 2002)

Hierarchical organization can also be viewed from a phylogenetic perspective. Simple organisms such as the sea slug (Aplysia californica) demonstrate a gill-and siphon-withdrawal reflex when a light tactile stimulus is applied (Hawkins, et al. 1989). Thus, simple reflexes can be classified as a motor behavior that do not depend on a superior brain structure. Likewise in humans, such simple reflexes are present in the spinal cord. The stretch reflex, when a doctor raps a patient's knee, or a withdrawal reflex, when a hot object is touched, are two examples of basic reflexes mainly controlled by spinal motoneurons. The next level within the motor hierarchy is the brainstem. It is composed of two parallel systems (Kandel, et al. 1996). The medial system is important for controlling posture by means of relating visual and vestibular information with somatosensory input. The lateral system controls distal limb muscles and is, therefore, important for execution of complete, goal oriented movements - especially of arms and hands. In addition, specific nuclei within the brainstem control eye and head movements (Kandel, et al. 1996). The last and highest level of the hierarchical organization comprises primary motor cortex, premotor areas and supplementary motor area (Kandel, et al. 1996). To summarize, over the course of evolution, nervous systems have become more and more complex by adding more levels, leading from a simple reflex action to a highly diversified motor behavior that integrates volition and pervious experiences, thus enabling reaction in different ways to the same distinct stimulus.

Neuroplasticity

Throughout its development, the human brain undergoes substantial changes given that a child's brain is different from that of an adult. This includes the ontogenesis of the homunculus. But once fully developed, the human homunculi are highly comparable in general terms. However, the somatotopical representation can be altered, since the brain remains 'plastic' throughout the whole life. Extensive training of a specific motor skill can lead to enlarged representational maps of areas controlling the trained extremities. For instance, the effect of the so-called neuroplasticity has been demonstrated in professional string players who demonstrated an increased cortical representation of the digits (Elbert, et al. 1995). Even moreso, the amount of cortical reorganization was correlated with the age at which the musicians have begun with to play. Amunts et al. (1997), investigating the intrasulcal length of the precentral gyrus (ILPG), showed that professional musicians had a less pronounced left-right asymmetry compared to healthy controls. Furthermore, IPLG size negatively correlated with the commencement of musical training. Jäncke et al. (2000) found functional differences in professional musicians who showed less brain activation within

motor areas while executing self-paced uni- and bi-manual tasks compared to healthy control subjects. The authors assumed that professional musicians required less “energy” to solve the task as their motor system was highly trained. Similar changes in the human homunculus were also observed in elite volleyball (Tyc, et al. 2005) and racquet players (Pearce, et al. 2000). Taken together, practice leads to morphological and functional changes within the brain.

Cortical plasticity has also been observed in patients who suffered brain (e.g. stroke, tumor) or spinal cord injury or traumatic amputation. Recovery after stroke occurs over weeks, months or even years and is related to neuroplastic processes that can be spontaneous or are supported by physical therapy. Several cortical areas contribute to these processes, including reorganizations in the affected and unaffected hemisphere. Involvement of non-motor areas of the affected hemisphere, motor areas of the unaffected hemisphere and bilateral non-motor areas were commonly observed (see Rossini et al. (2007; 2003) for review). Decrease of activation in contralesional areas, together with improvement of motor abilities, is a reliable marker for good recovery; whereas contralesional activation of primary motor areas seems to be an indicator of poor recovery. Therefore, Rossini et al. (2003) state “by use of the unaffected hemisphere, we can assess reorganization in the affected hemisphere and relate it to clinical recovery.” Motor activity and sensory feedback from the paretic limb are essential for the recovery process in that afferent stimulation from the periphery could enhance plasticity of the brain. Afferent stimulation can be achieved by neuromuscular facilitation techniques by a physical therapist or a rehabilitation robot supplying resistance to the affected limbs in specified movements in order to increase the afferent flow of nerve impulses from the proprioceptors (Sonde, et al. 1998). Another form of neuromuscular facilitation is functional electrical stimulation (FES) which stimulates sensory and motor nerves. Not only is the use of a limb important for supporting neuroplasticity processes but maintaining the cortical representation of the affected limbs is also relevant (Hallett 2001).

Peripheral deafferentation after a traumatic amputation can lead to reorganizational processes within the brain. Studies on monkeys (Merzenich, et al. 1983a; Merzenich, et al. 1983b) showed that after deafferentiation by means of nerve transaction or amputation, affected cortical areas were “invaded and occupied” by adjacent cortical representations. Similar topographic changes were observed in humans. For instance, after traumatic amputation of the upper extremity, stimulation of the lips lead to activations not only in the face area but also within the cortical region that would normally correspond to the amputated hand (Elbert, et al. 1997). However, patients skillfully using their affected limbs by either prosthesis or just by

daily use of the upper limb stump have motor cortical maps that show bilateral recruitment, having contralateral prominence, similar to the ones of healthy subjects (Cruz, et al. 2003). Thus, in accordance with the results found in stroke patients, a contralateral activation pattern elicited by use of the affected limb is a desired outcome of rehabilitation amongst motore recovery, which probably even precedes the visible success of therapy. Reorganization after SCI is controversially discussed. Curt, et al. (2002) reports in an fMRI study that finger movements elicited an increase in activation volume of the MI hand representation and additional activation in various non-primary motor areas such as SMA, dPMC, post-central and parietal areas as well as the cerebellum. Thus, the somatotopy was not very different to controls. Perseveration of the basic organization has further been demonstrated by Halder, et al. (2006) and Hotz-Boendermaker, et al. (2008) who showed that SCI patients had cortical control mechanisms over the affected limbs. Thus, the relevant cortical representations were not overtaken by adjacent areas. However, other studies report shifts into regions representing the disconnected limbs. For instance, Lotze, et al. (2006; 1999) demonstrated a shift of activation maxima during elbow movements towards the disconnected lower limb region. All in all, after SCI, a reorganizational process will occur demonstrated by a takeover of areas controlling the affected limbs and/or additional recruitment of other brain structures. Important for a rehabilitative strategy, the incorporation of these findings to improve motor function as an intact brain function is central to voluntary movement (Cramer, et al. 2005).

So far, only a few studies have related the therapy outcome to changes in brain activation patterns in terms of monitoring the recovery process in a long term setting with repeated neuroimaging sessions. During the course of therapy and with follow-up sessions investigating the maintenance of hopefully positive effects, a long term study design allows an assessment of the relationship between neural plasticity and rehabilitative setting. Thus the pattern of neuronal activity can be followed. For instance, Dobkin (2004) demonstrated with fMRI changes in representational maps that adults with chronic hemiparetic stroke evolved practice-induced representational plasticity associated with gains in speed, endurance, motor control, and kinematics for walking (Fig. 4). Liepert, et al. (1998) used transcranial magnetic stimulation to show changes in cortical motor area sizes in the damaged hemisphere of a single subject eliciting responses in abductor pollicis brevis muscle (APB) before and after constraint induced therapy[1]. In a PET study, (Nelles, et al. 2001) demonstrated an increased blood flow in bilateral inferior parietal cortex, premotor areas and in the contralateral

[1] Constraint induced therapy prevents the use of the non-affected hand in therapeutic tasks as well in activities of daily living. The patient is forced to repetitively use his / her affected hand leading to a concentrated training of the impaired extremity (Taub E et AL. , 1993; Vogelaar TW et al., 1999; Wolf et al.,1989).

sensorimotor cortex after stroke subjects underwent a specific arm training. In an exemplary fMRI study, (Johansen-Berg, et al. 2002) correlated the behavioral improvement of stroke patients with their corresponding brain maps. Increased fMRI signal change was seen in bilateral cerebellum, contralateral secondary somatosensory cortex and contralateral dorsal premotor cortex suggesting an altered recruitment of sensorimotor cortices and the cerebellum contributing to recovery of the applied therapy.

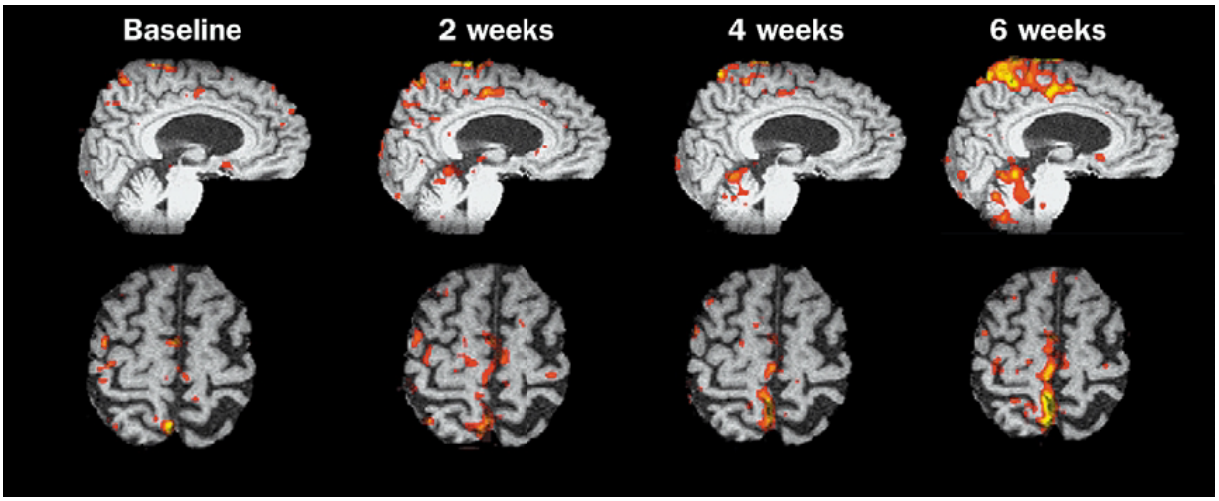

Figure I-4 Functional MRI series with the blood-oxygen-level dependent signal and analysis of regions of interest during voluntary ankle dorsiflexion (Dobkin 2004). The patient had chronic hemiparesis after a subcortical stroke 14 months earlier and still walked at less than 65 cm/s. The behavioral changes from baseline to the end of the first 12 training sessions were significant, so further therapy would probably not have been offered. The increase in fMRI activity, however, suggested ongoing recruitment within primary sensorimotor cortex (S1M1). Therapy was extended another six sessions in 2 weeks to see if gains in walking and recruitment had reached a plateau. There was a 20% increase in walking speed and improved motor control. The fMRI study at 6 weeks revealed an expansion of the foot representation medially into the representation for the back and hip muscles. Also, greater cerebellar and cingulate motor cortex activity developed. Two additional bouts of therapy led to greater motor control of the ankle during walking and focusing, rather than expanding fMRI activity within M1, consistent with greater synaptic efficacy (not shown).

In short, neuroplasticity is a phenomenon happening throughout the life span not only of human beings but of all organisms possessing a nervous system. It adapts to new situations in a learning process and deals with injuries finding a best possible functionality. Unfortunately, it may sometimes be maladaptive. Therapy seeks to support and improve remaining functions and to reverse adverse compensatory behavior. Neuroimaging helps to visualize the ongoing neuroplastic changes and may give conclusions about the success of an ongoing rehabilitative approach. To convincingly relate behavioral gains to changes in brain activation patterns over the course of therapy, Dobkin, et al. (2004) proposed 4 prerequisites:

- Employment of a well-defined rehabilitation strategy that emphasizes the practice of functionally important movements

- Application of an activation paradigm during neuroimaging that incorporates components of the rehabilitation strategy
- Relate changes in activated regions of interest over time to the intensity of duration of the rehabilitation strategy
- Use of behavioral outcome measures that monitor the gains over time that are relevant to what was practiced

Accomplishment of studies that follow these guidelines is challenging and needs careful designing. However if changes in brain activation evolve together with behavioral progress, then the fMRI results may serve as valuable predictors for the outcome of therapy.

Functional magnetic resonance imaging

There are several ways to investigate ongoing neuronal processes in the brain; and for further reading, two extensive books (Jancke 2005; Toga and Mazziotta 1996) are suggested. For this reason, this part is kept short and only some crucial points are mentioned. Electroencephalography (EEG) and magnetoencephalography (MEG) both rely on detection of electrical potentials emitted by neurons recorded with electrodes placed on the scalp (EEG) or with specific sensors within a head coil (MEG). The recording of electrical potentials reflects a direct measurement of neuronal activity. On the other hand, functional magnetic resonance imaging (fMRI) and positron emission tomography are indirect methods measuring neural events. They rely on the detection of metabolic signals, that is, changes in metabolism or blood flow while the subject lying in the scanner is engaged in a specific task. Neurons, as well as other cells of the body, need glucose and oxygen to function properly. Thus, PET and fMRI measure the consumption of oxygen (fMRI) or glucose (PET) that are transported by the vascular system since neuronal activity is derived from energy consumption of neurons.

BOLD – Blood oxygenation level dependent

The most often used fMRI-method measuring oxygen (O_2) consumption makes use of the blood oxygenation level dependent (BOLD) contrast mechanism (Jancke 2005). In plain language, red blood cells exhibit a conversion during "neuronal activation" in that it changes from an oxygenated state (hemoglobin concentrated blood, HbO_2) into a deoxygenated state (deoxyhemoglobin concentrated blood, Hbr). This conversion leads to a change of magnetic property. While HbO_2 is diamagnetic (no unpaired electron and no magnetic moment), Hbr is paramagnetic (unpaired electron and magnetic moment). Subsequently, Hbr behaves like a small bar magnet that causes susceptibility artifacts in a magnetic field, leading to a signal

decrease (Jancke 2005).Thus, hemoglobin acts as a convenient endogenous contrast agent, making fMRI a complete noninvasive method as it relies primarily on the magnetization difference between HbO_2 and Hbr. Figure 5 shows that the BOLD signal is a complex interaction of regional cerebral blood flow (rCBF), cerebral blood volume (CBV) and cerebral metabolic rate of O_2 consumption ($CMRO_2$).

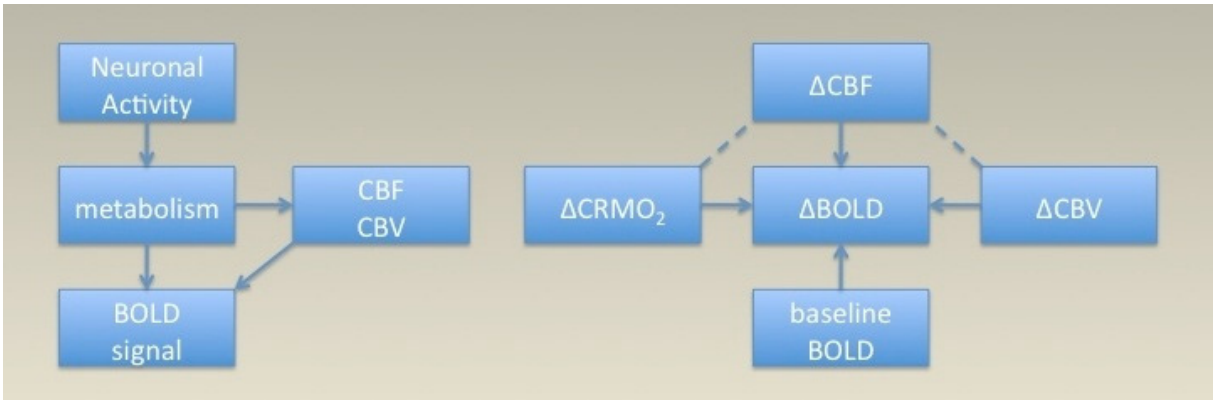

Figure I-5 Left: A block diagram showing the multistep path to the fMRI observables of blood flow,blood volume, and BOLD signal. Right: BOLD signal changes result from a combination of changes in CBF, CBV, and $CMRO_2$, together with an amplification factor than depends upon baseline physiology.The dashed lines indicate presumed coupling relationships (adapted after Toga and Mazziotta 2002).

A neuronal activity leads to an increase of rCBF. Local $CMRO_2$ is not increased to the same extent as HbO_2 that is available (the neural tissue is unable to absorb all of the excess oxygen), leading to an O_2 surplus and less signal inhibiting Hbr. During the beginning of neuronal activity, a local concentration of Hbr is found which is demonstrated in an initial dip in the hemodynamic response function (Fig. 6), causing magnetic field inhomogenities. The brain compensates this local Hbr-concentration with an HbO_2-supply that peaks apx. 5-8 seconds after stimulus onset, leading to a signal increase that plateaus if neuronal activity continues and returns to baseline after neuronal activity has stopped. The relationship of these parameters is apparently also affected by other factors such as energy demands of neurons (Jancke 2005). The interpretation of the BOLD signal requires a complete understanding of the underlying neuronal activity that gives rise to the hemodynamic response and the way these two factors are related - also called neurovascular coupling (Arthurs and Boniface 2002). However, the features of neurovascular coupling remain mostly unknown - including the nature and origin of the communicating signals between neuron and vessels (Arthurs and Boniface 2002). As shown in Figure 5, the common belief is that relative changes in CBF, $CMRO_2$ and CBV are all functionally coupled during brain activation (Toga and Mazziotta 1996).

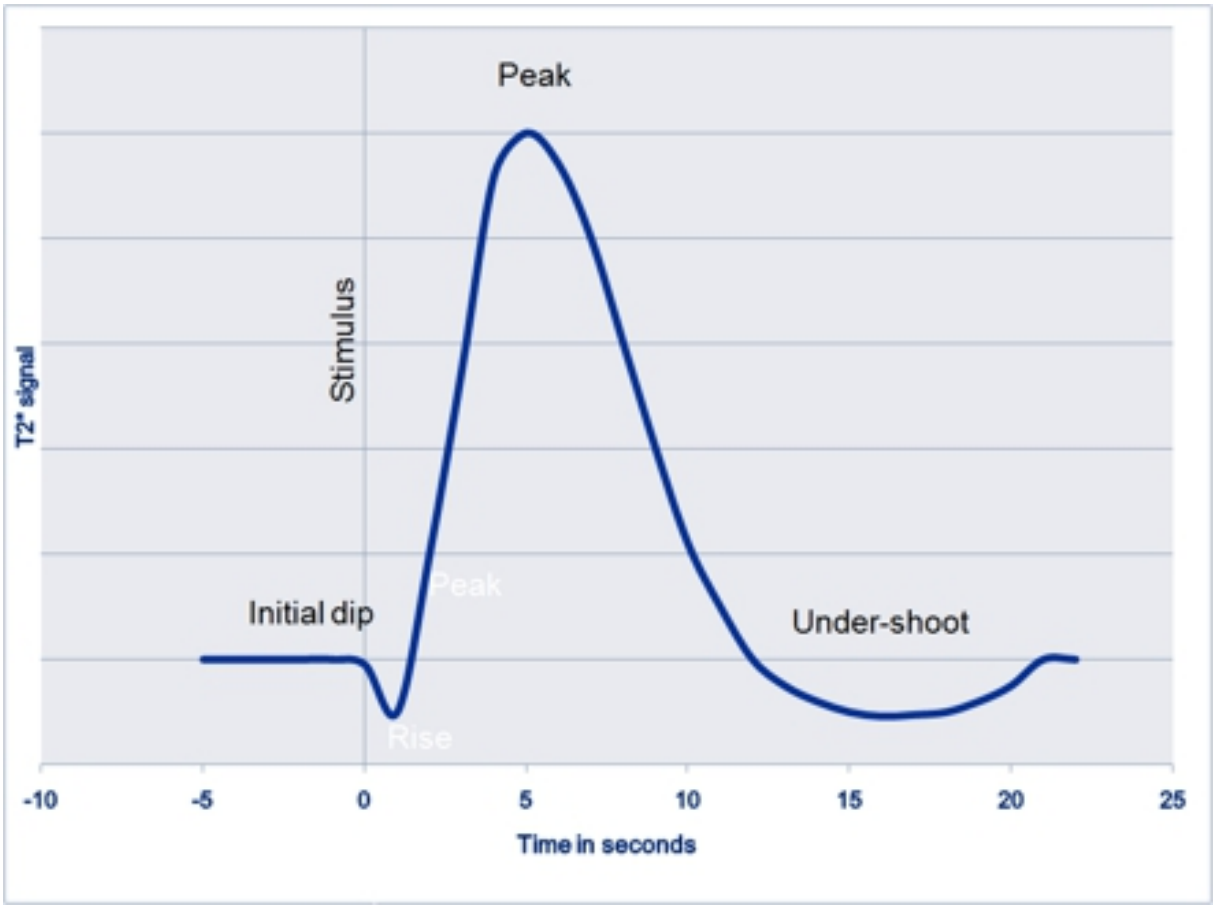

Figure I-6 Hemodynamic response function. During the beginning of neuronal activity, a local concentration of Hbr is found that is demonstrated in an initial dip in the hemodynamic response function causing magnetic field inhomogenities. The brain compensates this local Hbr-concentration with an HbO_2-supply that peaks apx. 5-8 seconds after stimulus onset, leading to a signal increase that plateaus if neuronal activity continues and returns to baseline after neuronal activity has stopped. (http://radiopaedia.org/articles/bold_imaging)

Another BOLD-related issue is the question of what is really measured (Culham 2008). Obviously, firing neurons requires energy and oxygen. But is it the output of, or the input to, a neuron that is reflected in the BOLD activation? Is activation inferred from excitatory or inhibitory inputs? Does the BOLD signal depict feedforward projections (lower subcortical to higher cortical areas) or feedback projections? Figure 7 illustrates these questions. Major progress in answering these questions has been made by the work of Logothetis and coworkers (for a review see Logothetis 2008). Their milestone work consisted of simultaneous recordings of electrical and fMRI data in primates (Logothetis, et al. 2001). They measured local field potentials (LFP) and multi-unit activities (MUA); the former reflecting not only post-synaptic activity (weighted average of synchronized dendro-somatic components of the input signals of a neural population) but also local perisynaptic activity in a region (Logothetis 2008), and the latter reflecting primarily the output of a neural

population. They found that the BOLD signal may reflect neuronal processing related to the input and the local processing in an area (LFP) rather than the spiking activity corresponding to the output of the area (MUA) (Logothetis, et al. 2001). Moreover, it has been found that where spiking activity was absent the hemodynamic response was not reduced (Logothetis, et al. 2001; Viswanathan and Freeman 2007).

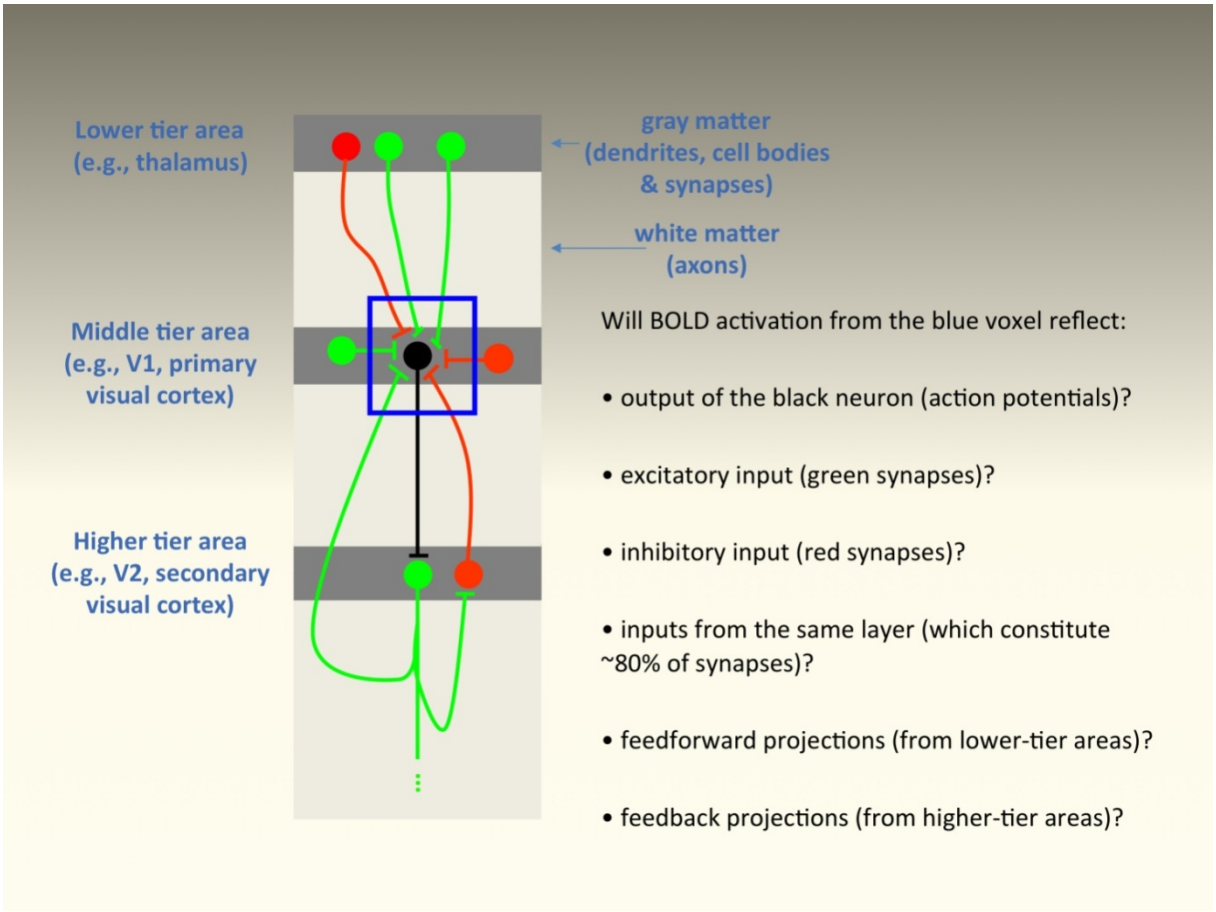

Figure I-7 What is measured with BOLD-imaging? Within the example, the blue voxel receives excitatory but also inhibitory influences from different layers (from Culham 2008)

Summarized, the limitations of fMRI are less related to physics and hardware issues (e.g. field strength of scanners) and more to the understanding of the neurovascular coupling and the circuitry and functional organization of the brain (Logothetis 2008). While fMRI cannot differentiate between excitatory and inhibitory signals, it is still unclear whether bottom-up or top-down processes are measured. Currently, $CRMO_2$ – one of the major variables effecting the BOLD - can still not be estimated accurately. Detection of activation in a very small number of neurons may be prevented by volume transmission that is related to states of motivation, attention, learning and memory and, therefore, dominates the hemodynamic response (Logothetis 2008).

Nevertheless, BOLD-fMRI is well correlated with results from other methods, making obtained results definitely valuable. fMRI is currently one of the best methods available for gaining insights into brain function. With the development of stronger scanners, the imaging resolution will permit activation detection at a small scale. Moreover, the combined approach with EEG/MEG has a millimeter / millisecond resolution potential . Logothetis (2008) nicely stated in his conclusion, "Today, a multimodal approach is more necessary than ever for the study of the brain's function and dysfunction. Such an approach must include further improvements to MRI technology and its combination with other non-invasive techniques that directly assess the brain's electrical activity, but it also requires a profound understanding of the neural basis of haemodynamic responses and a tight coupling of human and animal experimentation that will allow us to fathom the homologies between humans and other primates that are amenable to invasive electrophysiological and pharmacological testing."

Safety issues

The massive strength of the magnet makes safety essential. To compare, the earth's magnetic field corresponds to apx. 0.5 Gauss (= 0.00005 Tesla [T]) whereas we used a 3T scanner leading to a magnetic field which is 60'000 times stronger than our usual surroundings. This force can make thing fly – even big things! Chaljub, et al .(2001) lists in his report that a defibrillator, a wheelchair, a respirator, ankle weights, an IV pole, a tool box, sand bags containing metal filings, a vacuum cleaner and mop buckets have all been drawn into the MR-scanner. For this reason, it is absolutely mandatory to screen participating subjects for any magnetic objects outside (barrette, earrings, necklace, belt etc.) and inside (orthopedic implants, pacemaker, neurostimulators, metal splinters, etc.) before entering the MR-environment. Smaller objects such as barrettes might not be dangerous; but their magnetism will most likely affect the MR images, making them unusable for further analysis. Obviously, developing new devices for MR-imaging is challenging since it requires assembly parts that do not affect the imaging. But attention also has to be paid to the effect of magnetism with the functionality of the new device. For further information and reading about fMRI safety issues, the website www.mrisafety.com is very comprehensive and recommendable.

Functional electrical stimulation

Functional electrical stimulation (FES) is a technique widely applied in physical therapy, sports training and medicine. It is used in the treatment of muscle atrophy (Sheffler and Chae 2007), muscle force training (Gondin, et al. 2005; Maffiuletti, et al. 2002a), endurance

training (Marqueste, et al. 2003; Petrofsky, et al. 2000), pain treatment (DeSantana, et al. 2008; Emmiler, et al. 2008; Slavin 2008; Weiner, et al. 2008), functional movement therapy (Durmus, et al. 2007; Popovic, et al. 2001a; Robertson and Ward 2002) and in the restoration of a functional movement in disabled patients using so-called neuroprostheses (Mangold and Keller 2003; Mangold and Keller 2004). And its applications are continuously increasing.

FES uses short bursts of electrical pulses that generate action potentials in motoneurons attached to a muscle which cause the required muscle contraction (Fig.8) (Baker, et al. 1993).

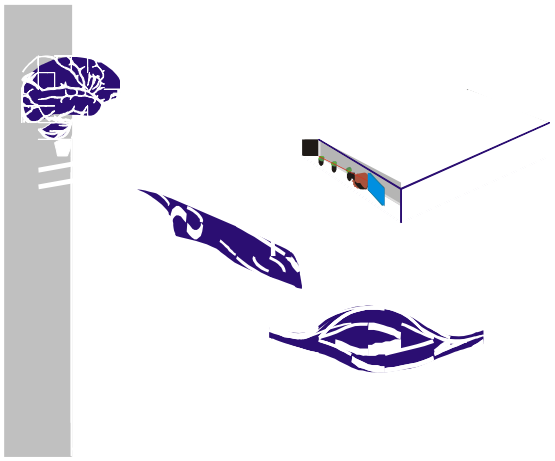

Figure I-8 The basic principle of FES. External electrical inputs travel along the relevant nerve bundles, resulting in a contraction of the targeted muscle

The artificial generation of an action potential may produce a similar muscle contraction to that evoked by voluntary activity. However, physiologic muscle contraction differs in recruitment order and synchronicity of excitation of individual motor units (Baker, et al. 1993). Small motoneurons with slow-fatiguing motor units are generally the first ones to be activated in a normal physiological condition followed by the recruitment of larger, faster, and more powerful units that fatigue more rapidly (Guyton 1991). With FES, the large neural fibers, supplying the mentioned larger and easily fatigable motor units, are the first to fire. The smaller, slower and deeper lying motor units capable of a longer contraction are only excited when stimulation intensity is increased. In short, FES results in a recruitment order that is the reverse of the normally physiologic order (Baker, et al. 1993).

FES is applied either through self adhesive surface electrodes, needles or implanted electrodes. The electric pulses are applied between pairs of electrodes. Ion currents are driven between the positive electrode (anode) and the negative electrode (cathode). At the anode, positive ions in the underlying skin are repelled and negative charged ions are simultaneously attracted. The cathode acts in the opposite way, resulting in a current of ions defined as the

movement of charged particles (Baker, et al. 1993). Since the electric current seeks the way of least resistance, it will flow more easily through tissue with low impedance. Thus, due to the high impedance of the skin with its horny layer, the electric current rather passes through the underlying structures. Most of the stimulating current bypasses the nerve fiber and flows through the extracellular fluid which has lower impedance. Because of this, only a fraction of the electrical current passes the membrane of an axon (Fig. 9). The relationship between the diameter of an axon and resistance to longitudinal flow (i.e. along the axon's axis) is reciprocal in that the larger the axon diameter, the lower the resistance to current passing across the membrane. Thus, larger nerve axons have lower current thresholds and are, therefore, more easily exited by peripherally applied electrical stimuli (Baker, et al. 1993).

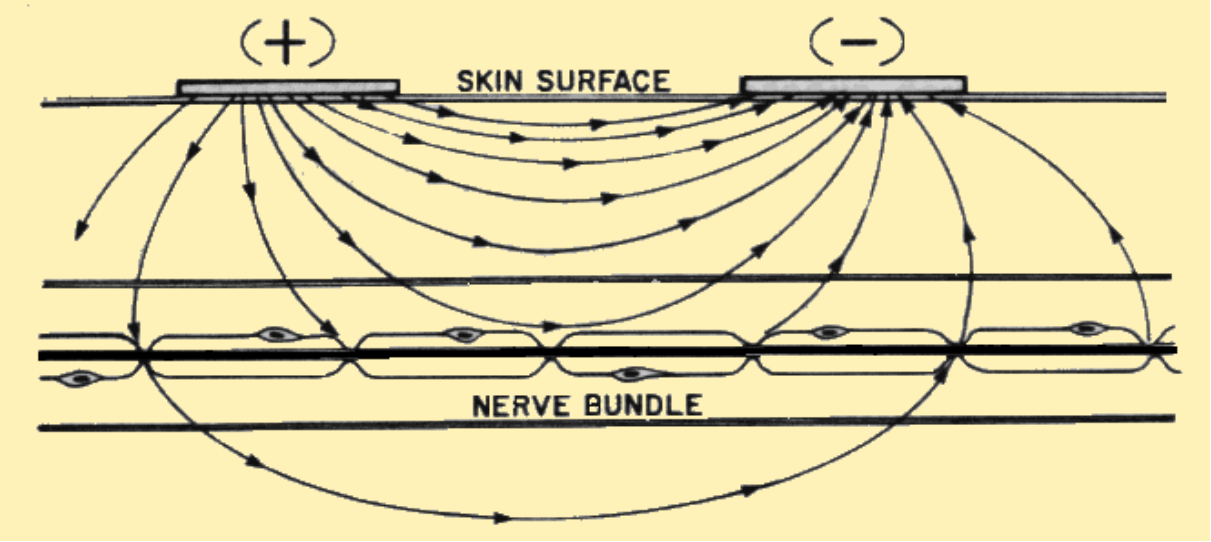

Figure I-9 Current density. The electric current seeks the way of least resistance. Only a fragment of the stimulation reaches the nerve bundle as most of the current travels through extracellular fluids, which have less impedance (Baker, et al. 1993). Factors influencing the current are impedance of body tissues, electrode size and position as well as stimulation parameters.

Placement of electrodes affects the stimulation in that electrodes that are placed close together cause most of the current to pass through surface tissue. This is because of the short distance and the subsequent lower impedance compared to the higher impedance if the current has to pass the skin and fat layer. However if electrodes are placed farther apart, the way of lowest impedance goes through the interstitial tissues and, therefore, allows stimulation of deeper tissues (Baker, et al. 1993). Furthermore, Adams et al. (1993) showed that the same electrode position does not activate the same muscles across different subjects. Variations in stimulation were most probably due to individual muscle architecture. Lang (2008) demonstrated that during a 4-week FES training the same electrode position did not elicit the

same stimulation force between two consecutive measurements. In order to achieve the best possible stimulation results, electrode placement has to be adapted in every session.

Stimulation parameters

The amplitude (intensity) of the applied pulse and its duration must be adequately adjusted to exceed the threshold of excitability of the stimulated tissue (Baker, et al. 1993). First, the closest fibers to the exciting electrode and then the ones with the largest diameter are stimulated. Increasing the amplitude leads to stimulation of additional fibers. Increased recruitment can also be achieved by extending the pulse duration. Figure 10 demonstrates the relationship between amplitude and pulse duration. The same excitation can be achieved by either varying amplitude or pulse duration.

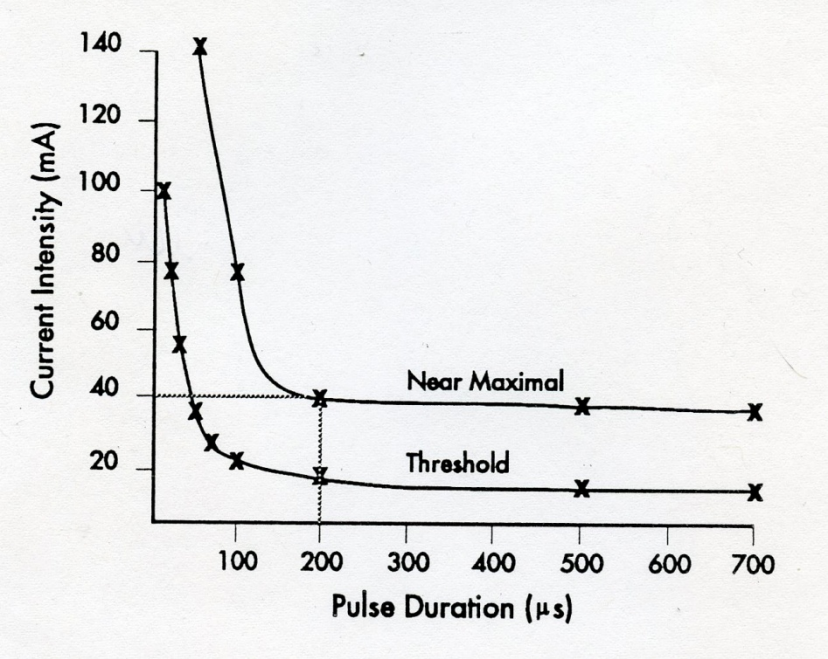

Figure I-10 The relationship between current intensity and pulse duration. With the same duration, muscle force can be adjusted from threshold to near maximal by varying the current intensity between 15 – 40mA. On the other hand by keeping the intensity constant at 40mA, a muscular response can be achieved by adjusting the pulse duration from 40 to 200μs (Baker, et al. 1993).

Frequency

The firing rate of neural fibers is dependent on the pulse repetition frequency that thereby influences the quality of the evoked motor response (Baker, et al. 1993). A single pulse leads to a muscle twitch. Increasing the frequency leads to a greater torque that is best achieved at frequency producing tetany (Fig. 11). In general, a frequency between 25 and 50 Hz is used for clinical applications (Baker, et al. 1993). By selecting the stimulation frequency, attention

has to be directed to the effect of muscle fatigue. Tetanic stimulation leads to a synchronous activation of the same nerve fibers; whereas during physiological contraction, neural activity is asynchronous. Smooth muscles contractions are achieved with individual neural discharge rates of only 5 – 25 /sec (Adrian and Bronk 1929) allowing repeated responses in the motor nerve with virtually no conduction failure. External stimulation activates only a small fraction of the motoneuron pool due to placement and orientation of electrodes. Furthermore, increasing frequency induces discomfort or pain because before activating large numbers of motor nerves, superficial sensory fibers will be excited as well.

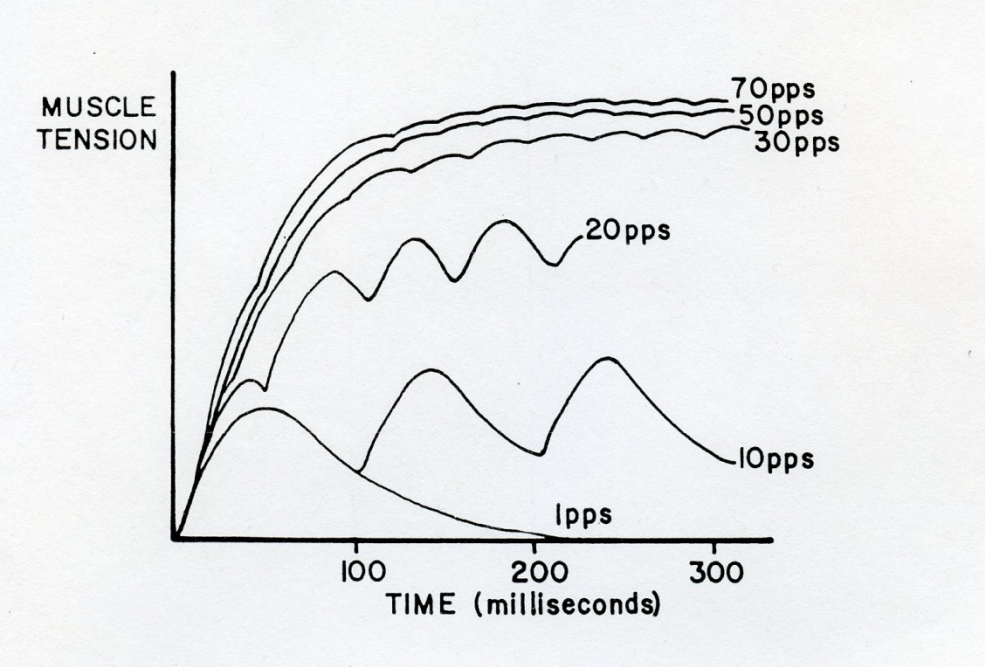

Figure I-11 Summation of contractions and tetanization (Baker, et al. 1993). In order to achieve the best result of a smooth muscle contraction without causing too much muscle fatigue, a frequency between 25 and 50Hz is usually used in clinical applications.

Wave forms

Motoneurons can be excited with many different waveforms (for detailed description, see (Baker, et al. 1993)). Nowadays monophasic and biphasic current or voltage pulses are applied (Peckham and Knutson 2005a). As previously mentioned, the applied electric charge depolarizes the membrane of the motoneuron leading to a generation of an action potential. Then, the applied charge should leave the body and not sum up. Thus, the secondary pulse of a biphasic waveform balances the charge injection of the primary pulse. For the sake of patients and applied stimulation, it is beneficial that the positions of anode and cathode alternate during stimulation (Peckham and Knutson 2005a). For this reason, the majority of

FES applications use bipolar current pulses, allowing control of the amount of charge administered to and removed from the body (Popovic, et al. 2001b).

FES applications

Several electrodes exist for the application of FES, such as surface (transcutaneous), needle (percutaneous) or implanted electrodes (Fig. 12). In general, surface stimulation requires self adhesive electrodes that are placed on the subject's skin over the nerves or over the motor points of the targeted muscles (Baker, et al. 1993; Peckham and Knutson 2005a). The advantage of surface stimulation is that it is non-invasive and relatively easy to apply. Furthermore, surface systems can be applied at a very early stage of rehabilitation, during the recovery and reorganization of the peripheral and central nervous systems, allowing early benefit for the patient (Popovic, et al. 2001b). Even patients can apply the electrodes when appropriately instructed. The development of textile neuroprostheses containing multiple embroidered transcutaneous electrodes that can be placed on the forearm to enable an electrically functional grasp will make the application for patients even more comfortable and reliable (Lawrence, et al. 2008). However, surface stimulation also has its disadvantages. Repeated application of electrodes in the appropriate locations requires some expertise and patience in order to achieve the desired outcome. Reducing fatigue requires activation of the deeper lying slower motor units (see above) but in sensitive skin, the stimulation may cause painful reaction because of cutaneous pain receptor activation, preventing a successful muscle contraction. In addition, a selective activation of specific muscle groups is difficult with larger electrodes, (Peckham and Knutson 2005a).

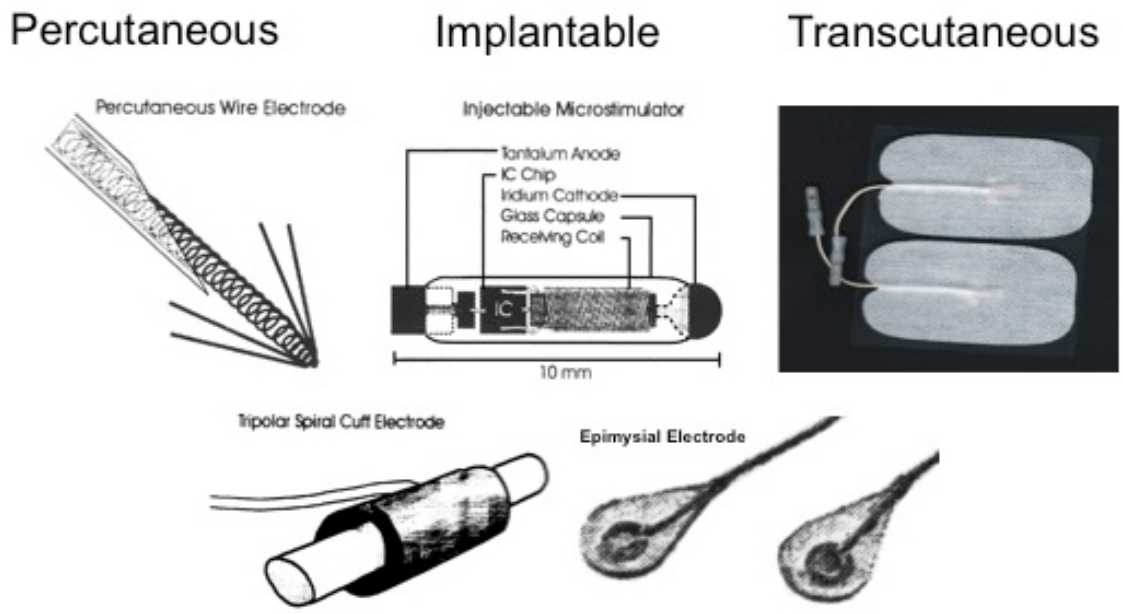

Figure I-12 Different types of stimulation electrodes

Percutaneous stimulation is done with wired electrodes that are implanted into the muscles with an epidermal needle. Due to its nature, a percutaneous electrode can selectively activate deeper lying muscles, provide isolated and repeatable contractions and produce less likely pain sensations in the skin as sensory afferents are bypassed. A self-adhesive electrode serves as charge removal electrode (Peckham and Knutson 2005a). Disadvantageous is the minimal invasive application that might be prone to infections at the stimulation point if not properly applied. Moreover, electrodes might break or move and have to be removed and replaced (Shimada, et al. 1996). Nevertheless, percutaneous systems may serve as precursors to fully implanted FES systems and have been shown to be suitable for long-term applications (Peckham and Knutson 2005a; Shimada, et al. 1996).

Implanted FES systems are generally used in a long-term set-up (Peckham and Knutson 2005a). In contrarst to transcutaneous and percutaneous systems, the stimulator is implanted in the patient's chest or abdomen and is connected through a radio-frequency telemetry link to an external control unit that provides power and command instructions, thereby eliminating the wiring outside of the body. The risk of infection is reduced as newer batteries have long service lives, therefore reducing the need for replacement (Peckham and Knutson 2005a). One other advantage of implanted FES systems is that, once implanted, there is no additional time required to put on and put off the stimulator compared to surface stimulation (Popovic, et al. 2001b). Implanted electrodes are attached to the muscles surface, within the muscle, motor neurons close to the muscle, around or close to a nerve (Peckham and Knutson 2005a;

Popovic, et al. 2001b). Similar to percutaneous stimulation, greater muscle selectivity is achieved so that smaller and deeper muscle can be controlled.

To summarize, it is recommendable to start with a transcutaneous application as soon as possible after an injury. Surface application is very flexible and can be adapted to the patient's needs (Popovic, et al. 2001b). An early application might support the plasticity of the peripheral and central nervous system and help to recover the lost functions as a result of the disease or injury. Popovic et al. (2001b) state […subjects would learn from the very early rehabilitation program to accept the neuroprostheses as a device they need to carry out in their daily living activities.] After successful daily applications of surface stimulation administered by the patient, one might consider a transition to an implanted system as long as the recovery of lost functions has not yet lead to a satisfactory state.

Rationale for using FES

FES aims to repeatedly stimulate relevant muscles or nerves that have been deafferented and / or deefferented. The goal is thereby mimicking neuronal and / or muscular signals through a sequence of electrical pulses that will generate inputs to the spinal cord. The increased flow of signals from distal sensory areas could enhance brain plasticity in stroke patients (Sonde, et al. 1998). Furthermore, feedback from the paretic limbs is believed to be essential for recovery (Rossini, et al. 2003). Several reports have shown the beneficial effects of somatosensory stimulation leading to higher cortical excitability (Kaelin-Lang, et al. 2002; Ridding, et al. 2000; Ridding, et al. 2001), enhancement of pinch grip strength in stroke patients (Conforto, et al. 2002) and the maintenance of beneficial effects over 30 days in a hand motor assessment in patients after a stroke (Conforto, et al. 2007).

FES can be applied in supporting either passive or active movements. The muscles of paralyzed limbs may not be voluntarily moved, but FES provides a possibility to externally activate them. Thus, electrical pulses lead to passively evoked muscle contractions. On the other hand, FES might support a voluntary contraction becoming more effective as reported in studies investigating the effect of FES-supported force training (Gondin, et al. 2005; Maffiuletti, et al. 2002a). Neuroimaging studies with PET (Nelles, et al. 2001; Nelles, et al. 1999) and fMRI (Enzinger, et al. 2008; Lotze, et al. 2003; Takahashi, et al. 2008) have shown that specific active or passive rehabilitation procedures induced significant changes in brain activations (Rossini, et al. 2003). Passive movements seem to have a similar effect to active movements on primary sensorimotor cortex in the affected hemisphere of stroke patients. Therefore, passive therapy during the acute stage may improve the outcome of recovery and active motor training in the subsequent, subacute and chronic stage of stroke may reverse

maladaptive brain reorganization (Rossini, et al. 2003). In short, FES merges the approaches of increased input from the periphery, somatosensory stimulation as well as active and passive training possibilities. Although several reports about the beneficial effects of FES have been published, very little literature exists about the relationship of FES and cortical reorganization mechanisms - especially when fMRI is used to monitor these changes. The aim of this thesis has been to demonstrate the application of FES during fMRI recordings and, much more important, to follow in a long-term setting the cortical and subcortical activation changes in the human brain related to a FES training.

Robot-assisted therapy

Robot-assisted movement therapy is a quite new field in rehabilitation treatment (for review see Prange, et al. 2006; Reinkensmeyer, et al. 2004; Riener, et al. 2005a). It will not replace the human therapist but rather assist him in order to provide the best possible rehabilitation program. Robot-assisted therapy provides good measurements of motor skills (speed, power, direction) whereas manually-assisted movement training lacks the standardization, repeatability and objective measures of performance and progress (Nef, et al. 2007). Robotic therapy generates more measurable results, thus providing a more powerful assessment of its outcome. Moreover, the use of robotics makes a long term automated training more affordable. The rationale of using robots in a rehabilitation therapy is basically the same as for FES: Task-oriented movements can improve performance and can lead to enlarged or more excitable motor output areas (Classen, et al. 1998; Karni, et al. 1995; Liepert, et al. 2000; Liepert, et al. 1998). And as previously mentioned, an additional input from the periphery is beneficial for an ongoing recovery process since a change in neuronal membrane excitability leads to better motor performances (Butefisch, et al. 2004). Furthermore, most robots may function in a passive and patient supporting active mode (e.g. Nef, et al. 2007; Takahashi, et al. 2008).

The list of rehabilitative robots is growing. Well-known devices for the upper extremities are amongst others MIT-MANUS (Hogan, et al. 1995; Krebs, et al. 1998), ARM-Guide (Reinkensmeyer, et al. 1999; Reinkensmeyer, et al. 2000), MIME (Burgar, et al. 2000; Lum, et al. 2002) and ARMin (Nef, et al. 2007). In general, it can be said that rehabilitative robots support ongoing recovery at least equal to conventional therapy (Aisen, et al. 1997; Fasoli, et al. 2004; Kahn, et al. 2006; Lum, et al. 2002; Reinkensmeyer, et al. 1999; Volpe, et al. 2000). But they seem not to be superior, which leads to the question of justifying the use of rehabilitation robotics. Robots can make therapy more efficient because patients can practice

more intensively and thereby allow the therapist to focus more on treatment plan as well as treat more patients at the same time (Riener, et al. 2005a).And as previously stated above, robots provide a better effectiveness criterion (objectiveness, reliability and validity) that substantiates a better analysis of outcome effects. However, outcome analysis has been mostly restricted to behavioral outcome while the underlying biological change has only been assumed. Furthermore, none of these machines are MR-compatible and, therefore, allow no direct monitoring of their effects on the human brain. The development of MR-compatible robotic devices might close this gap. fMRI allows the study of ongoing cortical and subcortical processes related to therapeutic interventions as they evolve over time. Much more importantly, neuroimaging might detect meaningful changes in the brain before behavioral improvement is visible. Thus beforehand, a rehabilitative training might have ceased because no change was observed. With neuroimaging, training might be continued because observed brain activation changes might indicate a behavioral change to appear simply later than expected.

Achieving this goal means to solve several issues that are tightly connected to motor research in an MR scanner. First of all, there is very little space in the scanner tube which prevents execution of every movement performed during rehabilitation sessions. Also, patients are in a supine position instead of sitting during task completion. MR-imaging requires the head to be as motionless as possible; otherwise image artifacts might prevent proper data analysis. These restraints minimize the possible tasks to be performed during an fMRI experiment. However, the fMRI-task should be as similar to a rehabilitative exercise as possible in order to gain insight into the reorganizational processes in the brain which are related to therapeutic intervention (Dobkin 2004). A possible approach is to develop a device with a few degrees of freedom, which limits the task selection. Furthermore, easy tasks predicting the amount of expected head movements and necessary countermeasures (fixation of trunk, head, shoulders, etc.) can be implemented. In a final fMRI experiment, an excerpt out of the rehabilitation program will be performed and conclusions about the effectiveness of therapy can be drawn. As discussed above, drawing conclusions about the recovery process on the basis of a simple motor task performed inside an MR-scanner is a tightrope walk since the whole therapy package is much more complex. However, using a robot inside the scanner might help to understand the effect of robotics in neuro-rehabilitation and allow for better tracking of neuronal changes related to the therapeutic task as well as the other above mentioned reasons as the rationale to develop such a device.

II. Hypothesis

The principles of FES and robotic devices regarding recovery rely on the plastic changes occurring in the brain after an insult independent of the clinical picture: (a) Long term potentiation (Karni, et al. 1995): task-oriented movement can induce plastic changes within the brain which again can improve movement performance (b) Unmasking of latent inhibition (Jacobs and Donoghue 1991): therapy serves to learn new motion strategies and connections become active since the inhibitory process through the affected area has ceased. It might also involve recruitment of neurons not normally devoted to the abolished function. (c) Change of membrane excitability (Butefisch, et al. 2004): sensomotoric feedback facilitates motor learning. rTMS-Studies have shown that higher excitability leads to better motor performances, i.e. practice induces changes in cortical excitability.

The goal of this thesis is to assess the relationship between neural plasticity and rehabilitative therapy. The corresponding hypothesis states that specific rehabilitation induced active and passive movements will lead to changes in the cortical activation patterns and its underlying organization (Rossini, et al. 2003). To achieve this goal, we planned to observe changes within the brain maps of mental activity using neuroimaging techniques (fMRI) and correlate them with behavioral measurement of motor output during and after the specific treatments. Before even addressing the question of FES-related neuroplastic changes, the feasibility of a FES-application within the MR-scanner had to be established. This was the basis for the first study in which two very simple standardized fMRI paradigms were used to evaluate the functionality of FES and its effects on brain activation patterns. The acquired data will be used as a normative database for further FES-application in fMRI studies. After successful implementation of MR-FES, a training study with healthy subjects was conducted. The goal was to test a long-term protocolthat can be used as a reference guide for patient studies.

The third study will test the newly built robotic device within the MR-environment. First a prototype for upper arm rehabilitation providing1 degree of freedom (1 DOF) will be built in order to check for its compatibility for use in the MR-environment. Initially, MR-measurements checking for the safety of the materials used will be conducted. Subsequently, feasibility experiments will be performed using simple motor tasks in healthy subjects. The movements targeted by the robot will be relevant to rehabilitation of essential motor functions (i.e. grasping, reaching etc.). The acquired data will be used as a reference for the further use of the device in patients.

III. Studies

Study 1 – Cortical and Subcortical Correlates of Functional Electrical Stimulation (FES) of Wrist Extensor and Flexor Muscles Revealed by fMRI. Armin Blickenstorfer, Raimund Kleiser, Thierry Keller, Birgit Keisker, Martin Meyer, Robert Riener, Spyros Kollias.

The main scope was to test the feasibility and reliability of FES in a MR-environment. We showed cerebral activation patterns in healthy subjects undergoing fMRI during FES stimulation. Wrist extensor and flexor muscles were stimulated in an alternating pattern while BOLD-fMRI was recorded. Both block and event-related designs were used to demonstrate their feasibility for recording FES activation in the same cortical and subcortical areas. Six out of fifteen subjects repeated the experiment three times within the same session to control intraindividual variance. In both block and event-related design, the analysis revealed an activation pattern comprising the contralateral primary motor cortex, primary somatosensory cortex and premotor cortex; the ipsilateral cerebellum; bilateral secondary somatosensory cortex, the supplementary motor area and anterior cingulate cortex. Within the same subjects we observed a consistent replication of the activation pattern shown in overlapping regions centered on the peak of activation. Similar time course within these regions were demonstrated in the event-related design. Thus, both techniques demonstrated reliable activation of the sensorimotor network and eventually can be used for assessing plastic changes associated with FES rehabilitation treatment.

Author contributions

AB & RK designed the experiment. **AB** recruited the subjects and performed the fMRI measurements. Data analysis was done by **AB** and RK. **AB** wrote the manuscript. TK programmed the FES-stimulation and corrected the FES part of the manuscript. Correction of the manuscript was completed by BK, MM, RR & SK

Study 2 - Effects of a 4-week FES-Training applied to the dominant forearm on brain plasticity and muscle strength. Armin Blickenstorfer, Kai Lutz, Martin Lang, Thierry Keller, Martin Meyer, Birgit Keisker, Robert Riener, Marie-Claude Hepp-Reymond, Spyros Kollias.

Functional electrical stimulation (FES) is used for muscle strengthening in humans and an increase in force has been repeatedly demonstrated following the training. We investigated the effects of FES in the sensorimotor organization of the dominant upper arm in healthy subjects using fMRI. The training consisted of 16 sessions over 4 weeks in which the forearm muscles were electrically stimulated, inducing a grasping movement of the hand against force. An MR-compatible dynamometer was used to record FES induced and voluntary grasp forces during scanning. Maximal voluntary grasp (MVG) was recorded at three time points: a) before and after one FES session before training, b) then weekly during the training period and c) once again following one month of training cessation. After 4 weeks of FES training, a significant force increase during the fMRI experiments was seen for trained subjects and, surprisingly, also for the controls. Assessment after one month of training cessation revealed a significant group difference between the training group, which maintained the force gains, and the controls who returned to their pre-training force level. However, MVG was not affected by the training. Cortical changes were reflected in decreased activations following training and cessation of training while no group differences were found. Possible reasons for the lack of correspondence between the fMRI activation patterns and the observed behavioral gains may be habituation effects and that a mere spinal process is not reflected in fMRI activation maps. The results may provide important insights into cortical and spinal processes relevant to the use of FES in neurorehabilitation.

Author contributions

AB & ML designed the FES training program. **AB** & KL designed the fMRI paradigm. TK programmed the FES stimulation. **AB** & ML recruited the subjects. **AB** performed the fMRI recordings. ML conducted the strength measurements and its consecutive analysis. **AB** analyzed the data of FES recordings during fMRI and the correspondent imaging data. The manuscript was written by **AB**. Its correction was done by KL, TK, BK, MM, RR, SK.

Study 3 - Comparison of MRI-Compatible Mechatronic Systems with Hydrodynamic and Pneumatic Actuation. Ningbo Yu, Christoph Hollnagel, Armin Blickenstorfer, Spyros Kollias, Robert Riener.

The strong magnetic fields and limited space make it challenging to design the actuation for mechatronic systems intended to work in MRI environments. Hydraulic and pneumatic actuators can be made MRI-compatible and arepromising solutions to drive robotic devices inside MRI environments. In this work, two comparable haptic interface devices - one with hydrodynamic and another with pneumatic actuation, - were developed to control one degree of freedom for translational movements by a user performing fMRI tasks. The cylinders were made of MRI-compatible materials. Pressure sensors and control valves were placed far away from the endeffector in the scanner connected via long transmission lines. It was then demonstrated that both manipulandum systems were MRI-compatible and yielded no artifacts to fMRI images in a 3T scanner. Position and impedance controllers achieved passive as well as active subject movements. With the hydrodynamic system, we achieved smoother movements, higher position control accuracy and improved robustness against force disturbances than with the pneumatic system. In contrast, the pneumatic system was back-drivable, showed faster dynamics with relatively low pressure, and allowed force control. Furthermore, it was easier to maintain and did not cause hygienic problems after leakages. In general, pneumatic actuation is more favorable for fast or force-controlled MRI-compatible applications, whereas hydrodynamic actuation is recommended for applications that require higher position accuracy, or slow and smooth movements.

Author contributions

NY designed the manipulandum systems. NY & CH & **AB** recruited the subjects. **AB** designed the fMRI paradigm and analyzed its imaging data. NY wrote the manuscript. CH, **AB**, SK and RR did the corrections.

Study 1

Cortical and Subcortical Correlates of Functional Electrical Stimulation (FES) of Wrist Extensor and Flexor Muscles Revealed by fMRI

Armin Blickenstorfer [1], Raimund Kleiser [1], Thierry Keller [2,3,4], Birgit Keisker [1], Martin Meyer [1], Robert Riener [3,4], Spyros Kollias [1]

[1] Institute of Neuroradiology, University Hospital Zurich, Switzerland

[2] Automatic Control Laboratory, ETH Zurich, Switzerland

[3] Sensory Motor Systems Laboratory, ETH Zurich, Switzerland

[4] Spinal Cord Injury Center, Balgrist University Hospital Zurich, Switzerland

Introduction

Functional electrical stimulation (FES) is a widely applied technique in medical treatment, physical therapy and sports training. Specific applications include treatment of muscle atrophy, build-up of muscle mass, endurance training, pain treatment, as well as functional movement therapy of paralyzed patients after brain or spinal cord injury (SCI) (Mangold & Keller, 2003 & 2004). The principle of FES lies in generating action potentials by short bursts of electrical pulses. The action potentials propagate along axons towards the target muscles resulting in a contraction (Popovic et al., 2001a). Since electrical stimulation activates nerves rather than muscles and the propagation of the electric impulse occurs along the axons, the motor nerves should not be deafferented (Peckham & Knutson, 2005). Possible peripheral mechanisms of FES include a training effect resulting in improved fitness and strength of the remaining motor units, improvement of flexibility and range of motion of affected limbs resulting in voluntary efforts becoming more effective, and reduced spasticity in the affected muscles (Rushton, 2003). FES is preferably applied when the lower motor neurons are excitable and the neuromuscular junctions, as well as the muscles, are intact. This is usually the case in patients with complete and incomplete SCI, stroke, head injuries, cerebral palsy, and multiple sclerosis (Peckham & Knutson, 2005). Several reports have demonstrated that motor training causes cortical reorganization (Karni et al., 1995; Pasqual-Leone et al., 1995; Nudo et al., 1996; Muellbacher et al., 2001) and somatosensory inputs lead to changes in the cortical excitability (Ridding et al., 2000, 2001; Kaelin-Lang et al., 2002). FES uses both somatosensory inputs and passive movements as means to improve motor performances (Uy et al., 2003; Bütefisch et al., 2004). Passive movements are frequently used in medical therapy when the affected limb, due to weakness or disability, cannot be moved voluntarily. Neuroimaging studies demonstrated that passive movements result in cortical reorganization, meaning mere external treatment caused changes in functional brain activations to resemble the ones elicited by active movements (Weiller et al., 1996; Carel et al., 2000; Loubinoux et al., 2001; Lotze et al., 2003). However, Lotze et al. (2003) and a recent study from Kaelin-Lang et al. (2005) found that active training leads to better motor performance and more prominent increases in fMRI activation than passive training. Their findings consolidate the pivotal role of voluntary drive in motor learning and neurorehabilitation.

Functional electrical stimulation merges these training approaches, in that it allows repetitive movements, generates a somatosensory input and can be actively and passively applied. However, the functional brain correlates of FES-elicited movements have yet to be determined.

The main scope of this study was to test the feasibility and reliability of FES in a MR-environment. Should the FES approach be successful, it would provide the means for assessing the central correlates of specific rehabilitation treatment and its effects on cortical organization. To our knowledge, only one study so far applied neuromuscular stimulation on healthy subjects in the fMRI environment (Han et al., 2003). This study reported findings only from three cortical regions of interest: namely primary motor, primary somatosensory and supplementary motor areas. Here we demonstrate the feasibility of performing fMRI during a simple FES-elicited motor task in healthy subjects and report activation patterns from the entire brain. We used a block experimental design, as well as an event-related design, to demonstrate the possible application of FES using two standard fMRI paradigms. We expected to observe identical activated areas elicited with both experimental approaches because the stimulation is thought to produce robust brain activations that do not vary as function of the experimental design. Furthermore, we addressed intra-subject reproducibility by performing repeated measurements in the same subject. Within the context of rehabilitation, it is important to know whether a treatment effect can be differentiated from intra-subject variability or methodological variations.

Methods

Subjects

Fifteen healthy male (n = 7) and female (n = 8) right-handed subjects (mean age 31.27 years, SD 7.85) participated in the study after given informed consent. Handedness was assessed with the Edinburgh Handedness Inventory (Oldfield, 1971), which showed a moderate to strong right-handedness for all subjects (mean 86.6, SD 15.1, range 60 – 100). The experiment was conducted with the approval of the local Ethics Committee.

Stimulation device and parameters

FES was carried out with the portable system “Compex Motion” (Keller, Popovic et al. 2002). The device is a microcontroller-based system with four current-regulated stimulation channels and is controlled with a chip card programmed by custom made software. For the fMRI experiments, only two channels were used. We first ran the same fMRI-protocol (see data acquisition) as with the healthy subjects using a water bottle phantom. Recorded images were objectively evaluated and no obvious artifacts or image distortions were observed. We applied

asymmetric, biphasic, charge balanced rectangular pulse shapes[2]. The depolarizing pulse had four times higher amplitude but was four times shorter than the charge compensating pulse. The depolarizing pulses had a width of 200μs[3] and frequency of 20Hz[4]. The wrist extensor muscles (WEM) and wrist flexor muscles (WFM) were each stimulated by a separate channel with a pair of 50mm × 50mm, "Synapse", self adhesive electrodes (Ambu A/S, Baltorpbakken 13, 2750 Ballerup, Denmark). For the WEM, the depolarizing electrode was placed on the forearm close to the elbow over the m. extensor carpi radialis longus and brevis, m. extensor digitorum communis, m. extensor carpi ulnaris, while the charge removing electrode was placed proximal to the wrist. For the WFM, the AP generating electrode was placed on the forearm distal to the elbow over the motor points of m. brachio-radialis, m. flexor pollicis longus with the charge removing electrode being placed distally under the wrist. The stimulation amplitude of the depolarizing pulse for both WEM and WFM was individually determined by palpation – a standard procedure in the clinical setting. Initially, current amplitude was increased stepwise by 1mA until muscle twitches could be sensed by the examiner, a clear sign of motor activation of the wrist muscles. Then, the stimulation amplitudes used during the experiment were adjusted to 150% of the individual motor threshold amplitude and the stimulation frequency was set to 20 Hz to achieve strong muscle contraction resulting in robust passive movements of the wrist in its range of motion between 50 - 70° for extension and flexion respectively (Fig 1a). However, some subjects felt discomfort and required lower amplitudes that were subsequently reduced. The resulting stimulation current amplitudes were in the range from 9 – 23 mA.

[2] Biphasic pulse forms are believed to be better suited for surface stimulation. The first pulse generates the action potential (AP) and the secondary pulse removes the injected charge from the body (Peckham & Knutson, 2005; Popovic et al., 2001).

[3] By means of short pulses more efferent compared to afferent nerves will be stimulated. Important is the selective stimulation of the relevant muscle groups (Keller & Dewald, 2004)

[4] In order to keep muscle fatigue at minimum and still producing smooth tetanic muscle contractions a pulse repetition frequency range in the range of 20 – 30 Hz is recommended (Keller & Dewald, 2004)

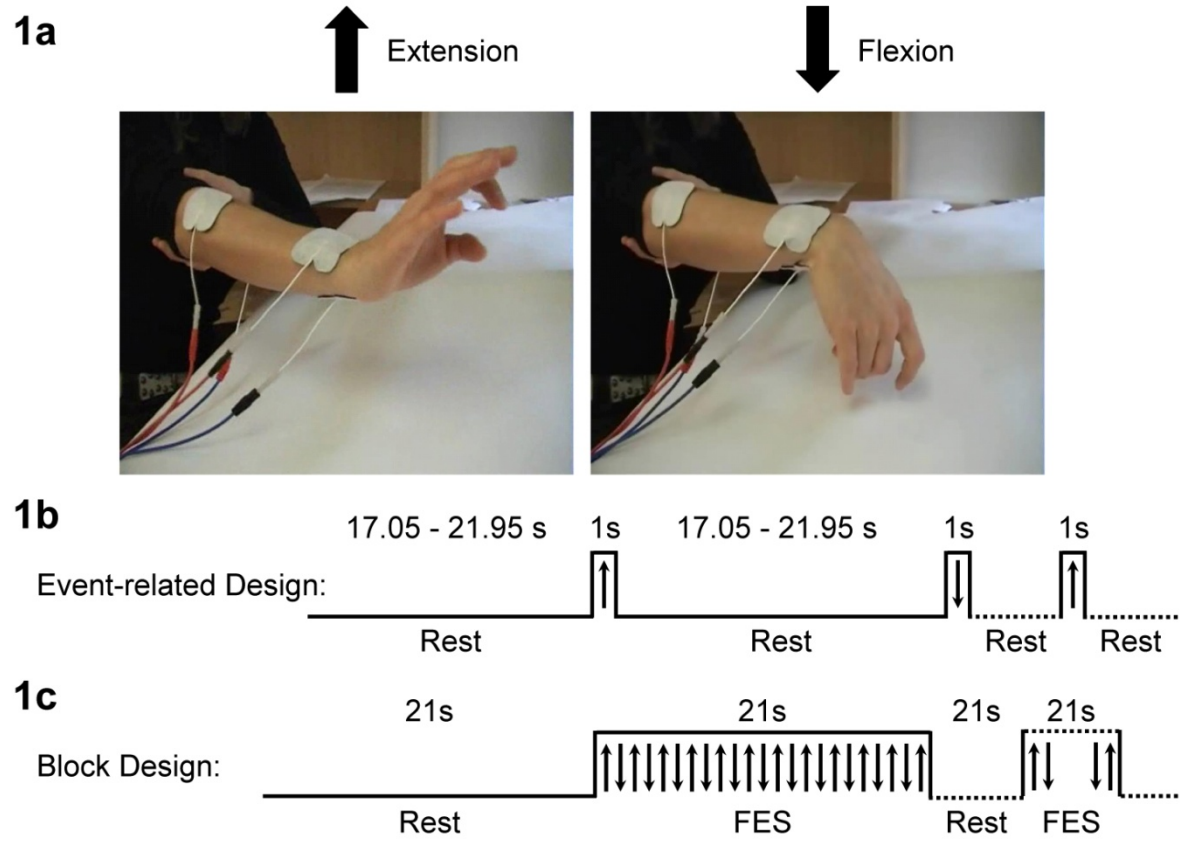

Figure III-1 Experimental paradigm. 1a. Electrode placement and maximal extent of electrically stimulated extension and flexion movement. 1b Event-related design. 22 single extension and flexion movements of each 1 sec duration were electrically elicited in an alternating pattern with an interstimulus interval lasting 17.05 - 21.95 sec. Total duration: 900 sec. 1c. Block design. 6 rest and 6 stimulation blocks each lasting 21 sec. The stimulation condition consisted of a repetitive extension flexion movement, stimulating alternatively WEM and WFM for 1 sec. Total duration: 252sec.

Stimulation induced wrist extension-flexion paradigms

Using a stimulation induced wrist extension-flexion task gives us the possibility to compare the cerebral activation patterns of FES-elicited movements with previous experience (Table 1) using similar motor (Carel et al, 2000; Loubinoux et al., 2001; Curt et al, 2002; Naito et al., 2002; Lotze et al, 2003) and sensory (Del Gratta et al., 2000; Sutherland & Tang, 2006; Arienzo et al., 2006) tasks. We predicted similar activation patterns within the primary and secondary motor and somatosensory areas as well as subcortical regions such as thalamus and cerebellum. Moreover, stimulation of the wrist is widely applied in rehabilitation treatments and is less likely to elicit head movements because these movements are considered an ignorable local event, especially when executed at a slow pace. Subjects were placed in the scanner with their right arm positioned along their body and supported by a pad to allow unobstructed flexion-extension movements of the wrist. The head was fixed with foam cushions in the MR head coil and straps around to torso were used to diminish any additional

movements. Subjects were asked not to perform any voluntary movements of their finger and wrist or contractions of the arm muscles. During the scanning procedure, subjects were told to keep their eyes closed. An event-related experiment was followed by a block experiment in the same imaging session. In the event-related design, an 'event' consisted of a single 1 sec stimulation of either WEM or WFM. In total 22 extension and 22 flexion movements were evoked. The interstimulus interval had a range of 17.05 to 21.95 sec. The event-related design lasted 900 sec (Fig. 1b). The block design consisted of 6 stimulation and 6 rest blocks, starting with the latter. One block lasted 21 sec. Within the stimulation block, the WEM and WFM were each stimulated in an alternating pattern for 1 sec (1 Hz) resulting in 11extension and 10 flexion movements. The block design lasted 252 sec (Fig. 1c).

Table III-1 fMRI Studies investigating a) active and / or passive movement of the wrist and b) the effect of electrical stimulation at the wrist

	Main activation loci to activated/stimulated wrist			
Task	**Contralateral**	**Ipsilateral**	**Bilateral**	**Reference**
a) Active and passive wrist movements	SIMI, SMA, cingulate	Cerebellum	IPL	(Carel, et al. 2000)
Active and passive wrist movements	SIMI, SMA, cingulate		SIMI, PMC, frontal cortex, SPL, IPL, cerebellum	(Loubinoux, et al. 2001)
Active wrist movements	MI, SI, insula, thalamus, putamen		SMA, SII, SPL, dPMC, vPMC, caudal cingulate motor	(Curt, et al. 2002)
Motor imagery of wrist movement and kinesthetic stimulation	SIMI, cingulate motor area, SMA, dPMC, IPS	Cerebellum		(Naito, et al. 2002)
Active and passive wrist movements	MI, SI, SII, thalamus	Cerebellum		(Lotze, et al. 2003)
b) Electric stimulation of median nerve at the wrist	SPL, SI, SMA		SII, PFC, STS	(Del Gratta, et al. 2000)
Electric stimulation of median nerve at the wrist			SI	(Sutherland and Tang 2006)
Electric stimulation of median nerve at the wrist	SI		SII, insula, ACC, SMA	(Arienzo, et al. 2006)

Abbrevations: ACC, anterior cingulate cortex; dPMC, dorsal premotor cortex; IPL, inferior parietal lobule; MI, primary motor area; PFC, prefrontal cortex; SI, primary somatosensory area; SII, secondary somatosenory area; SMA, supplementary motor area; SPL, superior parietal lobule; STS, superior temporal sulcus; vPMC, ventral premotor cortex.

Data acquisition

MRI was performed at 3.0-T MR system (Philips Medical Systems, Eindhoven, The Netherlands) equipped with an 8 channel SENSE™ head coil. For the functional acquisitions a T2* weighted, single-shot, field echo, EPI sequence of the whole brain (TR = 3012msec, TE = 40msec, flip angle = 82°, FOV = 220mm × 220mm, acquisition matrix = 128 × 128, in-plane resolution = 1.7 × 1.7mm, slice thickness = 3mm) with a SENSE factor of 2 was applied to collect signals from 39 contiguous slices. The event-related design consisted of 300 functional scans; the block design of 84 scans. Preceding each functional measurement, five dummy scans were performed in order to achieve magnetic field homogeneity. For testing intra-subject reproducibility, six subjects underwent the sequence (block design, event-related

design) three consecutive times within the same scanning session. Anatomical images of the whole brain were additionally obtained by using a 3D, T1-weighted, field echo sequence (TR = 20ms, TE = 2.3ms, flip angle = 20°, in-plane resolution = 0.9mm × 0.9mm, slice thickness = 0.75 mm, 210 slices).

Data analysis

Image preprocessing and data analysis was performed using BrainVoyager QX 1.7.9® software package (Brain Innovation B.V., Maastricht, The Netherlands). Data preprocessing included 3D motion correction by means of trilinear interpolation, spatial smoothing applying a Gaussian filter of 4mm FWHM, and temporal smoothing including linear trend removal and application of high pass filter with 3 cycles in time course (3 cycles / number of scans × TR). For the event–related design a correction for slice scan-time was performed by sinc interpolation. All images were co-registered to the participant's T1-weighted high-resolution anatomical scan, spatially normalized into standard stereotaxic space (Talairach and Tournoux, 1988). In the single subject analysis the stimulation condition was modeled using a general linear model (GLM) convolved with the standard two gamma haemodynamic response function resulting in t-contrast maps corrected for multiple comparisons with q(FDR) < 0.05 showing the contrast FES vs. rest. FDR has a higher power than Bonferroni correction as the threshold varies automatically across subjects with consequent gain in sensitivity. The parameter q has the advantageous feature of being comparable across studies. The correction accounts for cluster size, i.e. the bigger the cluster the more unlikely are unrandomly activations, hence accounting for less correction (Genovese et al., 2002). Analysis was performed on each subject to identify the network involved in the stimulation condition by comparing the activation with the rest condition. Group analysis was performed using random effects procedure to generalize the data to the population level. Single t-contrast maps were used as input. The data were corrected for serial correlations and multiple comparisons using the most conservative FDR threshold that revealed robust individual activations.

For determining intra-subject variability, a post-hoc region of interest (ROI) approach as described by Bosch (2000) was used. From all areas identified during the group analysis, we defined five functional ROI, namely supplementary motor areas (SMA), primary motor and somatosensory cortex (MI/SI), secondary somatosensory cortex (SII), anterior cingulated cortex (ACC) and cerebellum. These regions were selected according to the literature since

these regions have been reported as principle components of passive training (Weiller et al., 1996; Carel et al., 2000; Loubinoux et al., 2001; Lotze et al., 2003) and in wrist extension-flexion tasks (Carel et al, 2000; Loubinoux et al., 2001; Curt et al, 2002; Naito et al., 2002; Lotze et al, 2003). For each subject and run single t-contrast maps (FES vs. rest) of the whole brain were calculated to obtain the relevant coordinates of the peak of activation in the 5 ROIs. The location of these coordinates within the specified ROIs was verified based on the following anatomical landmarks: SMA was defined from vertex to the cingulate sulcus and from the precentral sulcus posteriorly to the line crossing perpendicular the AC-PC line at the level of the anterior commissure (see Chainay et al., 2004 for details). MI/SI was defined as the anterior and posterior bank of the central sulcus (Kollias et al., 2001) and the hand area as the hook-shaped segment of the central sulcus (Yousry et al 1997). SII comprised the post-central parietal operculum in the upper bank of the lateral sulcus (see Eickhoff et al., 2006 for details). The ACC was defined as the cortex lying within the cingulate sulcus (Fink et al., 1997; Arienzo et al., 2006). For the cerebellar ROI we have chosen Larsell's lobule V and vermal V representing the somatotopic organization of fingers and wrist respectively (Grodd et al., 2001). For each subject and for each ROI we identified three local maxima (i.e. one for each run), resulting in 90 data points. Subsequently, a cube with a side length of 3 voxels was defined with its center at the local maxima resulting in the final ROI.

In case it occurred that a local maximum was localized more than a side length of the cubes we chose the adjacent local maximum which was the closest to the other two centers resulting in three cubes with their centers within the same ROI. Single GLMs were again applied to the newly defined ROIs generating β-values for each run in order to evaluate the reliability across different individuals and experimental sessions. The resulting β-values were used as input for repeated measures ANOVA performed for each ROI separately, with time as a within-subject factor to test whether the haemodynamic responses collected from the three subsequent intra-session runs differ significantly. Furthermore, the approach described by was applied to assess the agreement between the measurements. For each ROI we plotted pair wise the mean of two measurements against the difference of the two measurements, resulting in three plots per ROI (measurement 1 (T1) vs. measurement 2 (T2), T1 vs. T3, T2 vs. T3). As proposed by Bland and Altman (1986) a good agreement is achieved when differences are less than two standard deviations. The reason for choosing an analysis of cubes instead of areas of activated voxels was two-fold: significant activated areas may differ in shape and amount of voxels between different runs in the same subject; voxels located at the border of these areas are close to threshold, which may lead to reduced mean z-values. The data were corrected for

serial correlations and the threshold was set at $p < 0.05$ uncorrected in order to achieve full cubes. No further corrections were applied. For the event-related data, an additional comparison of the corresponding time courses (z-transformed) within the ROI was performed.

Results

The Compex Motion stimulator did not distort the image quality of the functional and anatomical scans as no artifacts were present in any of the images. Furthermore, the subjects did not sense any differences in the intensity of the stimulation before and while scanning. No sensations of burning or other subjective discomfort were reported during the scanning sessions.

Group analysis – Block design

The contrast FES vs. rest condition (Table 2, Fig.2) FDR, $q < 0.03$ elicited activation patterns in MI/SI, intraparietal sulcus and superior parietal lobule contralateral to the stimulated right wrist. Bilateral activations were found in SMA, ACC, SII and ventral premotor cortex (vPMC). Ipsilateral activation was observed in the dorsal premotor (dPMC) cortex and insula. Subcortical regions were also significantly activated including the ipsilateral thalamus and contralateral putamen. Cerebellar activation (denotations after Grodd et al., 2001) was found mainly in ipsilateral Larsell's lobule HV spreading to the anterior vermis (vermal V). Minor contralateral activation was found in Larsell's lobule V.

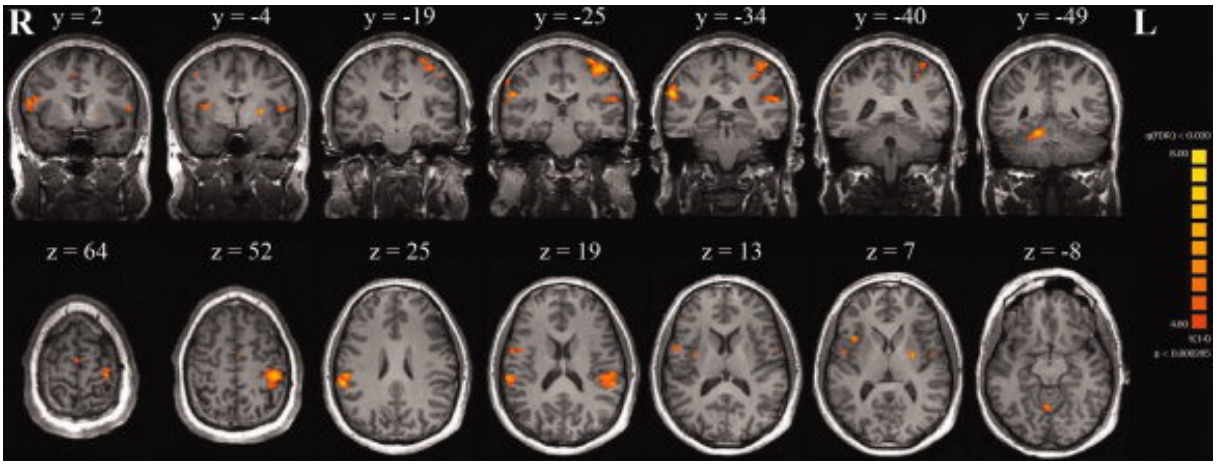

Figure III-2 Block design. Statistically significant activation maps FES vs. Rest (t(14) > 4.79, FDR q < 0.03 corrected). The cluster threshold was set at 10 voxels. Top row: coronar view, anterior-posterior direction; bottom row: transversal view, superior-inferior direction. Convention for lateralization is shown: R, right hemisphere; L, left hemisphere.

Table III-2 Activated brain regions in block design identified by random effect group analysis for all subjects (*N* = 15) [*t*(14) > 4.79, corrected for multiple comparisons FDR < 0.03]

	Functional	Contralateral					Ipsilateral				
Cluster	region	*x*	*y*	*z*	Max *t*	no. voxels	*x*	*y*	*z*	Max *t*	no. voxels
SFG	SMA	−6	−13	64	5.398936	46	3	−10	61	6.107354	88
PrCG,	SI	−42	−28	55	8.243153	4038					
PoCG, IPS	MI	−30	−25	64	6.796949	0					
	IPS	−27	−31	43	5.812412	0					
SPL		−27	−43	58	5.568961	97					
Cingulate	ACC	0	−7	52	5.39774	27	3	2	46	5.308772	17
dPMC							45	−4	46	5.705	59
SMG	SII						57	−28	43	6.629631	186
IPL							33	−46	37	6.016366	20
STG, RO, SMG	SII	−48	−31	22	6.721656	1066	57	−34	25	8.381711	1823
RO	SII						48	−1	7	5.600565	45
vPMC		−51	−4	10	6.041226	219	54	2	16	6.5513	591
Insula	Posterior						39	−1	4	6.360892	151
	Anterior						36	14	7	7.247239	149
IFG							45	35	10	6.317161	148
Putamen		−27	−4	7	8.584658	258					
Thalamus							12	−10	10	5.067441	3
Cerebellum	ant. Cerebellum						12	−49	−17	7.760526	1101
	Vermis	−3	−58	−2	7.132509	289	−21	−61	−20	5.485753	47

Coordinates depict voxel with the highest *t*-value. Abbreviations: ACC, anterior cingulate cortex; dPMC, dorsal premotor cortex; IFG, inferior frontal gyrus; IPS, intraparietal sulcus; MI, primary motor area; PrCG, precentral gyrus; PoCG, postcentral gyrus; RO, rolandic operculum; SFG superior frontal gyrus; SI, primary somatosensory area; SII, secondary somatosenory area; SMA, supplementary motor area; SMG, supramarginal gyrus; SPL, superior parietal lobule; STG, superior temporal lobe; vPMC, ventral premotor cortex.

Group analysis – Event-related design

The activation pattern found in the event-related design during FES was similar to that of the block design (Table 3; Fig. 3) FDR, q < 0.001. However, activation areas contained voxels with higher t-values when compared to those from the block design. During electrical stimulation contralateral activation was present in SI and MI. Bilateral activations were found in several cortical areas including SMA, SII, vPMC, ACC and insula. Activated subcortical regions comprised bilateral thalamus and contralateral putamen. Cerebellar activations were observed in vermal VB and VII, as well as ipsilateral Larsell's lobule V.

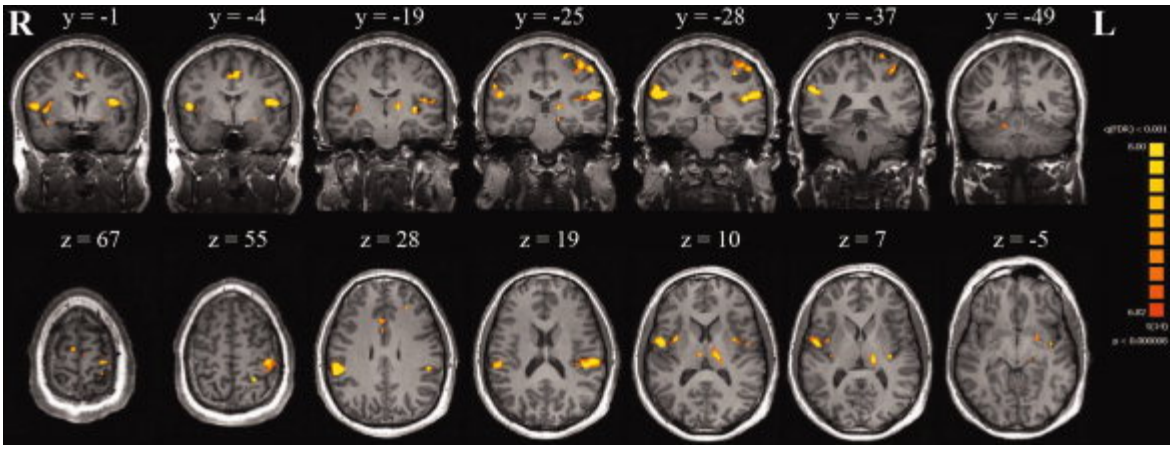

Figure III-3 Event-related design. Statistically significant activation maps FES vs. Rest (*t*(14) > 6.83, FDR <0.001 corrected). Top row: coronar view, anterior-posterior direction; bottom row: transversal view, superior-inferior direction. Convention for lateralization is shown: R, right hemisphere; L, left hemisphere.

Table III-3 Activated brain regions in event-related design identified by random effect group analysis for all subjects (*N* = 15) [*t*(14) > 6.83, corrected for multiple comparisons FDR < 0.001]

		Contralateral					Ipsilateral				
Cluster	Functional region	*x*	*y*	*z*	Max *t*	no. Voxels	*x*	*y*	*z*	Max *t*	no. Voxels
SFG	SMA	−6	−16	67	7.368715	4	9	−10	67	8.271598	53
PCS	SI	−24	−37	64	7.982056	38					
PrCG	MI	−24	−25	67	9.724324	85					
SPL	SI	−24	−46	55	11.44937	242					
PoCG,	SI	−51	−25	52	12.610755	1280					
IPL	SI	−33	−34	46	9.067326	696					
Cingulate	Anterior cingulate						3	17	34	10.221973	735
	Mid cingulate	−3	−4	46	10.554811	320	6	8	40	10.143863	695
		−6	−13	49	8.425615	34					
	Postcingulate	−12	−43	49	7.508058	6					
PoCG, SMG, LS	SII	−51	−25	19	11.711649	1922	54	−34	28	15.149926	2723
PrCG, Insula	vPMC	−42	−4	13	12.71619	871					
Insula		−39	−13	−2	9.505557	341	30	5	13	9.816894	396
							33	−19	7	7.553749	24
PrCG, IFG	vPMC						51	−4	10	11.59573	708
IFG		−48	5	1	9.569894	41					
Thalamus		−15	−22	7	9.832382	464	6	−16	10	8.626976	42
Putamen		−27	−10	7	7.649752	3					
Vermis		0	−58	−5	7.527245	8					
Cerebellum							12	−49	−17	7.529644	55

Coordinates depict voxel with the highest *t*-value. Abbreviations: ACC, anterior cingulate cortex; IPL, inferior parietal lobule; LS, lateral sulcus; MI, primary motor area; PoCG, postcentral gyrus; PrCG, precentral gyrus; SFG superior frontal gyrus; SI, primary somatosensory area; SII, secondary somatosenory area; SMA, supplementary motor area; SMG, supramarginal gyrus; SPL, superior parietal lobule; vPMC, ventral premotor cortex.

Intra-subject variability

Intra-subject variability has been tested in five functional ROIs selected by their consistent activation in both block and event related experiments in all single subjects as well as in the group analysis. Previous studies have shown that these areas are implicated in passive training (Weiller et al., 1996; Carel et al., 2000; Loubinoux et al., 2001; Lotze et al., 2003) and in wrist extension-flexion tasks (Carel et al, 2000; Loubinoux et al., 2001; Curt et al, 2002; Naito et al., 2002; Lotze et al, 2003) They included SMA, MI/SI, SII, ACC and cerebellum.

Our analysis showed a good reproducibility in repeated measurements. ANOVAs for both block and event-related design did not demonstrate a significant effect of time. The assessment of agreement for the repeated measurements within the block and event related designs showed minor differences, which, according to Bland & Altman (1986) were within the limits of agreement (mean difference ± 2 SD). However, two outliers were found: in the context of block design, one participant's difference for T1 vs. T2 slightly exceeded 2SD in SII. In context of event-related approach, one volunteer revealed a difference for T1 vs. T2 that slightly exceeded 2SD in MI/SI. Plots are available as supplementary data. The defined cubes around the peak activations in both block and event-related experiments overlapped, suggesting a reliable quantification of the repeated measurements (Table 4). The analysis of the time courses within the event-related design revealed a good match for each functional run (Fig.4).

Table III-4 Reproducibility of three consecutive measurements for block design and event-related design in six subjects

		Block design			Event-related design		
OI	**Subject**	**x**	**y**	**z**	**x**	**y**	**z**
SMA	BULI	−4.5 ± 6.36	−15 ± 2.12	68.5 ± 2.12	−4 ± 1.73	−16 ± 0.00	64 ± 3.00
	BURO	−7 ± 1.73	−9 ± 1.73	59 ± 6.93	−1 ± 1.73	−10 ± 0.00	62 ± 1.73
	EICH	−6 ± 0.00	−16 ± 0.00	69.5 ± 0.71	−9 ± 3.00	−16 ± 0.00	58 ± 6.00
	PREL	−5 ± 1.73	−16 ± 0.00	61 ± 0.00	−3.3 ± 0.58	−16 ± 0.00	63.7 ± 0.58
	ROST	−3 ± 3.00	−22 ± 3.00	54 ± 4.58	−3 ± 0.00	−22 ± 0.00	51 ± 1.73
	MEZE	0 ± 0.00	−10 ± 0.00	57 ± 1.73	−2 ± 1.73	−11 ± 1.73	60 ± 1.73
MISI	BULI	−39 ± 0.00	−22 ± 0.00	55 ± 0.00	−34 ± 1.73	−28 ± 0.00	61 ± 0.00
	BURO	−32 ± 1.73	−34 ± 0.00	55 ± 0.00	−30 ± 0.58	−34 ± 0.00	55.3 ± 0.58
	EICH	−36 ± 3.00	−24 ± 1.73	49 ± 6.00	−35 ± 1.73	−31 ± 3.00	60 ± 1.73
	PREL	−34 ± 1.73	−37 ± 5.20	62 ± 3.46	−30 ± 0.58	−31 ± 0.58	63.7 ± 0.58
	ROST	−32 ± 6.36	−43 ± 0.00	52 ± 0.00	−37 ± 1.73	−41 ± 1.73	57 ± 1.73
	MEZE	−35 ± 1.73	−28 ± 0.00	44 ± 1.73	−30 ± 0.00	−27 ± 1.73	43 ± 0.00
SII	BULI	−48 ± 4.24	−40 ± 21.21	14.5 ± 10.61	−46 ± 1.15	−25 ± 0.00	19 ± 0.00
	BURO	−53 ± 6.93	−20 ± 12.12	23 ± 1.73	−42 ± 0.00	−19 ± 0.00	22 ± 0.00
	EICH	−47 ± 1.73	−24 ± 3.46	13 ± 0.00	−48 ± 6.00	−32 ± 3.46	22 ± 1.73
	PREL	−54 ± 3.00	−20 ± 1.73	19 ± 0.00	−53 ± 1.73	−19 ± 0.00	19 ± 0.00
	ROST	−51 ± 0.00	−45 ± 1.73	25 ± 0.00	−59 ± 1.73	−30 ± 1.73	21 ± 1.73
	MEZE	−45 ± 3.00	−20 ± 1.73	23 ± 1.73	−48 ± 3.00	−20 ± 1.73	24 ± 1.73
ACC	BULI	−9 ± 0.00	−8.5 ± 6.36	46 ± 0.00	−7 ± 3.46	−10 ± 0.00	46 ± 0.00
	BURO	−11 ± 1.73	−18 ± 6.93	43 ± 5.20	−0.3 ± 0.58	4 ± 1.73	43 ± 0.00
	EICH	−5 ± 1.73	−29 ± 1.73	42 ± 1.73	−3 ± 5.20	−4 ± 3.00	43 ± 3.00
	PREL	−7 ± 4.58	−16 ± 3.00	48 ± 1.73	−4 ± 1.73	−14 ± 1.15	50.7 ± 1.53
	ROST	−7 ± 1.73	−8 ± 1.73	41 ± 1.73	−6 ± 0.00	−17 ± 1.73	43 ± 0.00
	MEZE	−9 ± 0.00	−31 ± 0.00	43 ± 0.00	−3 ± 0.00	−13 ± 0.58	45 ± 1.73
CEREBELLUM	BULI	18 ± 0.00	−46 ± 0.00	−20 ± 0.00	30 ± 0.00	−46 ± 0.00	−20 ± 0.00
	BURO	3.46 ± 0.00	0 ± 0.00	1.73 ± 0.00	4.58 ± 0.00	1.73 ± 0.00	0 ± 0.00
	EICH	12 ± 0.00	−50 ± 1.73	−20 ± 3.00	24 ± 10.82	−39 ± 6.24	−27 ± 4.58
	PREL	16 ± 1.73	−49 ± 3.00	−15 ± 1.73	21 ± 0.00	−49 ± 0.58	−16 ± 1.73
	ROST	6 ± 3.00	−49 ± 7.94	−9 ± 4.58	3 ± 3.00	−60 ± 1.73	−13 ± 1.73
	MEZE	18 ± 3.00	−48 ± 1.73	−17 ± 0.00	3 ± 0.00	−62 ± 1.73	−8 ± 0.00

Mean and standard deviations of individual talairach coordinates per ROI. Abbreviations: ACC, anterior cingulate cortex; MI/SI, primary motor / somatosensory area; SII, secondary somatosenory area; SMA, supplementary motor area.

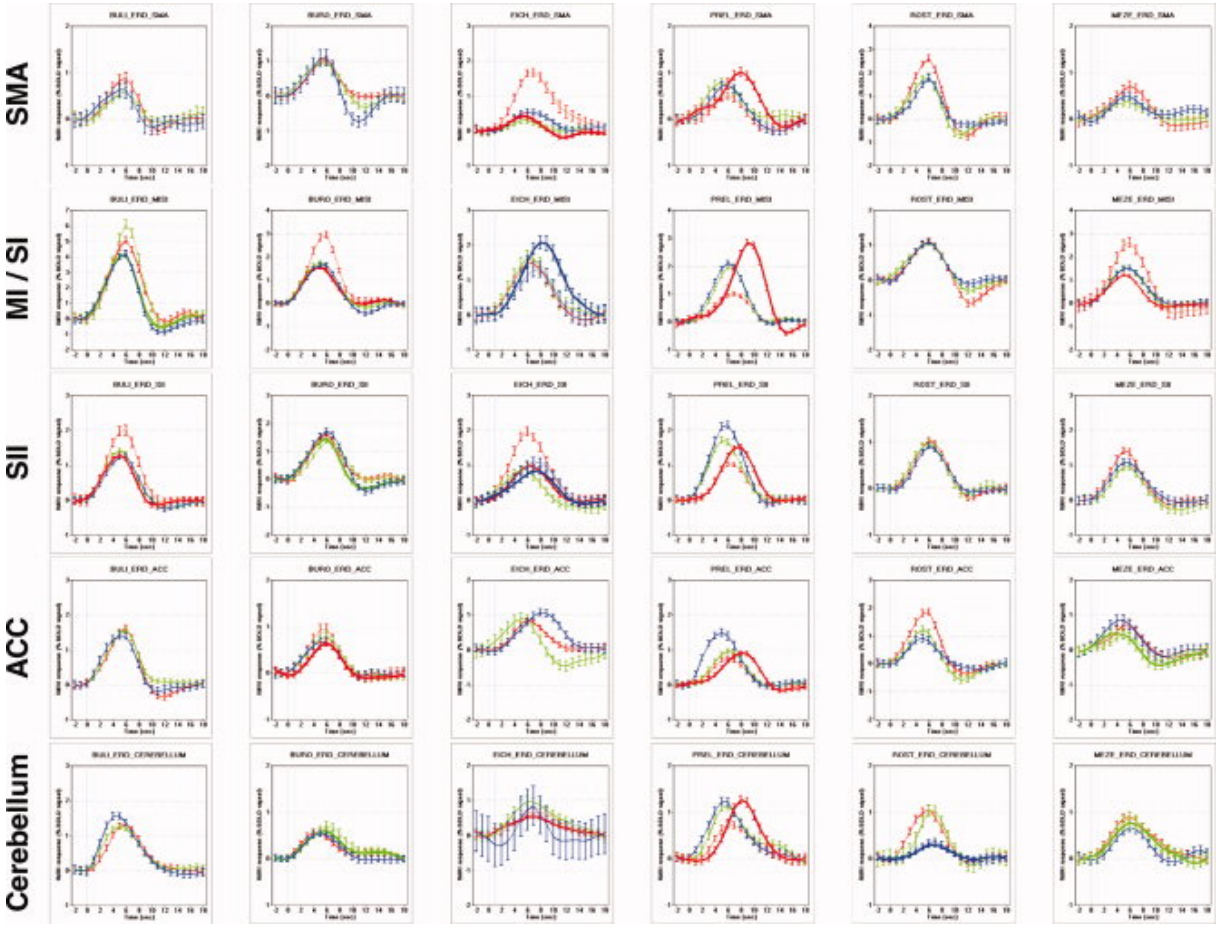

Figure III-4 Individual time courses of six subjects in five ROI in three consecutive runs within event-related design. Color represents order of runs: 1, red; 2, green; 3, blue. Bold curves represent ROIs which have been relocated adjacent to other 2 ROIs (see text for details)

Discussion

The motivation of this study was to show the safe application of FES in the MR-scanner, the comparison of two standard fMRI-paradigms using FES leading to similar cortical activation maps, and the demonstration of reproducibility of repeated measurements. Our results demonstrate that FES can be safely performed in the MR scanner, aiming to investigate the sensorimotor network activated during FES-elicited movements. No image artifacts were evoked and the stimulation was not influenced by the large magnetic field. FES elicited comparable activation patterns in both block and event-related design. Repeated measurements within the same subjects demonstrated overlapping regions of activation and similar time courses in three consecutive runs. Furthermore, ANOVA showed no significant time effect supporting a good intra-subject reproducibility of the results. A good agreement of measurement is achieved when differences lie between the limits of 2SD (Bland & Altman, 1986), as it is demonstrated by our results. Only in two out of 30 instances, minor differences were found slightly above this limit. However, remaining pair wise comparisons in the respective ROIs showed a good agreement leading to our suggestion of reproducibility.

These data indicate that the technique is suitable and may be used in longitudinal patient studies for assessing plastic changes associated with FES rehabilitation treatment.

Cerebral activation patterns of FES-elicited wrist movements

The stimulation induced wrist extension-flexion paradigm used in this study activated motor and somatosensory areas, which are concordant to those found in previous studies using either voluntary movements or sensory stimulations of the wrist (Carel et al., 2000; Loubinoux et al, 2001; Curt et al., 2002; Naito et al., 2002; Lotze et al, 2003). There is only one previous report (Han et al. 2003) on cortical activation patterns using neuromuscular electrical stimulation to elicit wrist extension movements in healthy volunteers. Their analysis was restricted to the MI/SI, PMC and SMA. However, several other cortical and subcortical areas such as, SII, ACC, insula, thalamus, putamen and cerebellum have been shown to activate during passive training (Weiller et al., 1996; Carel et al, 2000; Lotze et al, 2003; Ciccarelli et al., 2005) and have been implicated in functional recovery after rehabilitative therapy in patients with stroke (Johansen-Berg et al., 2002). Therefore, our study reports the effects of FES on the entire primary and secondary motor and somatosensory networks.

Five distinct brain areas, namely MI/SI, SMA, SII, ACC and cerebellum, known to contribute to active and passive motor tasks, showed significant and reproducible activations in our study. Strong activation has been elicited in MI/SI extending to the same degree in both somatosensory and motor areas adjacent to the central sulcus. These areas are closely connected, send efferent inputs to and receive afferent inputs from the distal extremities. Their co-activation was expected considering the nature of our stimulation and the motor output it produced. Activation of the primary motor cortex has been previously observed with passive movements even without electrical stimulation (Weiller et al., 1996; Han et al., 2003; Lotze et al., 2003; Ciccarelli et al., 2005).

In line with previous studies using wrist extension-flexion tasks (Carel et al, 2000; Loubinoux et al., 2001; Curt et al, 2002; Naito et al., 2002; Han et al., 2003) and in keeping with our predictions, we found activations in the SMA contralateral to the stimulated wrist. SMA plays an essential role in learning and initiation of a movement, as well as its execution (Picard & Strick, 1996). However, it is also reasonable that the electrical stimulus also contributed to SMA activation as this region is sensitive to somatosensory input (Picard & Strick, 1996; Del Gratta et al., 2000; Barba et al., 2005; Arienzo et al., 2006).

Bilateral activation within the SII was consistent in all subjects and was related both to the passive motor movement elicited by the FES and the sensory component of the electrical

stimulation. Studies investigating the effect of passive training on cortical plasticity (Carel et al., 2000; Loubinoux et al., 2001; Lotze et al., 2003; Ciccarelli et al., 2005) consistently report bilateral activations in SII. Moreover, several studies using electrical stimulation of the median nerve (Del Gratta et al. 2000; Arienzo et al., 2005; Sutherland & Tang, 2006) or stimulation of the fingers (Deuchert et al., 2002) found bilateral activation in SII. Ferretti et al. (2003), demonstrated a functional segregation of the SII in an anterior and a posterior area. The former was activated during painless and painful galvanic nerve stimulation, while the latter showed activation increase, which was related to the increase of pain. Our findings show a broadly extended activation pattern within SII encompassing both anterior and posterior parts, and despite the non-painful nature of our stimulus, a certain degree of unpleasant feeling may accounted for this observation. Individual attentive processes might also account for the observed activation patterns. Sterr et al. (2007) showed a modulation of SI and SII by attention. Subjects who perceived the stimulus as unpleasant presumably attended more to the stimulus.

Activation of the ACC is more likely attributed to the processing of the electrical stimulus itself rather than the passive movement of the wrist. The previously mentioned reports on passive training do not consistently report activation in cingulate areas. Carel et al. (2000) and Loubinoux et al. (2001) described activation within the cingulum, whereas others did not (Weiller et al., 1996; Lotze et al., 2003; Ciccarelli et al., 2005). However, studies using somatosensory stimulation (Ploghaus et al., 1999; Peyron et al., 1999; Wager et al., 2004; Mohr et al., 2005; Arienzo et al., 2006; Christmann et al., 2007) consistently demonstrate activations in the cingulate cortex.

Activation in cerebellum was mainly ipsilateral. Two main foci were found, one in vermal V and the other in ipsilateral Larsell's lobule V. This finding is in line with the sensorimotor mapping of Grodd et al. (2001). Fingers seem to be localized more lateral, whereas the wrist is somatotopically localized closer to the midline of the cerebellum in vermal V. Extension and flexion of the wrist co-activated also the fingers probably due to electrical stimulation of adjacent finger extension and flexion muscles. This pattern of cerebellar activation is in line with other studies using passive movements (Carel et al., 2000, Loubinoux et al., 2001; Lotze et al., 2003; Ciccarelli et al., 2005). The cerebellum plays an important role in the coordination and fine tuning of motor sequences (Trepel, 1999). A study using electrical stimulation of the lower extremities (Smith et al., 2003), reported that afferent spinocerebellar information from muscle, joint and tactile receptors is important for the preparation and correction of ongoing movement. Takanashi et al. (2003), using also electrical stimulation

demonstrated a similar somatotopical organization within the cerebellum. We conclude that the observed cerebellar activation pattern in our study has been elicited by the passive movement, as well as by the electrical stimulation itself.

Activation of pain network?

As previously mentioned, the stimulation was well tolerated, though not comfortable for all subjects. Two subjects, who were initially willing, eventually did not participate in the study due to uncomfortable sensations related to the electrical stimulation. Despite the non-painful character of the stimulus, activations within SMA and ACC may also be related to these subjective sensations of discomfort. The subjects in our study were lying in the scanner with their eyes closed anticipating the next burst of electrical impulses, which was the only stimulus perceived along the ongoing scanner noise. Arienzo et al. (2006) reported that SMA and ACC may play a role in individual processing of the electric stimulation in that the same stimulus is differently perceived by each subject. Studies investigating pain found activation within the SMA (Arienzo et al., 2006), ACC, insula, prefrontal cortex, thalamus, hippocampal formation and the cerebellum (Ploghaus et al., 1999; Peyron et al., 1999; Wager et al., 2004; Mohr et al., 2005; Arienzo et al., 2006). Moreover, studies investigating the anticipation of pain (Ploghaus et al., 1999; Wager et al., 2004) also reported activation in the same cortical areas.

Experimental design

We used both a block design and an event-related design to record cortical activation patterns. Our goal was not to directly compare these experimental approaches but to evaluate whether both experimental approaches result in activation of the same neuronal networks. In general, a block design shows robust results, has an increased statistical power and its BOLD signal change is relatively large related to baseline (see Amaro & Barker, 2006 for review), but it is also susceptible to habituation and anticipation (Liu et al., 2001). The event-related approach is advantageous in detecting transient changes in the BOLD signal, measuring unpredictable events and depicting the temporal dynamics of response (Rosen et al., 1998; Liu et al., 2001; Amaro & Barker, 2006). The illustrations of event-related time courses (Fig. 4) demonstrate that the haemodynamic response function of different brain regions was different for the same stimulus. This possibility of getting closer insight into the haemodynamic response of activated areas may potentially prove essential for studying recovery of motor functions following spinal cord injury or stroke. In our study, the two designs produced robust

activations of the sensorimotor network, with the event-related design showing activation maps with higher t-values as compared to the blocked design applying the same threshold. This difference may be attributed to habituation and anticipation effects associated with the block design, in that subjects got used to the enduring stimulation, lasting for 21 sec., which was repeated in a fixed order. Although learning processes were not expected to play an important role we cannot rule out that a learning process may have occurred. Even in the context of the passive stimulation used in our experiment, an episodic memory representation of the simple task (frequency, monotonous stimulation etc.) may have been formed in association with the experimental context (MRI, block design) (Loubinoux et al., 2001).which may also account for the decreased activity observed for the block design as compared to the event-related design.

A potential limitation of this study is that one cannot distinguish between the effects of stimulation and the effect of potentially voluntary wrist movement. With respect to the latter, we suggest that in the event-related design voluntary wrist movements can be excluded because the stimulation occurred in a random fashion and lasted only one second.

Despite obvious advantages of using an event related design, in the context of clinical studies, we propose the use of a block design for the following reasons. First, the results obtained from the block design are equivalent in strength to those collected during the event-related design. Second, the duration of the block design is considerably shorter, which makes it more comfortable for patients and increases the feasibility of clinical studies. Third, event-related designs have a lower statistical power compared to block designs as the ratio of task period to rest period is smaller (MacIntosh et al., 2004). Lastly, the block fMRI design is more similar to the real therapeutic use of FES, which is also applied in blocks of stimulation.

Reproducibility

Reproducibility was tested in six subjects undergoing the experiment three times within the same session. Intrasubject variability of local peak maxima and time courses within the predefined ROIs was ignorable as subjects showed robust activations within the previously discussed somatosensory network in both block and event-related design. Size and location of activation maps varied moderately across individuals. Similar findings have been reported in fMRI studies investigating the reproducibility of motor tasks (Tegeler et al., 1999, Loubinoux et al., 2001; Havel et al., 2006) and somatosensory stimulations (Kong et al., 2007) pointing out functional anatomic variations or different cognitive strategies. Yoo et al. (2005), using a sequential finger tapping task, demonstrated that intra-session recordings yielded slightly

better reproducibility measures as compared to ones obtained in other seven sessions, which were approximately eight weeks apart. In our study, long-term reproducibility was not tested but nevertheless, similar to what has been observed in previous studies, intrasession short-term reproducibility was high despite of minor variations in regional activations. Thus, we conclude that FES fMRI should be a reliable means for assessing plastic changes within the cortical areas related to rehabilitative therapy.

*Monitoring reh*ab*ilitation*

Several studies emphasize the beneficial effects of FES in a combined motor therapy (Chae & Yu, 1999; Barbeau et al., 2002; Rushton, 2003). The initial FES-therapy starts with a strengthening program followed by the functional training (Popovic et al., 2001). We demonstrated that fMRI experiments during FES are feasible and can be potentially applied to track rehabilitation induced recovery over time. Training related behavioral gains can be correlated with fMRI patterns in cortical activation to provide insight on plastic changes related to the specific rehabilitation treatment over time. So far there have been only few studies relating changes of the sensorimotor network over the course of a specific rehabilitation therapy (Liepert et al., 2000; Binkofski et al, 2001; Johansen-Berg et al., 2002; Dobkin et al., 2004; Winchester et al., 2005; Hamzei et al., 2006). The Compex Motion stimulator used in our study, emphasizes the practice of a simple functional movement, such as wrist extension-flexion, relevant to daily activities that can also be practiced within the fMRI environment to follow cortical changes related to functional gains. This approach, in combination with behavioral outcome measures, should be able to monitor with adequate sensitivity the progress of the patient (Dobkin, 2003).

Acknowledgments
We wish to thank Dr. Lars Michels (University Hospital Zurich) and Armin Heinecke (Brain Innovation B.V., The Netherlands) for their support on the statistical analysis with BrainVoyager software. This work was supported by the Swiss National Science Foundation grant, NCCR on “Neural Plasticity and Repair”.

Study 2

Effects of a 4-week FES-Training applied to the dominant forearm on brain plasticity and muscle strength

Armin Blickenstorfer [1,4], Kai. Lutz [2], Martin Lang [3,5,7], Thierry Keller [3,5,6], Martin Meyer [1,2], Birgit Keisker [1], Robert Riener [4,5], Marie-Claude Hepp-Reymond [8], Spyros. Kollias [1]

[1] Institute of Neuroradiology, University Hospital Zurich, Switzerland

[2] Department of Neuropsychology, University of Zurich

[3] Automatic Control Laboratory, ETH Zurich, Switzerland

[4] Sensory Motor Systems Lab, ETH Zurich, Switzerland

[5] Spinal Cord Injury Center, Balgrist University Hospital Zurich, Switzerland

[6] Biorobotics Department, Fatronik-Tecnalia, San Sebastián, Spain

[7] Institute of Human Movement Sciences and Sport, ETH Zurich, Switzerland

[8] Institute of Neuroinformatics, University and ETH Zurich, Switzerland

Introduction

Functional electrical stimulation (FES) is a widely applied technique in medical treatment, physical therapy and sports training. Sequences of short bursts of electrical pulses are applied through a pair of either transcutaneous, percutaneous or implanted electrodes, eliciting action potentials in motor nerves and thus leading to a contraction of the targeted muscles. Specific applications include treatment of muscle atrophy, build-up of muscle mass, endurance training, pain treatment, as well as functional movement therapy of patients suffering from paralysis after brain or spinal cord injury (SCI) (Mangold & Keller, 2003 & 2004). Possible peripheral mechanisms of FES include a training effect that results in improved fitness and strength of the remaining motor units, improvement of flexibility and range of motion of affected limbs increasing the effectiveness of voluntary efforts, and reduced spasticity in the affected muscles (Rushton 2003). The resulting increased muscle strength following long-term FES has been demonstrated in healthy subjects (Cannon and Cafarelli 1987; Gondin, et al. 2006a; Gondin, et al. 2005; Gondin, et al. 2006b; Hortobagyi, et al. 1999; Maffiuletti, et al. 2000; Maffiuletti, et al. 2002b), as well as in patient groups (Gordon and Mao 1994; Kowalczewski, et al. 2007; Shimada, et al. 2003). Two recent reviews focus on the application of FES as neuroprostheses in various patient groups (Peckham and Knutson 2005b; Sheffler and Chae 2007). FES uses both somatosensory inputs and passive movements as means to improve motor performances (Butefisch, et al. 2004; Uy, et al. 2003). Passive movements are used in medical therapy when the affected limb, due to weakness or disability, cannot move voluntarily.

Neuroimaging studies demonstrated that treatment with passive movements results in cortical reorganization by activating a brain network similar to the one elicited by active movements (Carel, et al. 2000; Lotze, et al. 2003; Loubinoux, et al. 2001; Weiller, et al. 1996). However, Lotze, et al. (2003) and a more recent study (Kaelin-Lang, et al. 2005) found that active training leads to better motor performance and more prominent increases in fMRI activation than passive training. Their findings consolidate the pivotal role of voluntary drive in motor learning and neurorehabilitation. Functional electrical stimulation merges these training approaches in that it allows repetitive movements, generates a somatosensory input and can be actively and passively applied.

Several reports have demonstrated that motor training causes cortical reorganization (Karni, et al. 1995; Muellbacher, et al. 2001; Nudo, et al. 1996; Pascual-Leone, et al. 1995) and somatosensory inputs lead to changes in the cortical excitability (Kaelin-Lang, et al. 2002; Ridding, et al. 2000; Ridding, et al. 2001). It is known that extensive practice over years as in

musicians can induce a reorganization of the motor network leading to different brain activation patterns when compared to untrained subjects (Jancke, et al. 2006; Koeneke, et al. 2004; Munte, et al. 2002). However, only few studies investigated the effect of a long-term motor training in the course of one study. Karni, et al. (1995) trained subjects on finger sequence movements for four weeks and found enlarged activation in primary motor cortex (MI). Floyer-Lea & Matthews (2005) used a task in which subjects were asked to track a continuous sequence by pressing a force sensor with their dominant hand. After 3 weeks of training, increases of activity were found in left primary motor and somatosensory cortex (MI/SI) and right putamen. Meister, et al.(2005) used movement sequences on a keyboard to find that the caudal part of dorsal premotor cortex (PMCd) and the supplementary motor area (SMA) were associated with long-term motor training, whereas MI did not show any changes related to the practice. Investigating the effect of practicing moving sequences with the left hand, Lehéricy, et al. (2005) demonstrated an activation decrease in a rostrodorsal area and an increase in a more caudoventral area of the putamen, suggesting a storage of motor skills in the sensorimotor territory of the basal ganglia.

So far, the relationship between FES and cortical activation pattern has not yet been thoroughly investigated. In a previous study (Blickenstorfer, et al. 2008), we successfully applied FES in a MR-scanner, eliciting reproducible brain activations in the sensorimotor network using a block- and event-related fMRI stimulation design. Smith, et al. (2003) demonstrated a dose-response relationship between the intensity of neuromuscular electrical stimulation (NMES) and the amplitude of activities as well as the volumes of activation in MI, SI, cingulate gyrus, thalamus and the cerebellum. Barsi, et al. (2008) evaluated cortical excitability by analyzing the relationship between TMS intensity and MEPs after subjects had a 20-minute FES session of finger flexor and extensor muscles. Their results indicated that a combination of voluntary effort and FES has greater potential to induce plasticity in the motor cortex and might be a more effective approach for rehabilitation than FES or repetitive voluntary training alone. However, the effect of long-term FES on human brain activation has not been investigated yet.

The main scope of this study was to assess the impact of a 4-week FES training on force output and its respective correlates on cerebral activation patterns. According to studies investigating the effect of long-term FES (Cannon and Cafarelli 1987; Gondin, et al. 2006a; Gondin, et al. 2005; Gondin, et al. 2006b; Hortobagyi, et al. 1999; Maffiuletti, et al. 2000; Maffiuletti, et al. 2002b), we expected that four weeks training with FES would lead to an increased force output and changes in the activation pattern of the sensorimotor system. To

investigate the effects related to training per se, the stimulation parameters during the entire time were kept constant to prevent cortical activity, which might be related to increase of stimulus intensity (Ferretti, et al. 2003; Smith, et al. 2003). According to Gondin, et al. (2005; 2006a,b), neural adaptations to the stimulation should become apparent after 4 weeks of FES – at least on the muscular level – and should be preserved for a longer period without training. According to previous neuroimaging reports on motor training (Debaere, et al. 2004; Floyer-Lea and Matthews 2005; Karni, et al. 1995; Petersen, et al. 1998), we expected increased activations following training, which persist over a period with no training, predominantly in the sensorimotor network including the contralateral primary sensorimotor cortex, cingulate motor cortex, cerebellum and basal ganglia. Kelly and Garavan (2005) propose in their review "that in sensory and motor tasks, which involve topographical representations, a primary outcome of practice is an extended representation within primary motor cortex resulting from increased connectivity within that area. This practice related change is associated with specific mechanisms of synaptic plasticity, primarily modifications in horizontal connections and is observed as increase in activation or an expansion in the area of activation." Alternatively, we could not exclude the possibility that training might lead to decreased activations in specific areas as a result of increased neural efficiency, i.e. decreased activations represent a concentration on stimulus processing (Poldrack 2000). Along this line, Koeneke, et al. (2004) used a complex finger movement task to demonstrate that musicians showed less cerebellar activations to matched controls, reflecting less neuronal recruitment for achieving the same behavioral response.

Methods

Subjects

Twenty healthy right handed male (n = 8) and female (n = 12) subjects (mean age 25 years, SD 2.15) participated in the study after given informed consent. Handedness was assessed with the Edinburgh Handedness Inventory (Oldfield 1971). The experiment was conducted with the approval of the local Ethics Committee of the University of Zurich.

Experimental schedule

Subjects were randomly assigned to either training (TRAIN, n = 10, 6 fem.) or control group (CTRL, n = 10, 6 fem.). Both groups underwent a baseline assessment (PRE, week 0) including fMRI and force and fatigue measurements (see Force measurement sessions below).

TRAIN completed four weeks of FES-training and four measurements sessions (weeks 1 – 4), whereas CTRL only attended four weekly measurements sessions without FES training. After 4 weeks, both groups underwent a second fMRI session (POST, week 4). Subsequently, both groups underwent fMRI and measurements sessions at the eighth week, following four weeks without any training (FOLLOW-UP, week 8).

Stimulation Device and Parameters

FES was carried out with the portable system "Compex Motion" (Keller, et al. 2002). The device is a microcontroller-based system with four current-regulated stimulation channels, which can be triggered using external signals. It is controlled with a chip card programmed by custom made software. We applied asymmetric, biphasic, charge balanced, rectangular pulse shapes[5]. The depolarizing pulse had four times higher amplitude but was four times shorter than the charge compensating pulse. The depolarizing pulses had a width of 180 μs[6] and frequency of 25Hz[7]. In order to grasp an object with optimal strength, the wrist must be extended by approx. 30° while keeping ulnar deviation at 0° (Fong and Ng 2001). Therefore, we stimulated both wrist extensor (WEM) and finger flexor muscles (FFM) by a separate channel with a pair of 50 mm × 50 mm, „Synapse", self-adhesive electrodes (Ambu A/S, Baltorpbakken 13, 2750 Ballerup, Denmark) resulting in a co-contraction. For the WEM, the depolarizing electrode was placed on the forearm close to the elbow over the m. extensor carpi radialis longus and brevis and m. extensor carpi ulnaris, while the charge removing electrode was placed proximal to the wrist. For the FFM, the AP generating electrode was placed on the forearm distal to the elbow over the motor points of m. flexor digitorum superficialis and m. flexor digitorum profundus with the charge removing electrode being placed distally. In order to assure same electrode placement throughout the experiment, locations of depolarizing electrodes were marked on the skin with a permanent marker. Determination of stimulation amplitudes was the same procedure for the fMRI paradigm and for the training sessions. However, for the fMRI experiment, subjects had to lie on a bench with their right forearm flexed at circa 90° on their abdomen; whereas for the training sessions, subjects were sitting with their right forearm flexed at 90° along the body. Different

[5] Biphasic pulse forms are believed to be better suited for surface stimulation. The first pulse generates the action potential (AP) and the secondary pulse removes the injected charge from the body (Peckham and Knutson, 2005; Popovic et al., 2001).

[6] By means of short pulses more efferent compared to afferent nerves will be stimulated. Important is the selective stimulation of the relevant muscle groups (Keller and Dewald, 2004)

[7] To keep muscle fatigue at minimum and still producing smooth tetanic muscle contractions a pulse repetition frequency in the range of 20-30 Hz is recommended (Keller and Dewald, 2004)

positioning caused slightly different amplitude settings for fMRI and training sessions (see below). For the fMRI experiment (FES condition), stimulation amplitudes of the depolarizing pulse for both WEM and FFM were individually determined by increasing the current stepwise by 1mA until subjects reported any discomfort. The individual amplitudes were retained throughout the experiment. Preliminary trials testing the fMRI setup showed that FES-induced contraction of WEM caused also finger extensions resulting in losing the grip of the dynamometer (see fMRI-Paradigm). Therefore, stimulation amplitudes were reduced to the value just below evoking finger extensions. The resulting stimulation current amplitudes were in the range from 12 – 30 mA (mean 18.05, 4.83 SD) for WEM and 15 – 42 mA (mean 32.25, 6.63 SD) for FFM. For the sensory condition within the fMRI experiment, stimulation amplitudes for both WEM and FFM were set at the individual sensory threshold i.e. current amplitude was increased stepwise by 1mA until subjects reported the sensation of the stimulation. The resulting stimulation current amplitudes were in the range from 5 – 14 mA (mean 7.15, 1.95 SD) for WEM and 5 - 8 mA (mean 6.15, 0.93 SD) for FFM. For the training sessions resulting stimulation current amplitudes were in the range from 17 – 32mA (mean 24.2, 4.32 SD) for WEM and 15 – 40 mA (mean 33.35, SD 6.3) for FFM.

fMRI-Paradigm

An event-related fMRI paradigm included three conditions (events): FES (stimulation induced finger flexion), VOL (voluntary finger flexion), SENS (sensory stimulation with no muscular contraction). Each condition lasted 4 seconds. The order of conditions was fixed: FES – VOL – SENS with an interstimulus interval (ISI) jittered between 12 – 15 sec. This sequence was repeated 24 times and lasted 22 min. The stimulator was programmed to stimulate WEM on channel 1 and FFM on channel 2. Figure 5 shows the course of one stimulation cycle. WEM-stimulation was followed by FFM-stimulation after a 1 sec delay and both channels were simultaneously stopped after 4 sec. Both stimulations included a 0.5 sec ramp up at the beginning and 0.5 sec ramp down at the end.

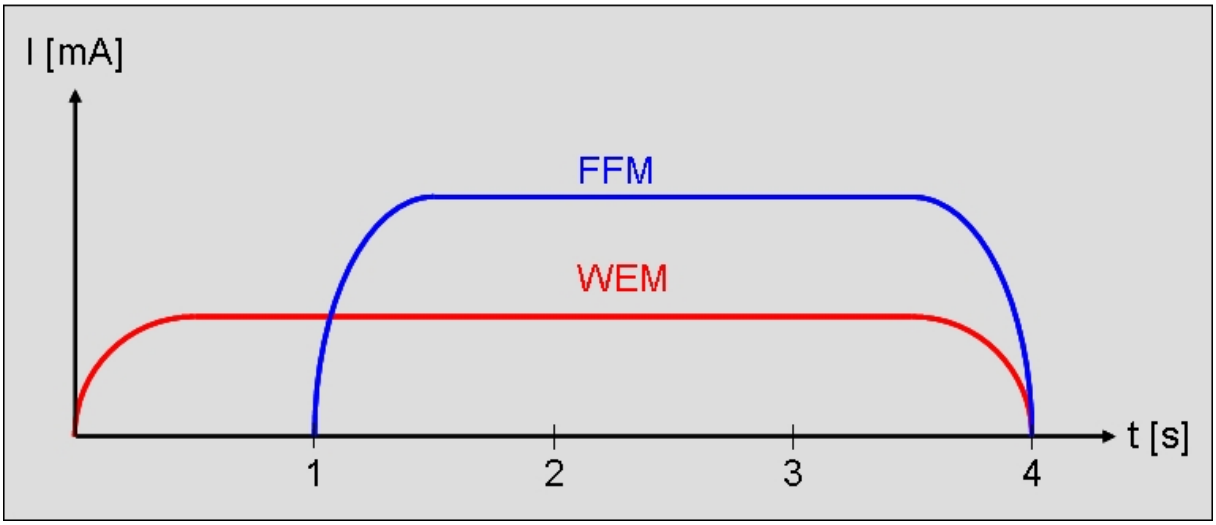

Figure III-5 Stimulation scheme of FES during fMRI experiment. FFM, Finger Flexor Muscles; WEM, Wrist Extensor Muscles

A custom made MR-compatible isometric dynamometer developed by the Sensory-Motor Systems Laboratory of the ETH Zurich (http://www.mrsensor.ethz.ch / Fig. 6) was used to record the applied forces of finger flexion. It is based on the optical force measurement principle and consists of a plastic handgrip containing optical fibers that transmit laser signals to an interface box, which produces analogue and digital force outputs. The measured signal is a linear function of the applied force. Multi-point calibration in the processing unit ensures good linearity and accuracy of the force sensor. The dynamometer was calibrated for each subject.

Figure III-6 MR compatible dynamometer

Subjects performed the tasks with visual feedback. A beamer projected the visual stimuli to a screen which was seen by the subjects through a double mirror mounted on the head coil. The

visual feedback consisted of two parallel vertical bars. In the FES-condition, electrical induced finger closing generated a force that led to a simultaneous increase of both bars to the maximal induced force. Within the VOL condition the left bar was set at the level of the previous FES condition. Subjects had to press the dynamometer until the right bar matched the left one and were instructed to keep on pressing at the same force level until visual feedback disappeared. During the SENS condition, subjects were stimulated at their sensory threshold and were instructed to watch their previous performance from VOL without applying any force to the dynamometer. Visual stimuli presentation and force recording (60Hz sampling rate) were executed with commercial experimental software (Presentation, Version 11.0 build 05.21.07, Neurobehavioral Systems, Albany, CA, USA). Subjects were placed in the scanner with their right arm positioned at a 90° angle on top of their abdomen holding the dynamometer. The head was fixed with foam cushions in the MR head coil to diminish any additional movements. Subjects were asked not to perform any voluntary movements with their fingers and wrist except during VOL.

Force measurement sessions

Assessment of maximal voluntary force was part of a study investigating the effects of FES to muscle fatigue (Lang 2008) and details of the experimental setup are described there. As described above, all subjects participated in the force measurements sessions; prior to the experiment, weekly during the training phase (4 weeks) and once after the four weeks detraining phase. This led to a total of six assessments. The force measurement sessions took place on different days than the fMRI recordings. Each session included the following sequences: maximal voluntary grasp force measurement (MVG), maximum stimulated grasp force measurement (MSG), measurement of single isometric finger force (SIFF), one training session (fatiguing task), a MSG and MVG in fatigued condition, i.e. after training. Both MVG and MSG were assessed with a standard handheld hydraulic dynamometer from Jamar, model 5030J1 (Sammons Prestion Rolyan, Chicago, Illinois, USA). During these tasks, subjects stood upright, the shoulder adducted in a neutral position and the elbow flexed in 90 degrees. The handle was adjusted to the most convenient grip for individual hand size. A MSG stimulation cycle lasted 6 sec. starting with stimulation of the wrist extensor muscles including a 0.5 sec ramp up at the beginning and a 0.5 sec ramp down at the end of the cycle. Stimulation of the wrist flexion muscles was started one sec later and stopped after 4 sec (incl. 0.5 sec ramp up at the beginning and ramp down at the end), while WEM-stimulation continued for one sec. Assessment of single isometric finger forces (SIFF) and wrist torques

was measured with a grasp and wrist assessment system (GAWAS)(Lawrence, et al. 2008). The elbow was held in a 90° angle and the wrist was firmly tightened into a cast. The single fingers were mounted onto load cells that detected the generated forces. Only MVG results will be presented and discussed; results from muscle fatiguing are reported elsewhere (Lang 2008).

Training

TRAIN-Subjects were instructed to sit comfortably, place the electrodes themselves on the spots marked on their forearms, start the stimulator and grab an object to hold on to (e.g. a plastic bottle). The stimulator was programmed as described above (Fig. 5). During WEM-stimulation (6 sec. duration), FFM-stimulation started after 1 sec delay and seized after 4 sec. ISI was set at 15 sec. One stimulation cycle was repeated 86 times (apx. 30 min duration). Training was performed 4 times per week for 4 weeks, within the premises of the institute in order to monitor the training sessions.

MR Data Acquisition

MRI was performed with a 3.0-T MR system (Philips Medical Systems, Eindhoven, The Netherlands), equipped with an 8 channel SENSETM head coil. For the functional acquisitions, a T2* weighted, single-shot, field echo, EPI sequence of the whole brain (TR = 3 sec, TE = 40 ms, flip angle = 82°, FOV = 220 mm × 220 mm, acquisition matrix = 128 × 128, in-plane resolution = 1.7 × 1.7 mm, slice thickness = 3 mm) with a SENSE factor of 2 was applied (Pruessmann, et al. 1999) to collect signals from 39 contiguous slices. 440 functional scans were recorded whereas the first three scans were discarded in order to achieve magnetic field homogeneity. Anatomical images of the whole brain were additionally obtained by using a 3D, T1-weighted, field echo sequence (TR = 20 ms, TE = 2.3 ms, flip angle = 20°, in-plane resolution = 0.9 mm ×0.9 mm, slice thickness = 0.75 mm, 210 slices).

Data Analysis

Force measurements

Data analysis was performed using the statistical software package SPSS (Version 15.0 for PC). To assess individual motor performances, each corresponding sample point was condition-wise plotted resulting in 3 × 24 single force curves (FES, VOL, SENS). Force curves (trials) were individually checked for errors (e.g. if subjects did not press the dynamometer during VOL) in which case, errors were discarded from subsequent analysis.

Curves of each condition were averaged resulting in a single mean force curve of FES and VOL (SENSE was not included in further analysis as this condition was mainly used for control purposes). Maximal values of these curves were used as parameters for group statistics. First, a group-wise explorative screening was used to identify outliers[8]. An ANOVA with repeated measurements was employed to investigate training effects of FES and MVG separately (within-group factor "time", 3 levels: PRE, POST, FOLLOW-UP) and group differences (in-between group factor "group", 2 levels). Differences, $p < 0.05$ were considered significant. Post-hoc tests included paired samples t-tests ($p < 0.05$, one sided) assessing training, and independent t-tests ($p < 0.05$, one sided) testing for group differences.

fMRI

Image preprocessing and data analysis were performed using statistical parametric mapping (SPM5, www.fil.ion.ucl.ac.uk/spm). All images were realigned to the first volume, corrected for motion artifacts, normalized (2 mm × 2 mm × 2 mm) into standard stereotaxic space (EPI-template provided by the Montreal Neurological Institute) and smoothed using a 6 mm full-width-at-half-maximum Gaussian kernel. Activated voxels were identified by the "General Linear Model" approach. Trials that were identified as errors (see force measurements above) were defined as 4th repressor - of no further interest. At the first level of analysis, a statistical model for each subject and each session was computed, applying a box-car model, convolved with a standard hemodynamic response set and eliminating low-frequency noise. Linear contrasts were employed for each subject and condition (Friston, et al. 1994), in which realignment parameters where used as repressors of no interest. The resulting set of voxel values for each contrast yields a statistical parametric map of the t-statistic [SPM(T)]. The following contrasts have been calculated for each subject over all three sessions and were tested for significance ($p > 0.05_{FWE\text{-}cor}$, corrected for multiple comparisons using Gaussian random field theory (Worsley, et al. 1996)): FES vs. baseline (FES1, FES2, FES3) and VOL vs. baseline (VOL1, VOL2, VOL3). Furthermore, contrasts of FES vs. VOL and VOL vs. FES for all subjects and sessions were computed. Second level analysis encompassed a group analysis (single t-test) for all subjects for the first session (FES1_ALL and VOL1_ALL) comparing activation vs. baseline ($p > 0.05_{FWE\text{-}cor}$). Additionally, t-maps depicting differences between these conditions were computed (FES1-VOL1_ALL and VOL1-FES1_ALL). Based on results from the MR force recordings, we calculated paired t-tests - investigating a training effect in both directions for all subjects for the first and second session (FES1-FES2_ALL and

[8] Distance of outliers to the median is more than 1.5 × interquartile range.

FES2-FES1_ALL; likewise for VOL). Within-group contrasts testing for the training effects of FES and VOL were calculated for both groups (TRAIN and CTRL) using paired t-tests (FES2-FES1, FES3- FES1, FES3-2; likewise for VOL). Between-group contrasts were calculated testing for group differences in FES and VOL over all three sessions between TRAIN and CTRL using two-sample t-tests. In case of voxel activations failing to reach significance level of $p < 0.05_{FWE\text{-}cor}$, we used a cluster level of $p < 0.05_{cor}$ (Poline, et al. 1997) to check whether there were clusters of significant activations at the chosen threshold.

Results

Force measurements during fMRI

Subjects did not report any difficulties executing the task. Table 5 shows the descriptive statistics of FES and VOL of both groups over all sessions revealing outliers (Fig. 7a) in TRAIN: FES1 (subject 6; 60.5N) and FES3 (8; 113.8N), VOL1 (6; 61.13N) and VOL3 (8; 116.06N), as well as in CTRL: FES1 (20, 49.41N). Repeated measurements ANVOVA for FES revealed a trend towards a main effect of time ($F_{2,17} = 2.679$, $p = .097$) while interaction time × group was not significant ($F_{2,17} = 1.405$, $p = .272$). Groups did not differ significantly ($F = 1.352$, $p < .26$). Repeated measurements ANOVA for VOL revealed a trend towards main effect of time ($F_{2,17} = 3.245$, $p = .064$), while interaction time × group was not significant ($F_{2,17} = 1.289$, $p = .301$). The two groups did not differ significantly ($F = 1.25$, $p < .278$) although the interaction diagram (Fig. 7b) shows a clear difference in FOLLOW-UP. Pair-wise comparisons of time demonstrated a significant force increase from PRE (FES: 34.98N (mean) ± 9.27 (SD), VOL: 35.84 ± 9.36) to POST (44.40N ± 18.97; 46.16 ± 19.09) for all subjects for FES ($t_{17} = -2.42$, $p = .026$) and for VOL ($t_{17} = -2.658$, $p = .016$) respectively. Analysis within each group using directed (1-tailed) paired t-tests, revealed in TRAIN an almost significant force increase ($t_9 = -1.821$, $p = .051$) from FES1 (35.81 ± 11.02) to FES2 (45.08 ± 22.68), whereas VOL1 (36.54 ± 11.11) vs. VOL2 (46.90 ± 22.97) were significantly different ($t_9 = -1.994$, $p = .039$). Comparison of FES1 (35.81 ± 11.02) vs. FES3 (49.04 ± 25.34) and VOL1 (36.54 ± 11.11) vs. VOL3 (50.44 ± 25.63) respectively, showed a trend towards significance ($t_9 = -1.652$, $p = .067$ and $t_9 = -1.706$, $p = .061$). Differences of FES2 vs. FES3 and VOL2 vs. VOL3 showed no significant effect ($t_9 = -.534$, $p = .303$ and $t_9 = -.462$, $p = .328$). Directed paired t-tests (CTRL) comparing FES1 (34.12 ± 7.66) vs. FES2 (43.722 ± 15.62) and VOL1 (35.14 ± 7.78) vs. VOL2 (45.41 ± 15.50) revealed a trend towards difference ($t_9 = -1.553$, $p = .078$) and ($t_9 = -1.698$, $p = .062$). Comparison of FES2 (43.722 ± 15.62) vs. FES3 (32.91 ± 11.13) and VOL2 (45.41 ± 15.50) vs. VOL3 (34.69 ±

11.68) respectively showed a significant force decrease (t9 = 1.853, p = .049 and t9 = 1.840, p = .05). Differences of FES1 vs. FES3 and VOL1 vs. VOL3 showed no significant effect (t9 = .255, p = .403 and t9 = .096, p = .463). Directed independent-samples t-tests demonstrated only significant group differences in FOLLOW-UP i.e. FES3 for TRAIN (49.04 ± 25.34) was higher (t18 = 1.842, p = .041) as in CTRL (32.91 ± 11.13). The same was found true for VOL3 where TRAIN (50.44 ± 25.63) had a significantly higher force output (t18 = 1.769, p = .047) compared to CTRL (34.69 ± 11.68) corroborating the effect in Figure 7b.

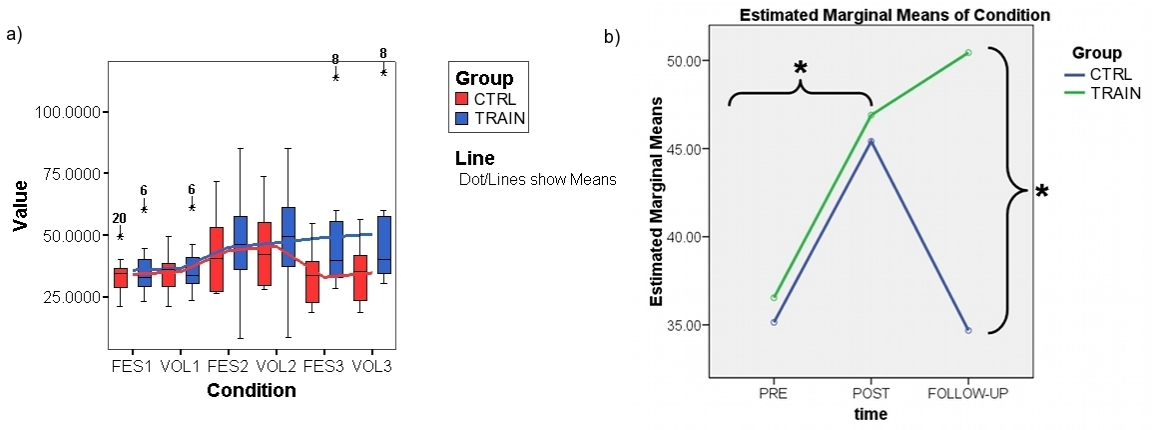

Figure III-7 a) Descriptive plot of TRAIN (blue) and CTRL (red) for FES and VOL. Boxes depict 25th to 75th percentile with median. Fences depict maximal and minimal values. b) Interaction diagram of mean FES for TRAIN (green) and CTRL (blue), * = p < 0.05

Table III-5 Descriptive statistics of FES and VOL during fMRI. Force output [N] measured with MR-compatible Dynamometer

	Time	PRE		POST		FOLLOW-UP	
Group	Condition	FES1	VOL1	FES2	VOL2	FES3	VOL3
CTRL	Mean	34.120	35.146	43.722	45.415	32.919	34.685
	Median	34.596	36.115	40.644	42.071	33.525	35.097
	Std. Deviation	7.654	7.778	15.625	15.505	11.130	11.685
	Minimum	21.029	21.183	26.429	27.804	18.604	18.500
	Maximum	49.413	49.608	71.629	73.721	54.600	56.146
TRAIN	Mean	35.814	36.542	45.082	46.898	49.041	50.442
	Median	32.934	33.580	46.127	49.571	39.892	40.296
	Std. Deviation	11.019	11.113	22.678	22.971	25.342	25.629
	Minimum	23.071	23.508	7.929	8.650	28.338	30.463
	Maximum	60.500	61.133	85.000	85.067	113.804	116.058

Summarized, a force increase was observed for both TRAIN and CTRL after 4 weeks of training. However after another 4 weeks without training (detraining), the observed effects were maintained in TRAIN whereas CTRL dropped back to the baseline level.

Maximal voluntary grasp (MVG)

Table 6 shows the descriptive statistics of MVG. Repeated measurements ANOVA of MVG did not demonstrate any significant effects for both main effect time ($F_{5,14} = 1.644$, $p = .213$) and interaction time × group ($F_{5,14} = 1.297$, $p = .320$). Independent t-tests demonstrated no significant group difference in all six assessments (MVG0, $t_{18} = -.972$, $p = .344$; MVG1, $t_{18} = -.703$, $p = .491$; MVG2, $t_{18} = -.804$, $p = .432$; MVG3, $t_{18} = -.749$, $p = .300$; MVG4, $t_{18} = -.1.204$, $p = .244$ MVG8, $t_{18} = -.691$, $p = .498$). We repeated the same ANOVA within the two groups separately in order to check whether changes over time would become significant. In TRAIN, no significant differences between time points were found. In CTRL, no main effect for time ($F_{5,5} = 1.818$, $p = .265$) was observed for MVG. Still, paired t-tests (2-tailed) between 0 (424.44 ± 107.85) and 4 (442.44 ± 123.22) ($t_9 = -2.288$, $p = 0.048$) and 4 and 8 (419.54 ± 118.31) ($t_9 = 3.863$, $p = 0.004$) revealed significant force increases and decreases respectively.

Table III-6 Descriptive statistics of maximal voluntary grasp (MVG) in Newton

	Time	**PRE**	**intra Training**			**POST**	**FOLLOW-UP**
	Week	**0**	**1**	**2**	**3**	**4**	**8**
Group	**Condition**	**MVG0**	**MVG1**	**MVG2**	**MVG3**	**MVG4**	**MVG8**
		Statistic	Statistic	Statistic	Statistic	Statistic	Statistic
CTRL	Mean	424.440	428.870	427.060	431.650	442.440	419.540
	Median	395.650	405.500	387.500	398.150	394.850	367.050
	Std. Deviation	107.851	111.007	111.052	111.749	123.219	118.313
	Minimum	291.000	304.100	295.900	305.700	279.600	281.200
	Maximum	616.400	626.200	578.800	652.400	657.300	624.600
TRAIN	Mean	380.470	393.390	388.140	377.360	381.450	385.700
	Median	329.050	323.750	325.350	320.450	341.750	333.550
	Std. Deviation	93.990	114.672	105.419	115.705	102.382	99.967
	Minimum	293.500	294.300	297.600	255.100	274.700	273.000
	Maximum	569.800	600.000	573.900	583.700	555.900	536.300

fMRI

Subjects did not sense any differences in the intensity of the stimulation during scanning. No sensations of burning or other subjective discomfort were reported. Contrasts without significant results are not reported.

FES

The results of the effect of FES vs baseline in all subjects at PRE (FES1_ALL) are shown in table 7 and Figure 8 a. Significant bilateral activations ($p < 0.05_{FWE\text{-}cor}$) were found in SI (postcentral gyri), supplementary motor areas (SMA), SII (postcentral gyrus, supramarginal gyrus, rolandic operculum), mid cingulum, and insula. Contralateral activation was observed in left precentral gyrus (MI), superior parietal lobules and thalamus. Cerebellar activation (denotations after (Schmahmann, et al. 1999)) was found mainly ipsilateral in posterior Larsell's lobule VI and anterior lobule V spreading to the anterior and posterior vermis (vermal V, VI). Small contralateral activation was found in Larsell's lobule VI.

Table III-7 Activated brain regions in all subjects (n = 19) for FES_PRE vs. Rest. Coordinates of local maxima (MNI) corrected for multiple comparisons p < 0.05 (FWE)

cluster-level			voxel-level					
p_{cor}	k_E	p_{unc}	$p_{FWE\text{-}cor}$	T	Z	p_{unc}	x,y,z {mm}	anatomical Region
0.000	158	0.000	0.002	9.63	5.65	0.000	22 -44 -32	Cerebellum ant R (Lobule V)
0.000	42	0.000	0.003	9.15	5.52	0.000	6 -56 -16	Cerebellum ant R (Vermis V)
0.000	23	0.000	0.003	9.26	5.55	0.000	-32 -64 -28	Cerebellum post L (Lobule VI)
0.000	134	0.000	0.000	12.06	6.23	0.000	-4 0 42	Cingulum mid L
0.000	13	0.000	0.003	9.2	5.53	0.000	-10 -26 44	Cingulum mid L
0.000	8	0.001	0.013	8.3	5.26	0.000	4 -10 44	Cingulum mid L
0.000	53	0.000	0.000	13.07	6.43	0.000	6 18 34	Cingulum mid R
0.000	52	0.000	0.002	9.41	5.59	0.000	-40 -4 -6	Insula L
0.000	307	0.000	0.000	12.83	6.39	0.000	42 6 -2	Insula R
0.000	18	0.000	0.002	9.43	5.6	0.000	36 -16 6	Insula R
0.000	28	0.000	0.002	9.38	5.58	0.000	42 -12 -14	Insula R
0.000	5	0.005	0.013	8.31	5.26	0.000	-24 -46 68	Parietal sup L
0.000	557	0.000	0.000	13.93	6.59	0.000	-34 -36 66	Postcentral L
0.000	6	0.002	0.007	8.66	5.37	0.000	-36 -46 56	Postcentral L
0.002	3	0.021	0.016	8.19	5.22	0.000	-60 -20 12	Postcentral L
0.015	1	0.158	0.034	7.77	5.09	0.000	-22 -36 70	Postcentral L
0.000	36	0.000	0.001	9.96	5.74	0.000	64 -22 38	Postcentral R
0.000	5	0.005	0.005	8.86	5.43	0.000	-32 -18 62	Precentral L
0.000	21	0.000	0.000	11.24	6.05	0.000	-40 -22 18	Rolandic Operculum L
0.005	2	0.053	0.010	8.49	5.32	0.000	-48 4 10	Rolandic Operculum L
0.000	141	0.000	0.000	10.86	5.96	0.000	48 -28 20	Rolandic Operculum R
0.000	7	0.001	0.004	9	5.47	0.000	48 6 16	Rolandic Operculum R
0.005	2	0.053	0.024	7.97	5.15	0.000	58 6 6	Rolandic Operculum R
0.000	23	0.000	0.008	8.61	5.36	0.000	-6 -4 64	SMA L
0.005	2	0.053	0.021	8.05	5.18	0.000	6 -4 70	SMA R
0.015	1	0.158	0.046	7.61	5.03	0.000	2 -2 66	SMA R
0.000	85	0.000	0.000	12.35	6.29	0.000	-60 -24 22	Supramarginal L
0.000		0.000	0.002	9.43	5.6	0.000	66 -24 18	Supramarginal R
0.002	3	0.021	0.021	8.04	5.18	0.000	-64 -26 32	Supramarginal L
0.000	6	0.002	0.008	8.61	5.36	0.000	-56 2 -2	Temporal sup L
0.000	49	0.000	0.000	10.6	5.9	0.000	-16 -22 4	Thalamus L

VOL

The activation pattern of VOL vs. baseline in all subjects at PRE (VOL1_ALL) was similar to that of FES (Tab. 8, Fig. 8 b). Additional significant activations ($p < 0.05_{FWE\text{-}cor}$) were found in bilateral intraparietal sulcus, inferior parietal lobe, inferior occipital lobe, occipitotemporal gyrus, ipsilateral occipital gyrus, superior parietal (while contralateral activation was absent), ipsilateral precentral gyrus and bilateral pallidum and putamen. Cerebellar activation was mainly bilateral.

Table III-8 Activated brain regions in all subjects (n = 19) for VOL_PRE vs. Rest. Coordinates of local maxima (MNI) corrected for multiple comparisons p < 0.05 (FWE)

cluster-level			voxel-level					
p_{cor}	k_E	p_{unc}	$p_{FWE\text{-}cor}$	T	Z	p_{unc}	x,y,z {mm}	anatomical Region
0.000	365	0.000	0.000	14.18	6.63	0.000	24 -50 -26	Cerebellum ant R (Lobule V)
0.000	113	0.000	0.000	11.02	6.00	0.000	-42 -52 -36	Cerebellum post L (Lobule Crus I)
0.000		0.000	0.000	10.80	5.95	0.000	34 -56 -28	Cerebellum post R (Lobule VI)
0.000		0.000	0.000	11.98	6.21	0.000	0 10 40	Cingulum mid
0.000		0.000	0.000	11.25	6.05	0.000	6 16 38	Cingulum mid R
0.000	6	0.002	0.009	8.52	5.33	0.000	-14 -26 40	Cingulum mid L
0.000	117	0.000	0.000	11.91	6.20	0.000	-42 -2 6	Insula L
0.001	4	0.009	0.010	8.49	5.32	0.000	-34 22 0	Insula L
0.000		0.000	0.000	12.14	6.25	0.000	36 20 -2	Insula R
0.000	8	0.001	0.001	9.89	5.72	0.000	-24 -62 58	intraparietal Sulcus L
0.000	7	0.001	0.007	8.71	5.39	0.000	26 -70 38	intraparietal Sulcus R
0.000	61	0.000	0.000	11.90	6.20	0.000	-44 -84 -4	Occipital inf L
0.000	24	0.000	0.001	9.93	5.73	0.000	28 -90 -8	Occipital inf R
0.000	11	0.000	0.011	8.43	5.30	0.000	-38 -94 0	Occipital mid L
0.000	14	0.000	0.001	9.69	5.67	0.000	-42 -72 -14	Occipitotemporal gyr lat L
0.002	3	0.021	0.016	8.19	5.22	0.000	44 -72 -16	Occipitotemporal gyr lat R
0.000	71	0.000	0.002	9.47	5.61	0.000	30 -98 2	occiptial Gyr R
0.002	3	0.021	0.003	9.25	5.55	0.000	46 -84 -2	occiptial Gyr R
0.000	5	0.004	0.012	8.36	5.28	0.000	-24 -14 0	Pallidum L
0.005	2	0.052	0.021	8.04	5.18	0.000	24 0 2	Pallidum R
0.000	17	0.000	0.006	8.78	5.41	0.000	-54 -28 46	Parietal inf L
0.001	4	0.009	0.016	8.21	5.23	0.000	36 -46 46	Parietal inf R
0.000	6	0.002	0.016	8.20	5.23	0.000	32 -58 58	Parietal sup R
0.000	282	0.000	0.000	18.37	7.25	0.000	-36 -34 56	Postcentral L
0.000	16	0.000	0.005	8.90	5.44	0.000	-52 -24 32	Postcentral L
0.000	57	0.000	0.001	10.09	5.77	0.000	62 -24 38	Postcentral, Supramarginalis R
0.000		0.000	0.000	12.50	6.32	0.000	-42 -20 52	Precentral L
0.000	18	0.000	0.002	9.37	5.58	0.000	54 12 32	Precentral R
0.000	13	0.000	0.001	10.22	5.81	0.000	-20 -12 -6	Putamen, Thalamus L
0.000	392	0.000	0.000	13.43	6.50	0.000	52 12 2	rolandic Operculum R
0.000	504	0.000	0.000	14.91	6.76	0.000	2 0 62	SMA R
0.000	6	0.002	0.005	8.88	5.44	0.000	60 -36 28	Supramarginal R
0.000	112	0.000	0.000	12.17	6.25	0.000	-10 -18 0	Thalamus L
0.000	11	0.000	0.001	9.69	5.67	0.000	18 -4 14	Thalamus R
0.000		0.000	0.013	8.35	5.27	0.000	8 -20 -2	Thalamus R

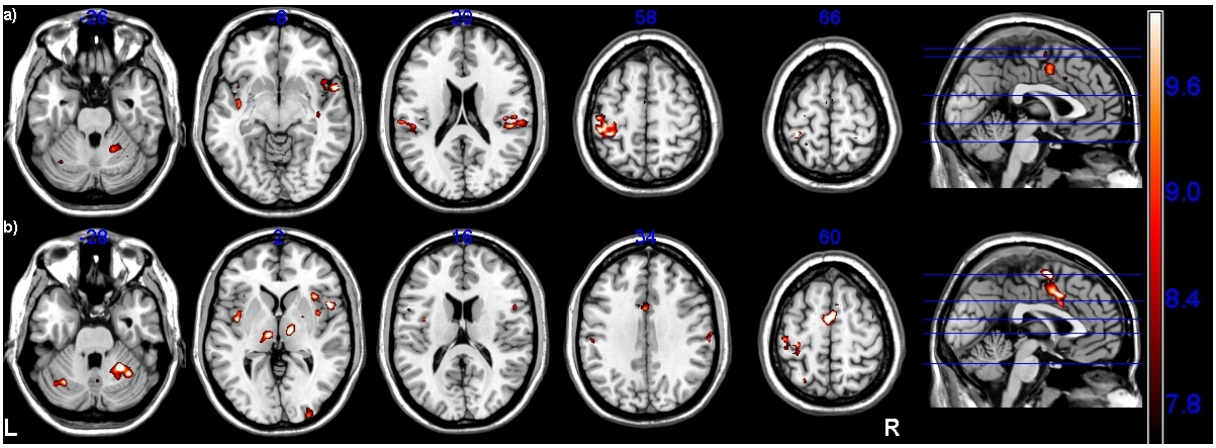

Figure III-8 Activation maps of all subjects after PRE for a) FES vs. Rest and b) VOL vs. Rest ($t(18) > 7.57$, $p < 0.05_{FWE\text{-}cor}$). Transversal view, convention for lateralization is shown: L, left hemisphere; R, right hemisphere.

General contrast between FES and VOL including all subjects

The contrast FES1-VOL1_ALL ($p < 0.05_{FWE\text{-}cor}$) revealed significant activations in bilateral insula, bilateral postcentral gyrus, which were clearly more dominant in the side contralateral to the stimulation, right rolandic operculum and left supramarginal gyrus both belonging to SII (Tab. 9 a, Fig 9 a). However, contrast VOL1-FES1_ALL showed no significant activation at level of $p < 0.05_{FWE\text{-}cor}$. Corrected at cluster level ($p_{cor} < 0.05$), significant activations were found in bilateral basal ganglia (mainly putamen and left pallidum), bilateral SMA, right precentral gyrus, right superior parietal lobule and right occipital regions (Tab. 9 b, Fig 9 b).

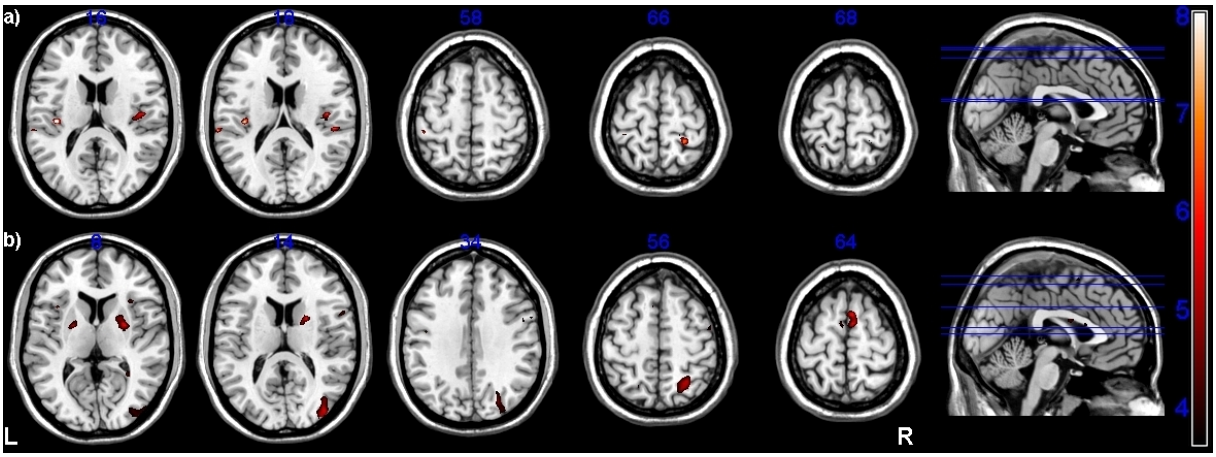

Figure III-9 Activation maps of all subjects for a) FES1 vs. VOL1 and b) VOL1 vs. FES1 ($t(18) > 7.57$, $p < 0.05_{FWE\text{-}cor}$). Transversal view, convention for lateralization is shown: L, left hemisphere; R, right hemisphere.

Table III-9 Activated brain regions in all subjects (n=19) for (a) FES1 vs. VOL1 and (b) VOL1 vs. FES1. Coordinates of local maxima (MNI) corrected for multiple comparisons using for (a) p < 0.05 (FWE) and (b) cluster-level p < 0.05

a)

cluster-level			voxel-level					
p_{cor}	k_E	p_{unc}	$p_{FWE-cor}$	T	Z	p_{unc}	x,y,z {mm}	anatomical Region
0.000	22	0.000	0.000	11.45	6.1	0	-38 -22 16	Insula L
0.002	3	0.021	0.015	8.26	5.25	0	-42 -26 2	Insula L
0.002	3	0.021	0.015	8.23	5.24	0	-40 -4 -16	Insula L
0.005	2	0.052	0.039	7.7	5.06	0	-36 -24 4	Insula L
0.000	53	0.000	0.001	9.84	5.71	0	38 -18 6	Insula R
			0.003	9.13	5.51	0	42 -14 18	Insula R
0.015	1	0.155	0.021	8.04	5.17	0	42 2 -16	Insula R
0.015	1	0.155	0.033	7.8	5.09	0	46 -10 -14	Insula R
0.000	12	0.000	0.004	9.01	5.48	0	-46 -32 58	Postcentral L
0.000	8	0.001	0.023	8	5.16	0	-34 -34 66	Postcentral L
			0.026	7.93	5.14	0	-40 -34 64	Postcentral L
0.015	1	0.155	0.028	7.89	5.12	0	-24 -46 68	Postcentral L
0.000	30	0.000	0.002	9.55	5.63	0	26 -38 64	Postcentral R
0.000	25	0.000	0.001	9.68	5.66	0	50 -28 20	Rolandic Operculum R
0.000	14	0.000	0.001	9.71	5.67	0	-64 -30 20	Supramarginal L
0.015	1	0.155	0.045	7.63	5.03	0	-64 -28 28	Supramarginal L

b)

cluster-level			voxel-level					
p_{cor}	k_E	p_{unc}	$p_{FWE-cor}$	T	Z	p_{unc}	x,y,z {mm}	anatomical Region
0.000	458	0.000	0.121	7.10	4.84	0.000	26 -4 4	Putamen R
			0.148	6.99	4.80	0.000	24 8 2	Putamen R
			0.789	5.72	4.27	0.000	22 4 14	Putamen R
0.000	177	0.000	0.187	6.87	4.75	0.000	-26 2 -2	Putamen L
			0.473	6.29	4.52	0.000	-24 -2 6	Putamen L
			1.000	4.70	3.75	0.000	-20 -6 0	Pallidum L
0.002	114	0.000	0.727	5.84	4.32	0.000	6 8 64	SMA R
			0.736	5.82	4.31	0.000	6 -2 62	SMA R
			1.000	4.17	3.44	0.000	-6 0 64	SMA L
0.014	83	0.000	0.829	5.64	4.23	0.000	46 -8 40	precentral R
			0.980	5.14	3.98	0.000	46 -10 50	precentral R
0.000	222	0.000	0.864	5.56	4.19	0.000	38 -88 16	occipital mid R
			0.999	4.72	3.76	0.000	40 -74 14	occipital mid R
			1.000	4.05	3.37	0.000	48 -82 10	occipital mid R
0.001	136	0.000	0.965	5.24	4.03	0.000	26 -56 56	Parietal sup R
0.002	114	0.000	1.000	4.67	3.73	0.000	26 -76 34	occipital sup R
			1.000	4.42	3.59	0.000	26 -88 38	occipital sup R
			1.000	4.18	3.45	0.000	32 -80 30	occipital mid R

Training effects in TRAIN

FES-contrasts in PRE and POST

Compared to the activation pattern of all subjects, FES1-FES2_TRAIN ($p_{cluster\text{-}cor} < 0.05$) showed only significant clusters in right pre-/postcentral gyrus (MI/SI) and insula (Tab. 10 a, Fig. 10 a). The contrast FES2-FES1 failed to show statistically significant differential activations.

FES-contrasts in PRE and FOLLOW-UP

Similar to FES1-FES2, significant activations for FES1_FES3_TRAIN ($p_{cluster\text{-}cor} < 0.05$) were only found in ipsilateral pre- and postcentral gyrus (Tab. 10 b, Fig. 10 b). However, no insula activation was seen.

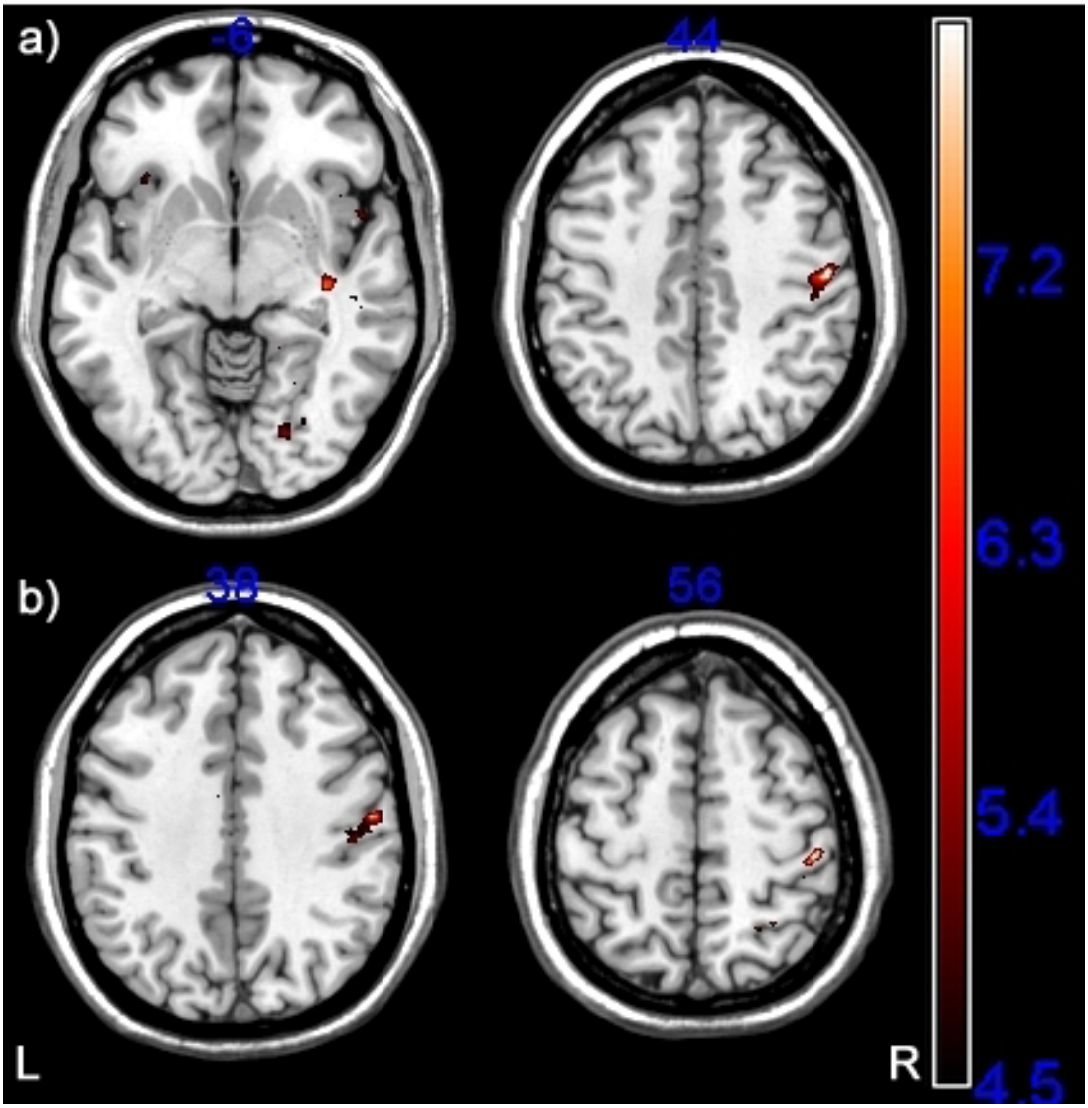

Figure III-10 Activation maps of TRAIN showing contrasts a) FES1 vs. FES2 and b) FES1 vs. FES3 (t(8) > 4.50, $p_{cluster\text{-}cor} < 0.05$) Transversal view, convention for lateralization is shown: L, left hemisphere; R, right hemisphere.

VOL-contrast in PRE and POST

Activation patterns resembled the ones found in all subjects (TRAIN and CTRL) (Tab. 10 c). However, cingulum and insula activations were not observed. Largest clusters size and highest t-values were found in the left posterior cerebellum (129 voxels, T8 = 10.58) and right precentral gyrus (216, 10.31) (Fig. 11 a).

VOL-contrasts in PRE and FOLLOW-UP

VOL1_VOL3_TRAIN ($p_{cluster\text{-}cor} < 0.05$) elicited activations in the left SMA and right postcentral gyrus. Two other clusters were located in the left lingual gyrus (Tab. 10 d, Fig. 11 b).

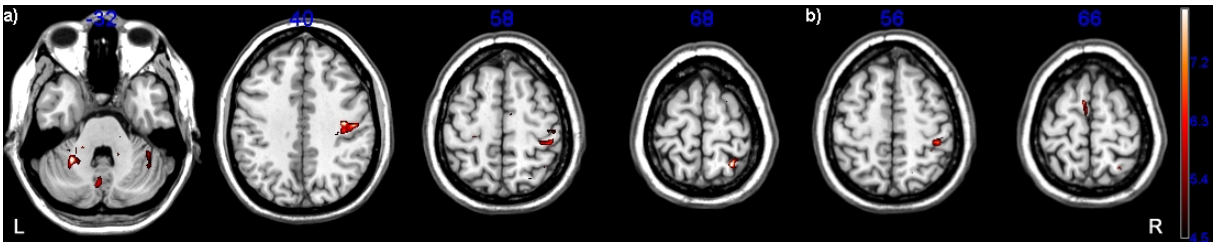

Figure III-11 Activation maps of TRAIN showing contrasts a) VOL1 vs. VOL2 and b) VOL1 vs. VOL3 (t(8) > 4.50, $p_{cluster\text{-}cor} < 0.05$) Transversal view, convention for lateralization is shown: L, left hemisphere; R, right hemisphere.

VOL-contrasts in POST and FOLLOW-UP

While VOL2-VOL3_TRAIN was not significant, VOL3-VOL2_TRAIN ($p_{cluster\text{-}cor} < 0.05$) depicted one cluster in the right parahippocampal gyrus (Tab. 10 e)

Table III-10 Activated brain regions in TRAIN (n = 9) for FES (a) PRE vs. POST, (b) PRE vs. FOLLOW-UP; for VOL (c) PRE vs. POST, (d) PRE vs. FOLLOW-UP, (e) FOLLOW-UP vs. POST. Coordinates of local maxima (MNI) corrected for multiple comparisons, using cluster-level p < 0.05

a)

cluster-level			voxel-level					
p_{cor}	k_E	p_{unc}	$p_{FWE-cor}$	T	Z	p_{unc}	x,y,z {mm}	anatomical Region
0.024	34	0.003	1.000	8.360	4.160	0.000	36 -20 -6	Insula R
0.000	200		0.097	13.240	4.890	0.000	52 -14 44	Pre-/ Postcentral R
		0.000	1.000	7.050	3.870	0.000	42 -18 40	Pre-/ Postcentral R
			1.000	6.750	3.800	0.000	46 -16 60	Precentral

b)

cluster-level			voxel-level					
p_{cor}	k_E	p_{unc}	$p_{FWE-cor}$	T	Z	p_{unc}	x,y,z {mm}	anatomical Region
	88		1.000	7.400	3.950	0.000	44 -18 42	Post-, Precentral R
0.002		0.000	0.898	9.880	4.430	0.000	46 -28 56	Postcentral R
0.000	10	0.000	1.000	7.670	4.020	0.000	54 -12 38	Postcentral R
	47		1.000	7.340	3.940	0.000	38 -30 50	Postcentral R
			1.000	5.460	3.430	0.000	50 -16 48	Precentral R

c)

cluster-level			voxel-level					
p_{cor}	k_E	p_{unc}	$p_{FWE-cor}$	T	Z	p_{unc}	x,y,z {mm}	anatomical Region
			1.000	8.98	4.28	0.000	-18 -38 -30	Cerebellum L ant (Lobule IV)
0.020	34	0.000	1.000	5.99	3.59	0.000	42 -48 -34	Cerebellum Post (Crus I)
0.000	129	0.000	0.532	10.58	4.54	0.000	-28 -50 -32	Cerebellum post L (Lobule VI)
0.028	32	0.000	1.000	6.63	3.77	0.000	-4 -72 -34	Cerebellum post L (Vermis VIII)
0.000	75	0.000	0.996	9.70	4.40	0.000	26 -54 68	Parietal sup R
			1.000	6.26	3.67	0.000	34 -54 62	Parietal sup R
			0.999	9.37	4.35	0.000	50 -16 50	Post-/ Precentral R
			1.000	7.65	4.01	0.000	34 -46 64	Postcentral / Parietal sup R
			1.000	8.08	4.10	0.000	46 -18 40	Postcentral R
0.015	36	0.000	1.000	6.57	3.75	0.000	44 -32 58	Postcentral R
			1.000	6.12	3.63	0.000	36 -34 58	Postcentral R
0.000	216	0.000	0.645	10.31	4.50	0.000	38 -16 40	Precentral R

d)

cluster-level			voxel-level					
p_{cor}	k_E	p_{unc}	$p_{FWE-cor}$	T	Z	p_{unc}	x,y,z {mm}	anatomical Region
0.000	54	0.000	1.000	8.120	4.110	0.000	-10 -70 -4	Lingual L
0.016	32	0.000	1.000	7.150	3.900	0.000	42 -34 56	Postcentral R
0.002	43	0.000	1.000	6.040	3.610	0.000	40 -20 38	Postcentral R
0.024	30	0.000	1.000	7.700	4.020	0.000	-6 2 66	SMA L

e)

cluster-level			voxel-level					
pcor	kE	punc	pFWE-cor	T	Z	punc	x,y,z {mm}	anatomical Region
0.023	33	0.000	1.000	7.110	3.890	0.000	32 -34 -24	parahippocampal Gyr R

Training effects (CTRL)

FES-contrasts in PRE and FOLLOW-UP

In contrary to FES2-FES1, bilateral basal ganglia activation was observed for FES3-FES1_CTRL (Tab. 11 a, Fig. 12), mainly in putamen but also in the pallidum.

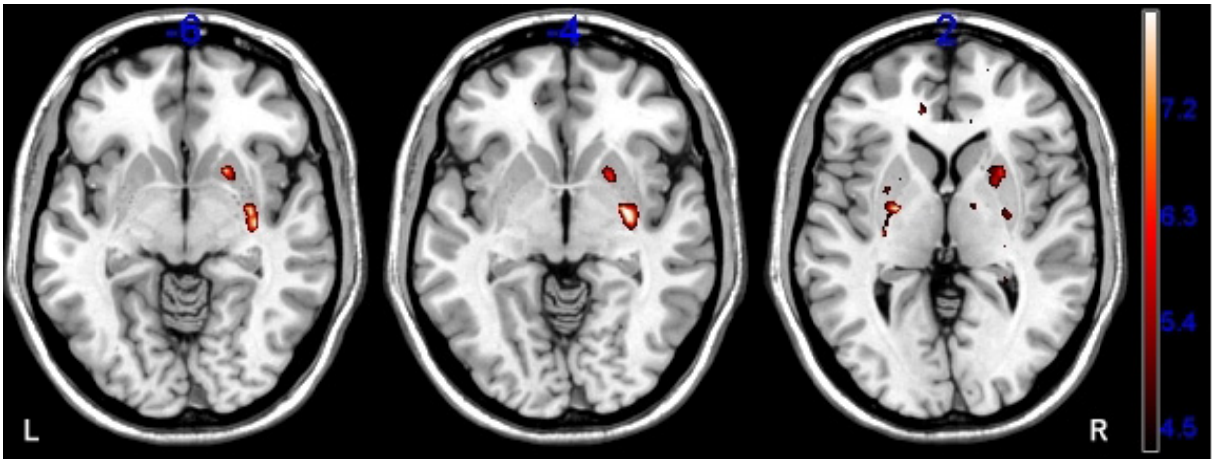

Figure III-12 Activation maps of CTRL showing contrasts FES3 vs. FES1 (t(9) > 4.30, $p_{cluster\text{-}cor}$ < 0.05) Transversal view, convention for lateralization is shown: L, left hemisphere; R, right hemisphere.

VOL-contrasts in PRE and POST

In VOL1-VOL2_TRAIN, only one significant cluster was found in the left superior parietal lobule extending to cuneus (Tab. 11 b, Fig. 13 a).

VOL-contrasts in PRE and FOLLOW-UP

VOL1-VOL3_CTRL ($p_{cluster\text{-}cor}$ < 0.05) activated a network encompassing the right superior parietal lobule, bilateral mid cingulum extending to left SMA, right inferior frontal gyrus overlapping with rolandic operculum, and right superior occipital gyrus (Tab. 11 c, Fig. 13 b).

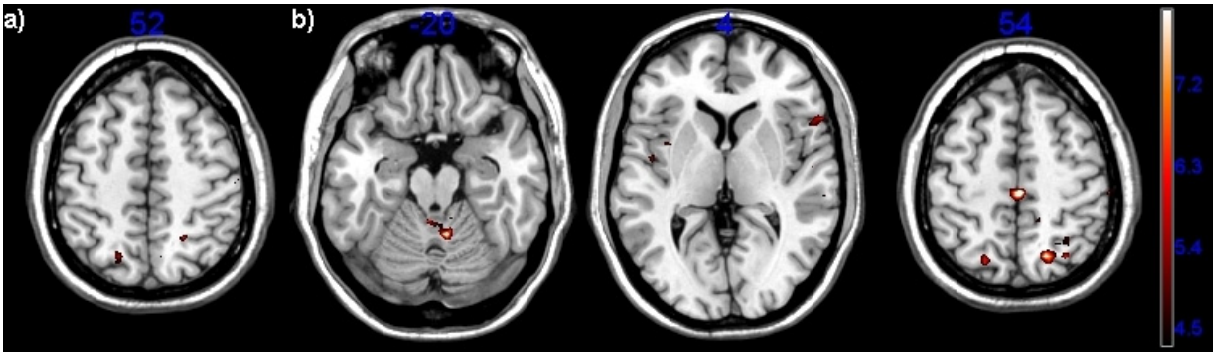

Figure III-13 Activation maps of CTRL showing contrasts a) VOL1 vs. VOL2, and b) VOL1 vs. VOL3 (t(9) > 4.30, $p_{cluster\text{-}cor}$ < 0.05) Transversal view, convention for lateralization is shown: L, left hemisphere; R, right hemisphere.

Table III-11 Activated brain regions in CTRL (n=10) for FES (a) PRE vs. FOLLOW-UP ; for VOL (b) PRE vs. POST, (c) PRE vs. FOLLOW-UP. Coordinates of local maxima (MNI) corrected for multiple comparisons, using cluster-level p < 0.05

a)

cluster-level			voxel-level					
p_{cor}	k_E	p_{unc}	$p_{FWE-cor}$	T	Z	p_{unc}	x,y,z {mm}	anatomical Region
			1.000	6.630	3.900	0.000	-30 -18 2	Putamen L
			1.000	5.380	3.510	0.000	-28 2 4	Putamen L
0.000	95.000	0.000	0.995	8.140	4.270	0.000	20 12 -6	Putamen R
			1.000	6.370	3.830	0.000	26 12 2	Putamen R
0.003	56.000	0.000	0.722	9.080	4.470	0.000	-24 -6 2	Putamen, Pallidum L
0.000	102.000	0.000	0.433	9.660	4.570	0.000	30 -8 -4	Putamen, Pallidum R

b)

cluster-level			voxel-level					
p_{cor}	k_E	p_{unc}	$p_{FWE-cor}$	T	Z	p_{unc}	x,y,z {mm}	anatomical Region
0.042	37.000	0.001	1.000	5.650	3.600	0.000	-18 -66 52	Parietal sup L

c)

cluster-level			voxel-level					
p_{cor}	k_E	p_{unc}	$p_{FWE-cor}$	T	Z	p_{unc}	x,y,z {mm}	anatomical Region
			1.000	6.410	3.840	0.000	-4 -44 -20	Cerebellum ant L (Vermis IV)
0.013	48.000	0.000	0.479	9.540	4.550	0.000	8 -52 -20	Cerebellum ant R (Vermis IV)
			1.000	5.350	3.500	0.000	-4 -60 -22	Cerebellum post L (Vermis VI)
0.002	66.000	0.000	1.000	5.450	3.540	0.000	6 -66 -28	Cerebellum post R (Vermis VI)
			1.000	6.780	3.940	0.000	-4 -18 60	Cingulate mid L, SMA
0.008	52.000	0.000	0.076	11.880	4.930	0.000	2 -26 54	Cingulate mid R
0.044	38.000	0.001	1.000	6.090	3.740	0.000	60 20 4	frontal inf R, rolandic Operculum
0.009	51.000	0.000	1.000	6.140	3.760	0.000	26 -92 30	Occipital sup R
			1.000	5.580	3.580	0.000	16 -92 28	Occipital sup R
			1.000	5.240	3.460	0.000	24 -86 38	Occipital sup R
0.000	138.000	0.000	0.971	8.620	4.380	0.000	18 -66 54	Parietal sup R
			1.000	7.130	4.030	0.000	30 -66 52	Parietal sup R
			1.000	5.420	3.530	0.000	24 -58 52	Parietal sup R
								Parietal sup R

Between group effects

Comparing groups in each condition for both FES and VOL, no significant group differences ($p_{cluster-cor} < 0.05$) were found.

Within group effects

Training Group

FES2-VOL2 revealed significant activations in bilateral postcentral gyrus, bilateral rolandic operculum and supramarginal gyrus. Furthermore, activations were present in right cerebellum and left inferior parietal lobule ($p_{cluster-cor} < 0.05$) (Tab 12 a, Fig 14 a). These two

regions were not found activated within the contrast, including all subjects FES1-VOL1_ALL which additionally showed left insula activation. After FOLLOW-UP, more activated clusters were observed for FES3-VOL3, namely in the right caudate nucleus, mid and posterior cingulum extending to precuneus, and bilateral insula (Tab 12 b, Fig 11 b).

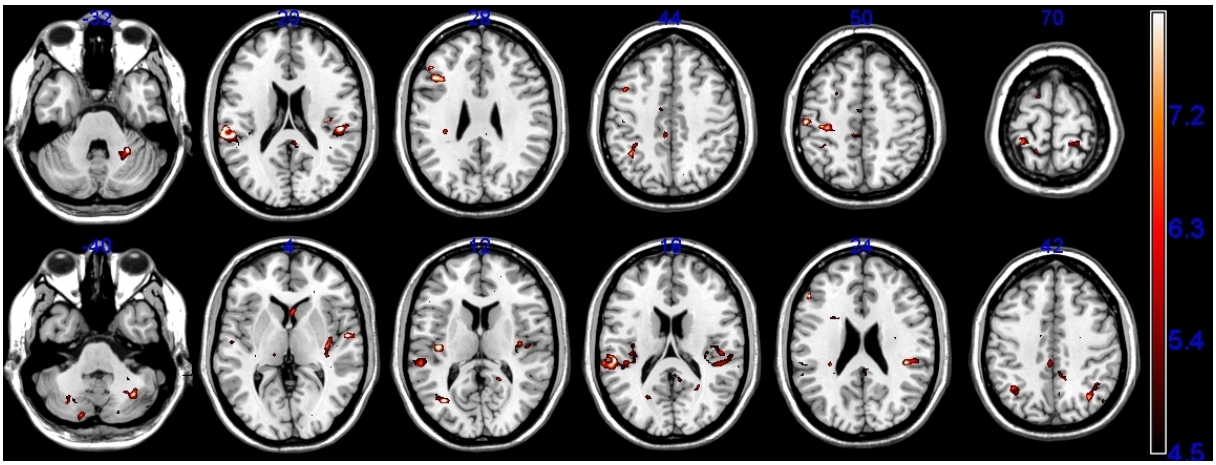

Figure III-14 Activation maps of TRAIN showing within-session contrasts a) FES2 vs. VOL2, and b) FES3 vs. VOL3 ($t(8) > 4.50$, $p_{cluster\text{-}cor} < 0.05$) Transversal view, convention for lateralization is shown: L, left hemisphere; R, right hemisphere.

For the inverse contrast VOL2-FES2_TRAIN (Tab. 13 a, Fig. 15 a), only one cluster in the right precentral gyrus was found to reach suprathreshold level whereas the contrast yielding all subjects, VOL1-FES1_ALL, showed activations within right precentral gyrus, parietal and occipital areas, bilateral putamen and SMA. However after FOLLOW-UP, VOL3-FES3 demonstrated four ipsilateral regions in which significant clusters could be observed: precentral gyrus, putamen together with pallidum and medial frontal gyrus (Tab. 13 b, Fig. 15 b).

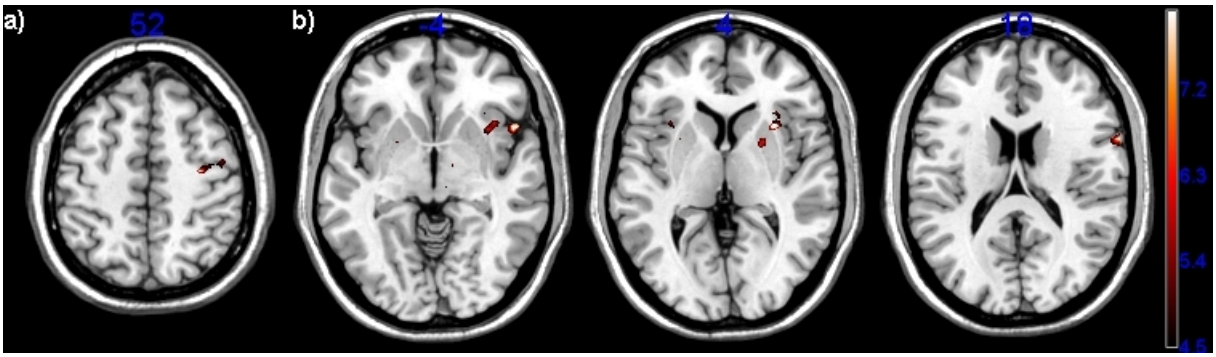

Figure III-15 Activation maps of TRAIN showing within-session contrasts a) VOL2 vs. FES2, and b) VOL3 vs. FES3 ($t(8) > 4.50$, $p_{cluster\text{-}cor} < 0.05$) Transversal view, convention for lateralization is shown: L, left hemisphere; R, right hemisphere.

Table III-12 Activated brain regions in TRAIN comparing FES vs VOL in a) POST, and b) FOLLOW-UP. Coordinates of local maxima (MNI) corrected for multiple comparisons, using cluster-level p < 0.05

a)

cluster-level			voxel-level					
p_{cor}	k_E	p_{unc}	$p_{FWE-cor}$	T	Z	p_{unc}	x,y,z {mm}	anatomical Region
			1.000	8.500	4.190	0.000	4 -56 -16	Cerebellum ant R (Vermis V)
0.000	380	0.000	0.332	11.290	4.640	0.000	28 -46 -32	Cerebellum post R (Lobule VI)
0.002	58	0.000	0.991	9.610	4.390	0.000	-44 22 28	Frontal inf triangularis L
0.000	73	0.000	1.000	8.420	4.170	0.000	-38 -50 44	Parietal inf L
0.008	48	0.000	0.451	10.840	4.580	0.000	-54 -20 50	Postcentral L
0.000	181	0.000	0.772	10.090	4.470	0.000	-42 -34 64	Postcentral L
0.000	105	0.000	0.997	9.200	4.320	0.000	-26 -30 54	Postcentral L
0.027	39	0.000	1.000	6.070	3.620	0.000	22 -40 70	Postcentral R
			0.561	10.530	4.530	0.000	-36 -32 12	Rolandic Operculum L
0.000	304	0.000	0.110	13.050	4.870	0.000	50 -26 20	Rolandic Operculum R
0.000	598	0.000	0.103	13.150	4.880	0.000	-62 -26 24	Supramarginal L
			0.117	12.940	4.860	0.000	-54 -32 20	Supramarginal L
			1.000	8.190	4.130	0.000	58 -4 -4	Temporal sup R
			0.994	9.440	4.360	0.000	50 -10 0	Temporal sup R / Insula

b)

cluster-level			voxel-level					
p_{cor}	k_E	p_{unc}	$p_{FWE-cor}$	T	Z	p_{unc}	x,y,z {mm}	anatomical Region
0.001	55	0.000	1.000	6.940	3.850	0.000	0 14 2	Caudate Ncl R
			1.000	6.890	3.830	0.000	4 22 8	Caudate Ncl R
0.003	45	0.000	1.000	6.070	3.620	0.000	-14 32 -2	Caudate Ncl R
0.000	118	0.000	0.533	10.620	4.550	0.000	34 -62 -40	Cerebellum post R (Lobule VI)
			1.000	5.960	3.580	0.000	-2 -32 42	Cingulum mid L
			1.000	5.790	3.530	0.000	4 -40 28	Cingulum post R
			0.997	9.700	4.400	0.000	-40 -18 12	Insula L
			1.000	7.980	4.080	0.000	36 -16 4	Insula R
0.005	43	0.000	0.238	11.820	4.720	0.000	-34 -68 12	Occipital mid L / temporal mid
			1.000	5.050	3.290	0.000	-36 -60 14	Occipital mid L / temporal mid
0.000	190	0.000	0.380	11.110	4.620	0.000	34 -64 40	Occipital mid R / Angular gyrus
0.023	33	0.000	0.364	11.170	4.630	0.000	-24 0 32	occipitofrontal fasciculus sup L
0.000	61	0.000	1.000	7.030	3.870	0.000	-38 -56 44	Parietal inf L
			1.000	7.290	3.930	0.000	38 -52 38	Parietal inf R / Angular gyrus
0.000	99	0.000	1.000	7.670	4.020	0.000	-22 -46 70	Parietal sup L
			1.000	6.640	3.770	0.000	-42 -36 64	Postcentral L
			1.000	5.630	3.480	0.000	-30 -34 60	Postcentral L
0.000	85	0.000	1.000	6.420	3.710	0.000	22 -36 66	Postcentral R
			1.000	6.090	3.620	0.000	22 -44 70	Postcentral R
			1.000	5.570	3.460	0.000	28 -36 74	Postcentral R
0.000	139	0.000	1.000	7.470	3.970	0.000	-34 -26 66	Precentral L / Postcentral
			1.000	8.440	4.180	0.000	-42 -34 20	Rolandic Operculum L
0.000	413	0.000	0.272	11.610	4.690	0.000	56 -6 4	Rolandic Operculum R
			0.405	11.020	4.610	0.000	42 -32 24	Rolandic Operculum R
0.000	286	0.000	0.304	11.440	4.670	0.000	-54 -30 18	Supramarginal L
0.002	48	0.000	1.000	8.500	4.190	0.000	-46 -22 -10	Temporal mid L

Table III-13 Activated brain regions in TRAIN comparing VOL vs FES in a) POST, and b) FOLLOW-UP. Coordinates of local maxima (MNI) corrected for multiple comparisons, using cluster-level p < 0.05

a)

cluster-level			voxel-level					
p_{cor}	k_E	p_{unc}	$p_{FWE-cor}$	T	Z	p_{unc}	x,y,z {mm}	anatomical Region
0.016	43	0.000	0.998	8.970	4.280	0.000	32 -12 52	precentral R
			1.000	5.270	3.370	0.000	46 -6 52	precentral R

b)

cluster-level			voxel-level					
p_{cor}	k_E	p_{unc}	$p_{FWE-cor}$	T	Z	p_{unc}	x,y,z {mm}	anatomical Region
			1.000	6.150	3.640	0.000	38 18 -4	Insula R
0.023	33	0.000	1.000	8.550	4.200	0.000	64 8 18	Precentral R
0.000	100	0.000	0.110	13.070	4.870	0.000	30 16 4	Putamen R
			1.000	6.250	3.670	0.000	22 4 4	Putamen R / Pallidum
0.046	29	0.000	0.433	10.920	4.590	0.000	52 16 -4	Frontal inf Operculum R

Control group

After POST, FES2-VOL2 showed two additional activated clusters compared to FES1 vs. VOL1_ALL: one in the left precentral gyrus (MI) and one in superior parietal lobule (Table 14, Fig 16 a). Insular activation was not observed. Similar to TRAIN, assessment after FOLLOW-UP FES3-VOL3 depicted a larger network additionally encompassing, bilateral cerebellum with a clear right dominance, bilateral pars triangularis of the inferior frontal gyrus, left medial and superior orbitofrontal cortex and bilateral precuneus (Table 15, Fig 16 b).

Table III-14 Activated brain regions in CTRL comparing FES vs VOL in POST. Coordinates of local maxima (MNI) corrected for multiple comparisons, using cluster-level p < 0.05

cluster-level			voxel-level					
p_{cor}	k_E	p_{unc}	$p_{FWE-cor}$	T	Z	p_{unc}	x,y,z {mm}	anatomical Region
0.003	64	0.000	1.000	5.500	3.550	0.000	-16 -54 70	Parietal sup L
0.000	189	0.000	1.000	7.210	4.050	0.000	-34 -36 62	Postcentral L
0.004	60	0.000	0.995	7.910	4.220	0.000	22 -44 68	Postcentral R
			1.000	5.410	3.520	0.000	-28 -24 64	Precentral L
0.000	123	0.000	0.961	8.720	4.390	0.000	-60 -32 14	Supramarginal L
			1.000	5.610	3.590	0.000	-64 -32 26	Supramarginal L
0.000	108	0.000	1.000	6.810	3.950	0.000	56 -28 22	Supramarginal R
			1.000	6.310	3.810	0.000	66 -22 22	Supramarginal R / rolandic Operculum

Table III-15 Activated brain regions in CTRL comparing FES vs VOL in FOLLOW-UP. Coordinates of local maxima (MNI) corrected for multiple comparisons, using cluster-level p < 0.05

cluster-level			voxel-level					
p_{cor}	k_E	p_{unc}	$p_{FWE-cor}$	T	Z	p_{unc}	x,y,z {mm}	anatomical Region
0.002	63	0.000	1.000	6.940	3.990	0.000	30 -52 34	Angular gyrus R
			1.000	6.310	3.810	0.000	40 -50 32	Angular gyrus R
0.007	53	0.000	1.000	7.150	4.040	0.000	20 -50 -32	Cerebellum ant R (Lobule V)
0.000	166	0.000	0.991	8.180	4.280	0.000	4 -54 -14	Cerebellum ant R (Vermis IV)
			1.000	6.340	3.820	0.000	-16 -60 -18	Cerebellum post L (Lobule VI)
			1.000	5.040	3.390	0.000	24 -58 -32	Cerebellum post R (Lobule VI)
0.004	57	0.000	0.984	8.410	4.330	0.000	-34 34 4	Frontal Triangularis inf L
0.000	96	0.000	0.648	9.220	4.490	0.000	50 34 28	Frontal Triangularis inf R
			0.419	9.720	4.580	0.000	44 -12 -18	Insula R
			0.461	9.600	4.560	0.000	42 -14 12	Insula R
0.038	39	0.001	1.000	7.370	4.090	0.000	-14 42 -8	Orbitofrontal med L
			1.000	5.300	3.480	0.000	-24 38 -12	Orbitofrontal sup L
0.000	300	0.000	1.000	6.320	3.810	0.000	-28 -32 56	Postcentral L
			1.000	5.580	3.580	0.000	-16 -38 74	Postcentral L
			1.000	4.500	3.180	0.001	24 -38 64	Postcentral R
0.000	81	0.000	0.316	10.050	4.640	0.000	22 -44 70	Postcentral R / Parietal sup
0.044	38	0.001	1.000	6.090	3.740	0.000	-62 -18 10	Postcentral L / Temporal sup
0.000	265	0.000	0.127	11.200	4.830	0.000	-38 -22 18	Rolandic Operculum L
			1.000	4.370	3.120	0.001	-50 -22 10	Rolandic Operculum L / Temporal sup
0.000	778	0.000	0.311	10.070	4.650	0.000	50 -26 16	Rolandic Operculum R
0.003	62	0.000	1.000	6.770	3.940	0.000	-62 -30 14	Supramarginal L / Temporal sup
			1.000	6.040	3.730	0.000	-58 -38 20	Supramarginal L / Temporal sup

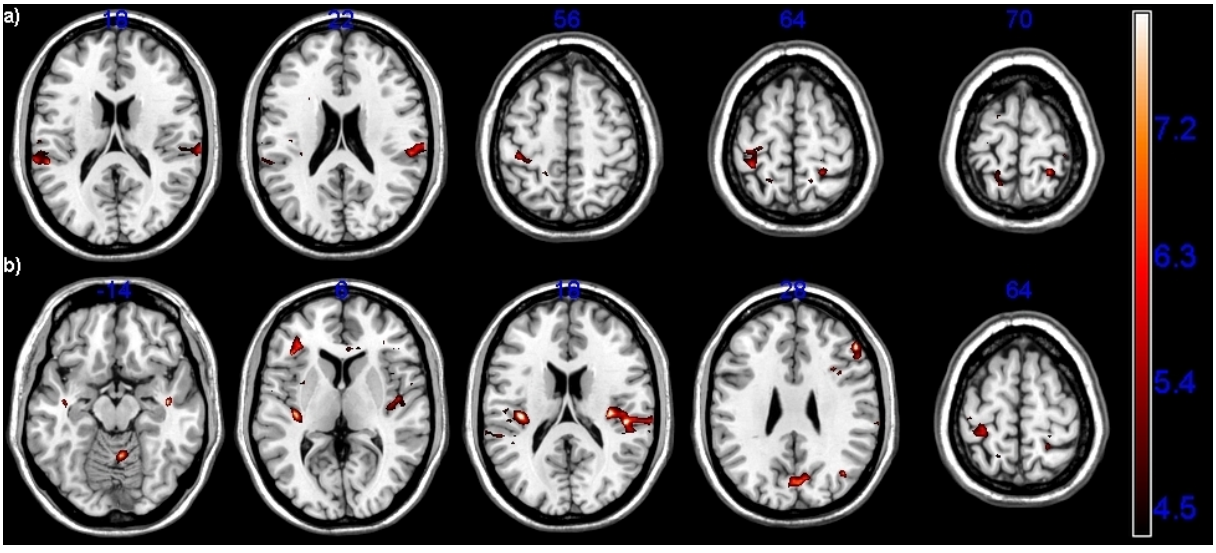

Figure III-16 Activation maps of CTRL showing within-session contrasts a) FES2 vs. VOL2, and b) FES3 vs. VOL3 (t(9) > 4.30, $p_{cluster-cor}$ < 0.05) Transversal view, convention for lateralization is shown: L, left hemisphere; R, right hemisphere

Discussion

The primary goal of this study was to demonstrate the modulator effect of a 4-week FES training applied to the dominant forearm with respect to the behavioral outcome and cortical activation patterns. Our experimental set-up led to a significant force increase in both; the subjects undergoing the four weeks systematic training as well as the controls. However after four additional weeks of no training, a significant group difference became apparent in that the trained group maintained a higher force output, whereas in the control group force decreased to baseline. Assessment of maximal voluntary grasp (MVG) did not show any significant changes - neither for time nor for group. However in controls, significant changes were observed for MVG showing force increase after week 4 as compared to the week 0. A significant force decrease was seen between week 4 and week 8. This pattern resembles the one found during fMRI.

The overall cortical activation by FES confirms the results reported in our previous study (Blickenstorfer, et al. 2008). Furthermore, activation patterns within the motor network due to VOL corroborate the successful application of FES in fMRI experiments as similar regions were activated. We could successfully distinguish between motor and sensory networks, revealed by contrasts comparing the voluntary with the functional stimulation task. Higher activations in basal ganglia; SMA and precentral gyrus were found for VOL; whereas FES revealed higher activations in bilateral postcentral gyrus, bilateral insula and bilateral SII which encompassed the right rolandic operculum and the left supramarginal gyrus.

However, contrasts depicting training effects showed no enlarged cortical activation clusters in both groups. This was true for both experimental conditions FES and voluntary movements. Furthermore, no differences were seen in the comparison of both groups.

For both groups, we further compared separately the two experimental conditions within each session, resulting in a trend of more activation clusters from PRE to POST to FOLLOW-UP for the contrast FES-VOL. However, VOL-FES showed a different pattern. While in TRAIN, fewer clusters were observed after POST and more after FOLLOW-UP; in CTRL, no significant activations were found for both VOL2-FES2 and VOL3-FES3. These findings more likely support our hypothesis in that over time additional areas were activated with regard to FES.

FES related changes

A 4-week FES training led to force increases which were maintained after four weeks of no training. This finding is consistent with previous studies (Gondin, et al. 2006a; Marqueste, et al. 2003) investigating the effect of long-term FES and its resulting beneficial adaptations after a period of no training also referred as detraining. However, the effect of force increase in CTRL from PRE to POST was somewhat unexpected. The reason for this could be due to the fact that CTRL participated in the fatiguing task, which was the same as the one during training. Although CTRL had four times less training compared to TRAIN, it seemed sufficient to gain force after four weeks, but not enough to maintain a lasting effect after detraining. Supporting results were described in clinical studies (Beekhuizen and Field-Fote 2005; Sterr, et al. 2002). Sterr, et al. (2002) investigated the effect of a 3-hour versus a 6-hour daily training of constraint induced therapy in brain injured patients. Movement abilities improved significantly in both groups and were even maintained in a follow-up period. However, shorter training was less effective as clinical improvements were stronger in participants who underwent the longer training. Beekhuizen and Field-Note (2005) investigated the effect of massed practice versus massed practice with median nerve stimulation in patients with incomplete cervical spinal cord injury. Patients receiving additionally electrical stimulation benefitted more, showing significantly better clinical scores. However, assessment of cortical excitability with TMS showed no group differences. Our data from healthy subjects support these clinical findings further emphasizing the importance of studies required to establish optimal training paradigms.

Maximal voluntary grasp did not improve in the training group. However for the control group, significant force increases were observed after four weeks, which then decreased after 4 weeks of detraining. The effect of more power in the non-trained controls is surprising and contradictory to the observations of the above mentioned studies (Beekhuizen and Field-Fote 2005; Sterr, et al. 2002) where subjects with more intensive training gained at least equal improvements as their counterpart controls. Early FES applications require constant adjustments of stimulation frequency and intensity as well as electrode placements in order to achieve the desired output and avoid early muscle fatigue (Popovic, et al. 2001a). In this study, we kept electrode placement and stimulation parameters constant during the entire study in order to avoid confounds with the brain activation. Median nerve stimulation studies have demonstrated that increasing stimulation intensity has been associated with increased amplitudes and broader activation maps within the human brain (Smith, et al. 2003). Likewise, increasing stimulus frequency led to more activated pixels and higher signal

amplitudes (Kampe, et al. 2000). Thus, by keeping stimulation parameters constant, a significant gain in MVG after 4 weeks of FES training probably was prevented.

Training related brain activations

Training effects in FES for TRAIN were demonstrated as more activated clusters were found in PRE (right pre- and postcentral cortex and insula), whereas no considerable significant activations were found in POST and FOLLOW-UP. No significant changes were observed between POST and FOLLOW-UP in either contrast. For CTRL, no training effects were seen between PRE and POST for either contrast. Thus, the 4 weekly FES assessments did not result in enhanced or enlarged brain activations, although a significant behavioral response was observed.

FES

We observed no FES related activation differences in PRE and POST for CTRL. This leads us to believe that activations found for TRAIN in PRE as opposed to POST were related to the FES training. Interestingly, these activations were located within primary sensorimotor areas and insula on the ipsilateral side to the stimulated arm. Ipsilateral activations have been previously reported with simple one-sided motor tasks (Alkadhi, et al. 2002b; Butefisch, et al. 2004; Ciccarelli, et al. 2005; Dai, et al. 2001; Koeneke, et al. 2006) or sensory inputs (Ferretti, et al. 2003; Golaszewski, et al. 2004; Korvenoja, et al. 1999; Peyron, et al. 1999; Shibuya and Ohki 2004; Sutherland and Tang 2006). Ipsilateral MI activation is linked to the global cortical activation within the cortical motor system, and it is somatotopically organized (Alkadhi, et al. 2002b). Another explanation for the ipsilateral MI activation may be its engagement in interhemispheric competition between homonymous representations. Applying TMS over ipsilateral MI can deteriorate the effects of motor training (Butefisch, et al. 2004) due to enhanced inhibitory drive over the trained hand. Therefore, activation within ipsilateral MI plays an important role in learning new motor task. Supporting this idea, Dai and collaborators (2001) reported that ipsilateral activity might be a result of precision control of the power grip to execute the task at low force levels. The pathway to ipsilateral SI activations is still unclear. Sutherland and Tang (2006) proposed two possibilities: callosal inputs from contralateral SI and / or uncrossed ipsilateral inputs. Peripheral electrical stimulation might lead to ipsilateral SI activation through group 1a, b and II afferents and their direct or transcallosal projections to sensorimotor cortex (Golaszewski, et al. 2004). Further insight comes from pain studies, which implicate an anticipatory role to the ipsilateral primary sensory areas (Peyron, et al. 1999) and emotional as well as attentional coloring of the

stimulus by insular regions, similar to a habituation effect. FES-related ipsilateral activation in PRE might demonstrate a reaction to the electrical stimulus itself. As subjects became used to the stimulus in the subsequent sessions, the anticipatory role became unnecessary.

The activation pattern found for PRE vs. FOLLOW-UP in TRAIN is similar to the one in PRE vs. POST except no insular activation was present. We speculate this to be related to familiarization with the experimental setup, thus, an emotional reaction was absent.

During FOLLOW-UP significant activations were observed within bilateral basal ganglia and left precuneus. The former can be related to storage and execution of automatic motor sequences (Debaere, et al. 2004; Doyon, et al. 2003; Wu, et al. 2008) while the latter is predominantly involved with storage processes (Halsband and Lange 2006; Shannon and Buckner 2004). The involvement of storage related process at FOLLOW-UP could be a delayed formation of memory of FES.

VOL

Training effects for TRAIN in VOL showed a similar pattern to the FES related activation patterns. More activated regions were seen in PRE (right pre- and postcentral gyrus, right superior parietal lobule, bilateral cerebellum, left SMA) whereas in POST and FOLLOW-UP no significant additional activations were observed. For CTRL, left superior parietal lobule activation was seen in PRE but no activations in POST. However, FOLLOW-UP vs. PRE showed activations within bilateral cerebellum, bilateral mid cingulate gyrus, and left SMA.

Although training was different for TRAIN and CTRL, the fMRI task was not different for both groups. The voluntary task led in both groups to activations within SPL. Parietal activations are related to visuo-sensory integration (Elsinger, et al. 2006; Tunik, et al. 2007; Vaillancourt, et al. 2003). Opposed to the FES condition, subjects had to press the dynamometer until the visually displayed goal was reached. Therefore, VOL required the visuo-sensory processes to complete the task, which was not necessary during FES. Keisker et al. (2008) used the same dynamometer for a visually guided grip force task and found that posterior parietal cortex activations play an important role in the control of lower forces. The forces elicited by FES were apx. 10-15% of MVG, which corresponded to the force level required for eliciting maximal parietal activations (Keisker, et al. 2008).

Bilateral cerebellar activations were observed for TRAIN in PRE vs. POST and for CTRL in PRE vs. FOLLOW-UP. The cerebellum plays an important role in the coordination and fine tuning of motor sequences (Trepel 1999). A recent review (Halsband and Lange 2006) proposes three roles for the cerebellum: (i) control of the actually performed movement by feedback processes using proprioceptive and visual information as well as error detection and

correction, (ii) control of initial motor learning, especially within left posterior cerebellar hemisphere, and (iii) involvement in storage of an acquired motor skill. The higher activation in PRE as opposed to POST can be therefore related to the learned and stored representation of the trained grip. However, these findings are contradictory to the results of Loubinoux, et al. (2001) who found an increase in cerebellar activation over time that was related to consolidation processes, and persisted for 2 months. On the other hand, cerebellar activation has been found to be decreased when the execution of a motor task has become automatic (Poldrack, et al. 2005; Wu, et al. 2008). This may be an explanation for the decreased cerebellar activation observed in POST as compared to PRE.

Left SMA showed increased activation in PRE as opposed to FOLLOW-UP for both groups. SMA plays an essential role in learning and initiation of a movement, as well as its execution (Picard and Strick 1996), even for simple movements (Kollias, et al. 2001). It is also proposed that increased SMA activation may be related to automation of a learned movement (Doyon, et al. 2002; Halsband and Lange 2006).

Right parahippocampal gyrus was found to be significantly activated for TRAIN in FOLLOW-UP vs POST. This effect is probably related to a late memory formation of the motor task (Muller, et al. 2002) paired with its visual stimulus in terms of a visual associative recognition memory (Duzel, et al. 2003).

Behavioral gain with an ab*sent cortical pattern?*

Effect of expertise and habituation

The question remains why barely any activation was found following 4 weeks of training, which is contradictory to studies reporting enlarged representations after a specific training (Debaere, et al. 2004; Floyer-Lea and Matthews 2005; Karni, et al. 1995; Petersen, et al. 1998). Indeed, there are also studies reporting less activations after a training (Loubinoux, et al. 2001; Morgen, et al. 2004; Pascual-Leone, et al. 1994). Pascual-Leone, et al. (1994) used TMS to investigate the development of implicit and declarative knowledge of a motor task. Improvements in task execution reflecting implicit learning led to enlargement of cortical motor output maps. However, after gaining explicit knowledge of the task, map topography returned to baseline. Morgan et al. (2001) used simple repetitive thumb movements as an fMRI paradigm. They found reduced task-specific activations in executive motor areas, which are involved in generating the required output, suggesting that a more automated processing of the output required less neuronal resources. Loubinoux, et al. (2001) found controversial results in a study investigating the reproducibility of simple active and passive tasks in

different sessions. After a second session, activation increases were found in contralateral premotor cortex and ipsilateral anterior cerebellum and concurrent decreases in primary sensorimotor cortex, parietal cortex and posterior SMA, which were dependent on the timing of the second session (5 hours, 1, or 2 months). These findings were interpreted in the context of habituation to the fMRI experiment, including both the MRI environment and the performed task. However, these changes were reversed at the third examination except in left parietal cortex and in the cerebellum, where they went on augmenting. This could have been due to a learning process, which formed a long-term memory consolidation of the sensorimotor task - not only of its characteristics (e.g. amplitude and frequency) but also of its context (fMRI). We used a very simple task for which no learning was required. Therefore, the frequently reported working memory activation increases within prefrontal as well as inferior and superior parietal lobules while developing knowledge about a motor task (Eliassen, et al. 2001; Hazeltine, et al. 1997), were not observed in POST and FOLLOW-UP sessions. Furthermore, our experimental paradigm was not designed to investigate a proceeding learning process as the three fMRI sessions were four weeks apart. By then a consolidation of memory has already taken place. Thus, subjects had rather gained an expertise reflected in habituation leading to lesser activations. Finally, it can be said that brain activations are dynamic in nature and may be afflicted simultaneously by at least two mechanisms that change the degree of activation, a learning-related increase and a habituation, adaptation or repetition-related decrease (Eliassen, et al. 2001). These findings corroborate our alternative hypothesis that cortical activation following long-term training decreases as a result of a more efficient neuronal network.

Methodological aspects

We observed a gain in force with no enhanced cortical activity after training. A similar finding was observed in stroke patients who underwent a NMES training (Kimberley, et al. 2004). Patients achieved functional improvements with no change in motor cortex activation. One important factor might have been the missing cognitive effort or problem solving associated with the task. There is evidence from animal studies that a simple task alone does not produce reorganization of cortical maps, whereas adding a cognitive component leads to changes within the functional activation (Kleim, et al. 1997; Nudo, et al. 1996; Plautz, et al. 2000). The simplicity of our task could, therefore, be one reason for missing increased activations. A more direct way to investigate the effect of electrical stimulation is TMS. Several studies have shown a training related effect in terms of enlarged cortical maps (Koeneke, et al. 2006) or higher motor evoked potentials in the trained muscles (Kaelin-Lang,

et al. 2002; Muellbacher, et al. 2001). However, these effects were observed directly after a training intervention, whereas we performed fMRI one to three days after cessation of training. This effect of delayed reversion to pre-stimulation has been demonstrated in a study (Stefan, et al. 2000) using TMS paired with low-frequency median nerve stimulation. After 30 minutes of stimulation, a higher cortical excitability was observed which decreased after few hours.

Physiological aspects

Absent enlarged cortical representations after a 4-week FES training despite the observed gain in behavioral force could be explained by changes within the spinal cord without associated changes on brain activation maps. Electric stimulation evokes action potentials in both targeted muscles and afferent cutaneous receptors, which in turn co-activate spinal cord motoneurons (Collins, et al. 2001). Also, cross-education effects demonstrate the involvement of intra-spinal processes (Hortobagyi, et al. 1999). A recent report (Gondin, et al. 2006a) investigated the effect of detraining after 5 weeks of NMES on neural drive representation. The results indicated that the H-reflex pathway[9] was not affected by detraining in that the efficiency of the reflex transmission between the 1a spindle afferent input and the α-motoneuron pool was not changed (Gondin, et al. 2006a). Thus, the observed behavioral gain without an obvious cortical epiphenomenon could be explained by spinal processes. However, we are well aware that the spinal effects reported above were demonstrated in the lower extremities and may not be directly related to the observed effects in the upper extremities.

Conclusion

The present study is the first to investigate the effect of 4-week FES training on brain activation using fMRI. The potential of FES is illustrated by the fact that subjects increased their passive force output significantly although training loads were different for both training and control groups. After 4 weeks of detraining, a training effect was demonstrated in that the training group showed a preservation of force output; whereas controls returned to their pre-training levels. Maximal voluntary force showed no change after training; however, we suspect this to be related to keeping stimulation regime constant. FES training with additional voluntary effort has been shown to increase muscle force resulting from stimulation. Training related brain activation patterns were manifested in stronger activations in the pre-training assessment. Several reasons were discussed, which could have lead to this phenomenon

[9] The H-reflex can be used to assess the excitability of α-motoneurons, reflecting the transmission efficiency in Ia afferent synapses (Aagaard et. al. ,2002).

including interhemispheric competition and efficiency increasing processes, as well as spinal processes which could have acted independently from top-down processes.

Acknowledgments
We wish to thank Mike Brügger from the Department of Neuropsychology, University of Zurich, for his great help in the SPM analysis. We thank the participating subjects for their invested time. This work was supported by the Swiss National Science Foundation grant, NCCR on "Neural Plasticity and Repair".

Study 3

Comparison of MRI-Compatible Mechatronic Systems with Hydrodynamic and Pneumatic Actuation

Ningbo Yu [1], Christoph Hollnagel [1], Armin Blickenstorfer [2], Spyros Kollias [2], Robert Riener [1]

[1] Sensory Motor Systems Lab, ETH Zurich, Switzerland

[2] Institute of Neuroradiology, University Hospital Zurich, Switzerland

Introduction

Mechatronic systems and devices that are compatible with magnetic resonance imaging (MRI) technology find wide range of applications in academic and industrial fields (Tsekos, et al. 2007; Yu and Riener 2006). MRI is an established clinical diagnostic method. MRI-compatible mechatronic devices can be applied to assist in image-guided surgery (Chinzei, et al. 2000b; Elhawary, et al. 2006; Hempel, et al. 2003; Kim, et al. 2002; Krieger, et al. 2005; Larson, et al. 2004; Masamune, et al. 1995) and to diagnose diseases (Bishop, et al. 1998), etc. Functional MRI (fMRI) is an advanced research and clinical tool in neuroscience. An MRI-compatible robot could perform well controlled and reproducible sensorimotor tasks, while the subject's motor interactions with the robot are recorded during the fMRI procedures and translated into brain images (Fig. 17). Therefore, MRI-compatible robots can be applied with fMRI to map brain functions (Golaszewski, et al. 2002; Harrington, et al. 2000), investigate human motor control (Gassert, et al. 2005; Khanicheh, et al. 2006), monitor rehabilitation induced cortical reorganization in neurological patients (Riener, et al. 2005b), etc. Such kind of fMRI-robotic systems could provide insights into the cortical reorganization mechanism after damage to the central or peripheral nervous system, offer a better understanding of therapy-induced recovery, and, eventually, help to derive more efficient rehabilitation strategies.

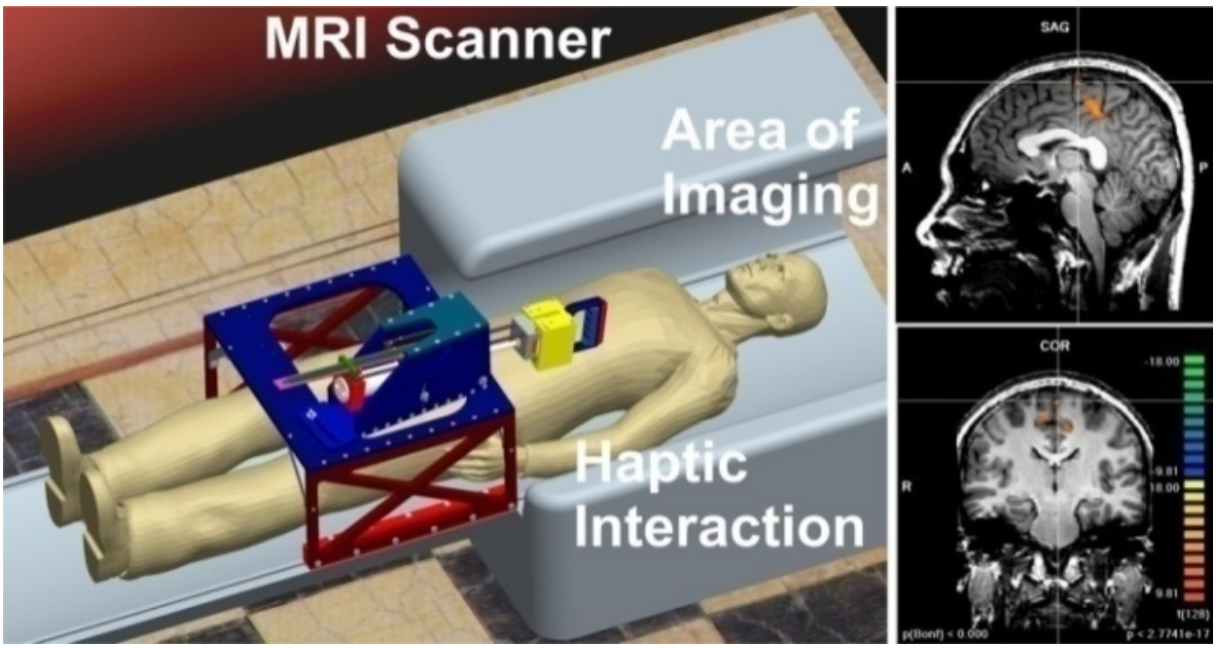

Figure III-17 fMRI-compatible robot and fMRI images

To construct MRI-compatible devices is rather challenging. First, the device must not disturb the scanner magnetic field and ensure image quality. Second, proper functionality of the device must be guaranteed when it is placed inside the MRI environment. During fMRI, the scanning sequences are more sensitive to magnetic field inhomogeneities than during anatomical MRI sequences, because fMRI measures the magnetic field inhomogeneities that are caused by changes of magnetic susceptibility of oxygenated and deoxygenated blood flow in the brain. Third, the device must be small and compact to fit into the limited space inside the MRI scanner bore. The bore diameter of most closed MRI scanners varies between only 55 cm and 70 cm (Chinzei, et al. 2000a; Tsekos, et al. 2007).

The strong magnetic field limits the choice of materials, sensors and actuators to be used in the MRI environment. Traditional ferromagnetic materials are not allowed to be placed into the MRI environment as they can be attracted by the strong magnetic field, thus endangering patient, personnel or the scanner system. Non-ferromagnetic conductive metals can also be problematic when they move in the magnetic field or when the strength of the magnetic field changes, because eddy currents and local magnetic fields can be induced that interfere with the spatial encoding magnetic field of the scanner. Thus, for moving parts, the electrical conductivity of the material must be strictly limited. Stiff polymer materials are a good alternative for applications in the MRI environment. Sensors and actuators based on electrical recording or actuation principles should also be avoided because, first, the electrical information can be disturbed by the magnetic fields and, second, the electrical fields generated by the device may fluctuate and cause magnetic inductions disturbing the image quality. Electrical components may be brought into the MRI environment if their electrical signals are of low frequency and low amplitude, and if the components are placed at a certain distance from the scanner and/or they are shielded (Flueckiger, et al. 2005; Gassert, et al. 2005; Khanicheh, et al. 2006). Sensors with optical recording principles have been widely employed to measure position (Gassert, et al. 2006; Khanicheh, et al. 2006), force and torque (Chapuis, et al. 2004; Khanicheh, et al. 2006; Riener, et al. 2005c).

Typical MRI-compatible actuation technologies are based on hydraulic or pneumatic principles, special electromagnetic principles, shape memory alloys, contractile polymers, piezoelectric actuation, materials with magnetostriction properties, or bowden cables (Hollerbach, et al. 1992a; Tsekos, et al. 2007; Yu and Riener 2006). A recent actuation principle has been realized by electro-rheological fluids (ERFs) (Khanicheh, et al. 2006). Among these working principles, fluidic actuations are promising solutions for MRI-compatible robots that are intended to perform defined functional movement tasks, because

1) the fluids are magnetically inert in nature and the moving endeffector can be made MRI-compatible,
2) the power can be generated distantly from the endeffector and sent to the endeffector inside the MRI scanner via transmission hoses,
3) the actuators can provide large movement ranges and large forces,
4) the force-to-mass ratio is high, and
5) the transmission can be made flexible so that they can be placed adaptively to the work environment (Hollerbach, et al. 1992b; Yu and Riener 2006).

In the literature, many efforts have been made for the application of pneumatic actuation technologies to MRI-compatible robotic systems (Diedrichsen, et al. 2005) and devices (Briggs, et al. 2004; Golaszewski, et al. 2002; Zappe, et al. 2004). Hydrostatic actuation was applied in master-slave setups in order to interact with human motion (Gassert, et al. 2006) or to position a forceps for surgery (Kim, et al. 2002). Reported problems were leakages which resulted in pollution of the lab, performance degeneration, and entrance of air bubbles. Furthermore, image deterioration occurred due to the high magnetic susceptibility of materials used for the systems (Kim, et al. 2002; Wang, et al. 2006). For each degree of freedom, the hydrostatic system in a master-slave configuration needs a second cylinder and a motor to drive. A possible problem is that leakages between the chambers and to the external environment will change the system property after long time. In contrast, a hydrodynamic system driven by a pump has the advantages of long-time stability, easier setup and maintenance.

Traditional hydrodynamic or pneumatic actuation techniques cannot be directly transferred to MRI-compatible applications. The fluid power generators, i.e., hydraulic pumps or pneumatic compressors, consist of ferromagnetic materials. They must be placed outside of the scanner room for safety reason. Control valves are normally actuated by magnetically driven solenoids. Furthermore, valves and pressure sensors also contain ferromagnetic materials. Thus, they must be positioned far away from the scanner and the endeffector to avoid electromagnetic interferences causing malfunction and/or image artifacts. Therefore, long hoses have to be used to transmit the fluid power from the compressor to the control valves and then to the endeffector.

This arrangement results in several challenges for both construction and control. First, the endeffector must be made of MRI-compatible materials so that it can work close to or inside the MRI scanner bore. This can result in friction and stiffness problems at the fluidic cylinder, which is required to transfer fluidic pressure into force and motion. Second, valves and

pressure sensors are distant from the endeffector, causing delay and measurement inaccuracies. Third, long hoses result in high inertia and compliance. Fourth, the system will interact with the user, so that the working pressure must be limited to ensure safety. Reduced pressure may also increase the compliance of the system. Finally, position and force sensors used inside the MRI scanner must be made MRI-compatible, which may reduce their signal quality. The mechatronic setup, including sensor, actuator and controller must be able to cope with these challenges and work in an, accurate, stable and robust way.

In this work two comparable haptic interface devices, one with hydrodynamic and another with pneumatic actuation, were developed and implemented to control a translational one degree of freedom movement for fMRI studies. The interface devices are equipped with MRI-compatible position and force sensors. Position and impedance/admittance controllers were realized to achieve active as well as passive subject movements, which are both required to investigate different fMRI-relevant motion tasks. The two systems were evaluated and compared with respect to control performance. Furthermore, both manipulandum systems were examined for MRI-compatibility in a 3 Tesla MRI scanner.

Technical Concept and Implementation of The MRI-Compatible Mechatronic Systems

Requirements and Concept

The required manipulandum has to be MRI-compatible. To be applicable for functional MRI tasks, it should cover a maximum movement range of 20 cm, maximum velocity of 10 cm/s, and a maximum force of 100 N. Furthermore, it should allow subject passive movements (guide the user's hand to follow a designed position) as well as subject active movements (simulate a virtual spring so that the subject can push or pull against the system). The linear movement range of 20 cm enables full range of wrist extension/flexion and about 40 degrees of elbow extension/flexion, assuming a lower arm length of 30 cm. The low velocity as well as smooth movement is required to avoid head motion, and, thus, artifacts to brain images. Control performance will be compared regarding to the two modes "position control" and "impedance control".

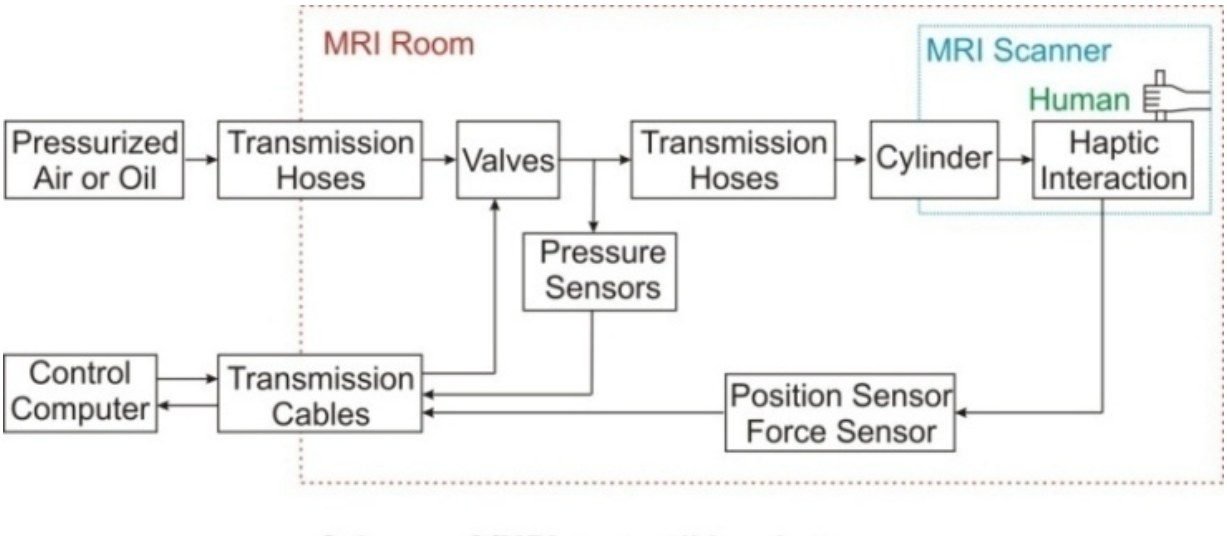

Figure III-18 Scheme of the MRI-compatible manipulandum

This device has one translational degree of freedom and is driven by a hydraulic or pneumatic cylinder to interact with the user's hand (Fig. 18). Position, force and pressure sensors send the respective information to the control computer. The fluidic power of the pressurized air or oil is generated out of the MRI scanner room, regulated by computer controlled valves, and then sent to the cylinder via long transmission hoses.

Construction Materials

All the materials put inside or close to the MRI scanner must have low magnetic susceptibility and low electric conductivity. Therefore, PET and PVC plastic were taken as the main construction material for frames and mechanical adapters. Nevertheless, metals have to be used for some parts required to be stiff, such as the cylinders that will work under high pressure and force. Both cylinders were specially designed and manufactured, with aluminum being the housing material. The moving piston of the pneumatic cylinder is made of PET, while that of the hydraulic cylinder is made of bronze to sustain the higher forces due to the significantly higher pressures. Both aluminum and bronze have low magnetic susceptibilities (20.7×10^{-6} and -0.879×10^{-6}), comparable with oxygenated and deoxygenated blood (about -9.0×10^{-6} and -7.9×10^{-6} (Schenck 1996)). Bronze was chosen for piston because its electrical conductivity ($7.5\times10^{6}\ \Omega^{-1}m^{-1}$) is small.

Force & Position Sensors, Signal Transmission

Both manipulandum systems are comprised by a force and a position sensor. The force sensor consists of a processing circuit and three optical glass fibers, one with emitting laser light and

two with receiving laser light (Fig. 19). The processing circuit, which is located outside the scanner room, generates the laser signal I0. This laser signal is sent to the hand bar by the emitting fiber, and picked up by the receiving fibers. Then, laser signals I1 and I2 are sent out of the MRI room via the receiving fibers, measured by the processing circuit, and read into the control computer. When a pulling or pushing force is applied to the hand bar, the emitting fiber is slightly displaced, thus, changing the light intensities in the two receiving fibers. As a result, the force is detected by the change of the ratio of light intensities I1 and I2.

An optical encoder, LIDA 279 by HEIDENHAIN, works together with a resistive potentiometer, MTP-L 22 by RESENSO, to measure the hand bar position. The voltage on the potentiometer is 10V DC and the resulting current is about 0.13 mA. A shielded cable connects the sensors with the processing circuit. Both the optical encoder and the resistive potentiometer (which works with low DC current only) are MRI-compatible (Yu, et al. 2007).

Hydrodynamic & Pneumatic Actuation, Power Transmission

The oil used in hydrodynamic actuation is Orcon Hyd 32, which is accepted as a lubricant with incidental food contact (H1). Hence, it is appropriate for biomedical applications.

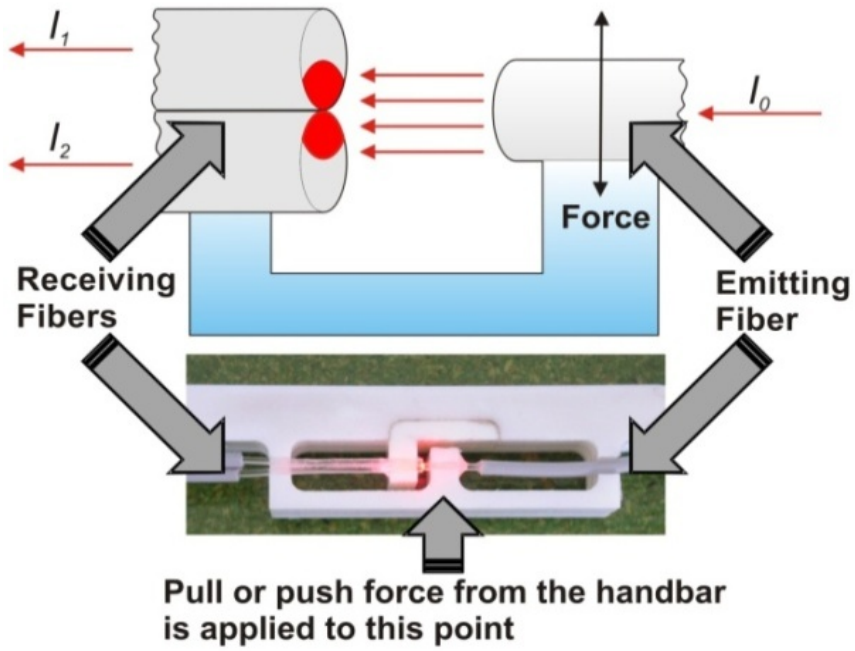

Figure III-19 Custom made MRI-compatible force sensor based on an optical measurement principle

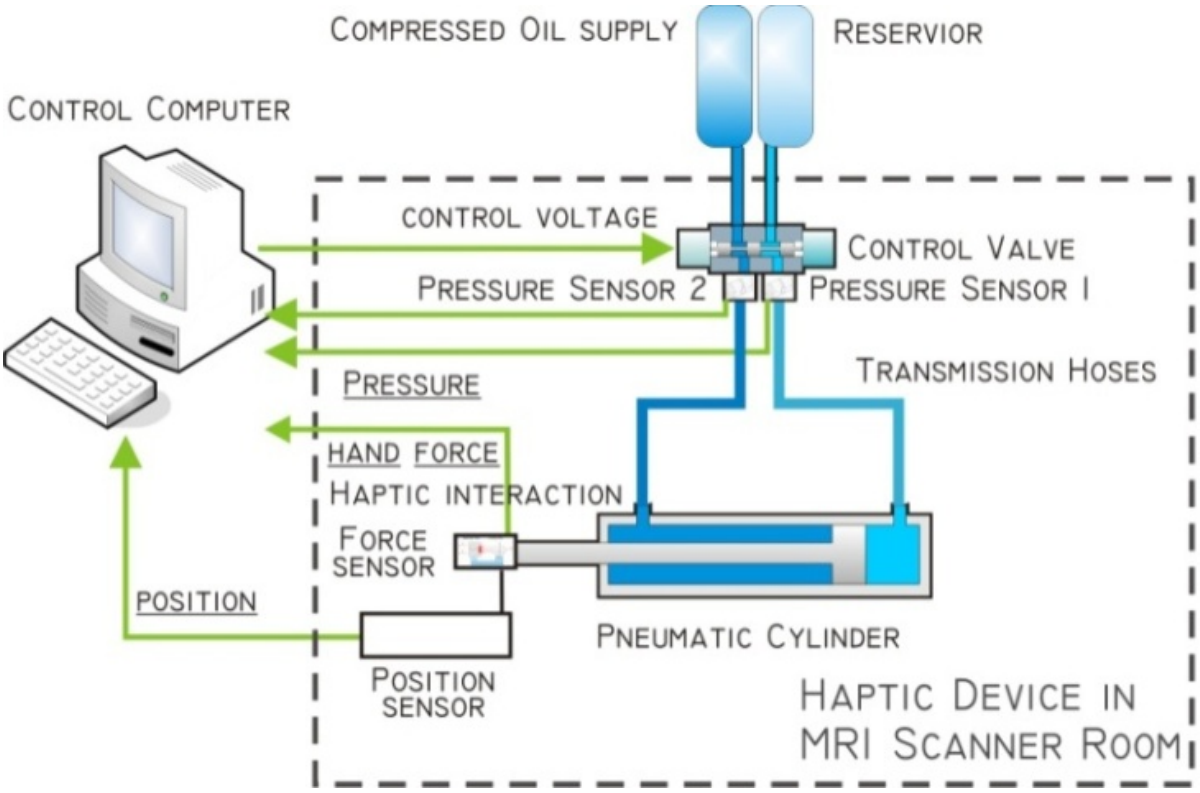

Figure III-20 Overview of the hydrodynamic system

The supply oil pressure from the compressor is 15 bar or 25 bar. A directional valve regulates oil flow and, thus, controls the movement of the actuation cylinder (Fig. 20). Two pressure sensors were mounted on the valve manifold. The bulk modulus of oil is rather large (Table 16), so it is nearly incompressible. The actuation system is not back-drivable, in the sense that the piston cannot be easily moved when the directional valve is powered off since it is closed.

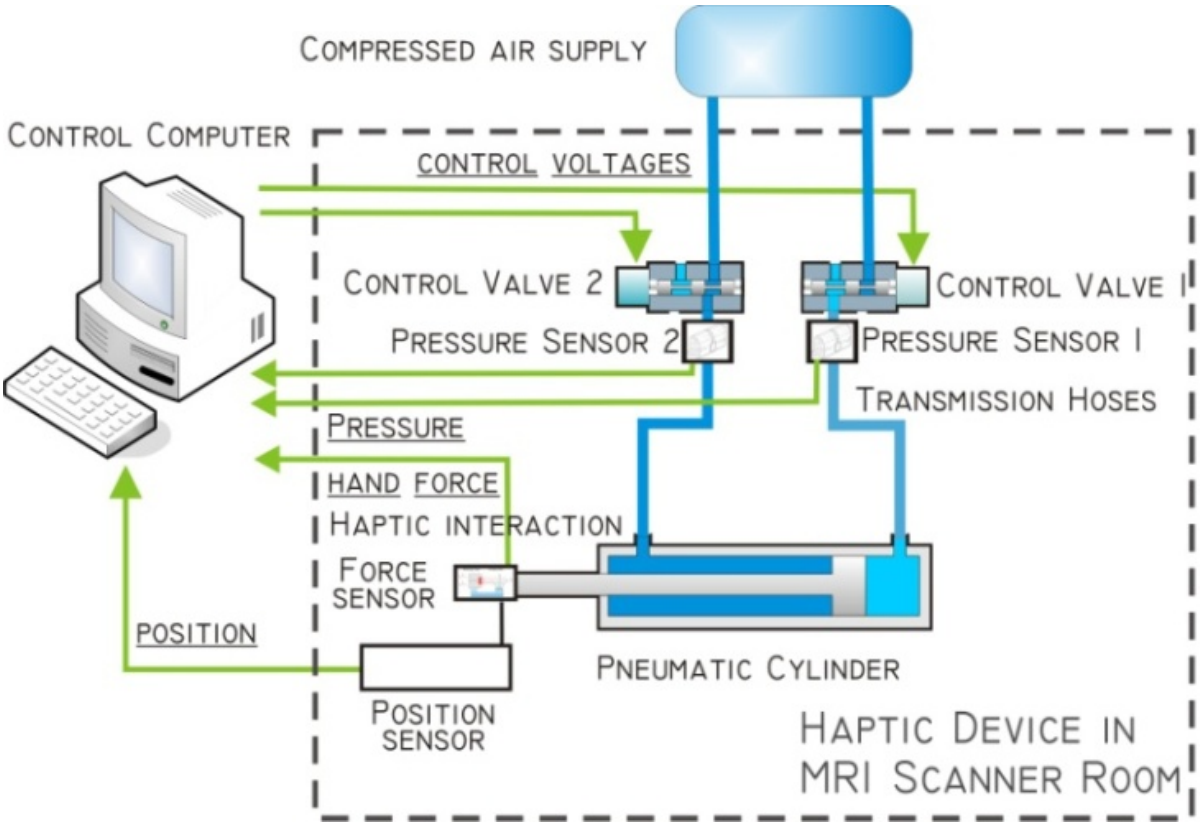

Figure III-21 Overview of the pneumatic system

For pneumatic actuation, the supply air pressure is 5 bar, as in conventional applications. Both flow control and pressure control can be implemented. Flow control is appropriate for position regulation such as point-to-point movements, and it can be achieved by a directional flow valve in a similar structure as the hydrodynamic system (Fig. 20). Pressure control is considered superior to flow control to overcome limitations of compressibility, friction and external disturbances (Hollerbach, et al. 1992a). In our application the manipulandum interacts with human subjects and the interaction force varies within a large range, so that we preferred pressure control. For each cylinder chamber, one valve regulates the pressure with the feedback from a pressure sensor (Fig. 21).

The hydraulic and pneumatic transmission hoses between the control valves and the cylinders are 6 m and 5 m long, respectively. The valves were located at the corner of the scanner room, far from the scanner isocenter. The scanner magnetic field decreases rather quickly with increasing distance from the scanner bore and comes to be only 0.2 mT at the valve location (Philips 2007) (For comparison, the magnetic field of the earth is about 0.03 – 0.06 mT).

Table III-16 Hydrodynamic and pneumatic system configuration

Properties	Hydrodynamic	Pneumatic
Power generation		
Compressor type	Bucher hydraulics, QX21-016-R	Jun Air compressor, Quite Model 6-15
Supply pressure Ps	15 bar* (≤ 25 bar*)	4 bar*
Exhaust pressure Pe	0.4 bar*	0 *
Fluid media		
Bulk modulus K	1.25×104 bar	Absolute pressure P
Density ρ	856 kg/m3	P/Pe×1.2 kg/m3
Kinetic viscosity υ	3.1×10-5 m2/s	1.5×10-5 m2/s
Custom Made double acting cylinders		
Housing material	Aluminum	Aluminum
Piston material	Bronze (CuSn8)	PET
Cross section A1	2.54 cm2	9.62 cm2
Cross section A2	1.41 cm2	7.85 cm2
Stroke L	0.24 m	0.25 m
Working pressure limit	25 bar	6 bar
Transmission Hose		
Type	Festo PUN-H-8*1.25 tube	Parker Push-lok 831 hose
Length Lt	6 m	5 m
Cross section At	0.317 cm2	0.283 cm2
Dynamics		
Force range	-194…356 N	-314…384 N
Velocity range	-0.11…0.19 m/s	-1.51…1.67 m/s
Reynolds Number (laminar flow: <2300)	0…494 always laminar flow	0…22731 laminar and turbulent flow

*: Relative to environment air pressure;
Pressure unit: 1 bar=10^5 Pa; Environment pressure is about 1.013 bar

Cables for electronic signal transmission (position sensors, pressure sensors and control valves), tubes for fluidic power transmission, as well as glass fibers for laser transmission, entered the scanner room through two tunnels in the wall. In the tunnel, the shielding layers of cables were connected to the shielding layer of the MRI room. Thus, noise in the control room is prevented from going to the imaging system.

Control Software and Data Acquisition

The controllers were designed in MATLAB Simulink and then compiled to the control computer that runs an xPC target and communicates with the system by a data acquisition card (AD622, HUMUSOFT). The sampling frequency was 1 kHz.

MRI-Compatibility Examination

The MRI-Compatibility of the two mechatronic systems must be examined by fMRI scanning. The fMRI experiments were conducted in each of the following experimental conditions: 1) no device; 2) silent device: the haptic interface was in the scanner bore and not in operation; 3) functioning device: the manipulandum was in the scanner bore and in operation. In condition 2) and 3), valves and sensors were put far away from the scanner isocenter.

Two methods were taken to evaluate whether artifacts have been introduced into the fMRI images. The signal-to-noise ratio (SNR) quantitatively estimates whether additional noise has been introduced into fMRI procedures. Image noise comes from fluctuations in electrical currents. These currents generate fluctuating magnetic fields, which induce noise signals in the MRI recording coils. The SNR values were calculated according to the signal-background method (McRobbie 2003)

$$\text{SNR} = \frac{0.66 \times \text{mean signal}}{\text{average of noise region standard deviations}}$$

For an acquired image, signal is given by the mean pixel value from a region of interest (ROI) within the phantom, while the noise is computed by the average standard deviation in four selected regions out of the phantom. The region of interest covers about 75% of the phantom area. A second method is image subtraction. This is a qualitative method to check whether image shifts or deformations did occur.

Closed-Loop Control Strategies

Hydrodynamic Controller Design

Hydraulic oil compressibility is characterized by the bulk modulus K. Changes of pressures P_1 and P_2 in the cylinder chambers can be written as

$$\begin{aligned} \dot{P}_1 &= \frac{K}{V_1}(-\dot{V}_1 + q_1) \\ \dot{P}_2 &= \frac{K}{V_2}(-\dot{V}_2 + q_2) \end{aligned} \quad (1)$$

Here $V_1 = V_{10} + xA_1$ and $V_2 = V_{20} + (L - x)A_2$ are the total fluid volumes on two sides of the cylinder, L is the stroke of the cylinder, x is the position of the piston, V_{10} and V_{20} are the dead volumes, A_1 and A_2 are the cross sections of cylinder chambers, $q_1$and q_2 are oil flows that are dependent on the chamber oil pressure, supply oil pressure or reservoir oil pressure, and also on the control signal u (Sohl and Bobrow 1999).

According to (1), the velocity of the piston is:

$$\begin{aligned}\dot{x} &= \frac{1}{A_1}q_1 - x\frac{\dot{P}_1}{K} - \frac{V_{10}}{A_1}\frac{\dot{P}_1}{K} - \frac{1}{A_1}\dot{V}_{10} \\ &= \frac{-1}{A_2}q_2 + (L-x)\frac{\dot{P}_2}{K} - \frac{V_{20}}{A_2}\frac{\dot{P}_2}{K} - \frac{1}{A_2}\dot{V}_{20}\end{aligned} \quad (2)$$

First, we consider the steady situation. Pressure changes and dead volume variations are ignored. In this case, $\dot{P}_1$, $\dot{P}_2$ and $\dot{V}_{10}$, $\dot{V}_{20}$ are all equal to zero. Thus, the velocity of the piston is fully determined by the oil flows q_1 and q_2:

$$\dot{x} = \frac{1}{A_1}q_1 = \frac{1}{A_2}q_2 \quad (3)$$

When the piston moves at a constant speed, the pressures P_1 and P_2 are constants, too. Thus, the oil flows q_1 and q_2 only depend on the proportional valve. As a result, the control voltage to the proportional valve regulates the velocity of the piston, which can be modeled by a lookup table (Fig. 22 and 23).

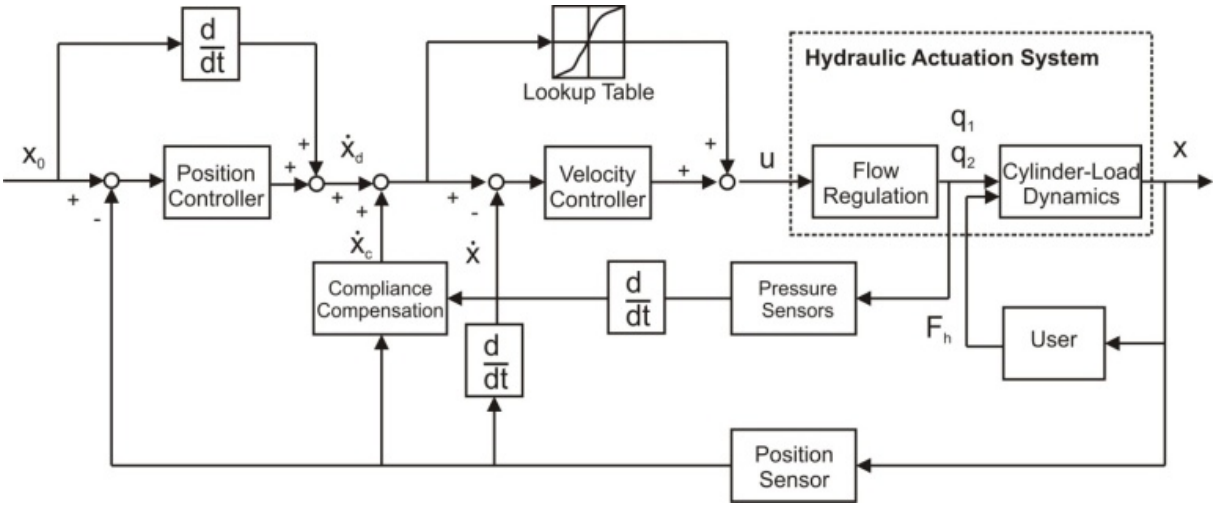

Figure III-22 Position controller for the hydrodynamic system

A velocity controller was designed to deal with model uncertainties, external disturbances, and most important in our application, compliance from the hydrodynamic system. This controller consists of a compliance compensation component and a proportional component (Fig. 22 and 23).

In our hydraulic system, compliance comes from pressure variations $\dot{P}_1$, $\dot{P}_2$, long hose volumes V_{10} ,V_{20} and their variations $\dot{V}_{10}$, $\dot{V}_{20}$. It can significantly affect the system performance. The dead volumes are the transmission hose volumes $V_{10} = V_{20} = L_t A_t$ When the hydraulic system works at 15 bar supply pressure, the velocity range is [-11, 19] cm/s (Tab. 16). Both $\dot{P}_1$ can rise up to 124 bar/s, which results in

$$\left| -x\frac{\dot{P}_1}{K} \right| = 0.24 cm/s, \qquad x = L$$

$$\left| -\frac{V_{10}}{A_1}\frac{\dot{P}_1}{K} \right| = \left| -\frac{L_t A_t}{A_1}\frac{\dot{P}_1}{K} \right| = 0.74 cm/s$$

These terms are relatively large in the working velocity range and cannot be neglected. It can also be seen that the long hoses are the main source of high compliance. Additionally, we have observed by visual inspection that the hose volumes also change as the inside pressures change, but cannot detect that quantitatively. We design the compliance compensation component as:

$$\dot{x}_c = -\frac{1}{2}\left[-x\frac{\dot{P}_1}{K} - \frac{V_{10}}{A_1}\frac{\dot{P}_1}{K} + (L-x)\frac{\dot{P}_2}{K} + \frac{V_{20}}{A_2}\frac{\dot{P}_2}{K} \right] \quad (4)$$

Besides compliance, cylinder pressure variations, model errors, external disturbances, as well as uncompensated compliance components - $(1/A_1)\dot{V}_{10}$, - $(1/A_2)\dot{V}_{20}$, also deteriorate the control performance. The proportional controller handles these problems and makes the whole system robust. The coefficient was experimentally adjusted to be 0.12 V/(cm/s). The user force F_h affects pressures P_1 and P_2, and causes a shift in the voltage-velocity lookup table. The velocity controller can correct this shift. A proportional-derivative (PD) position controller was designed to work in cascade with the velocity controller to guide the user's hand and track the given position trajectory (Fig. 22).

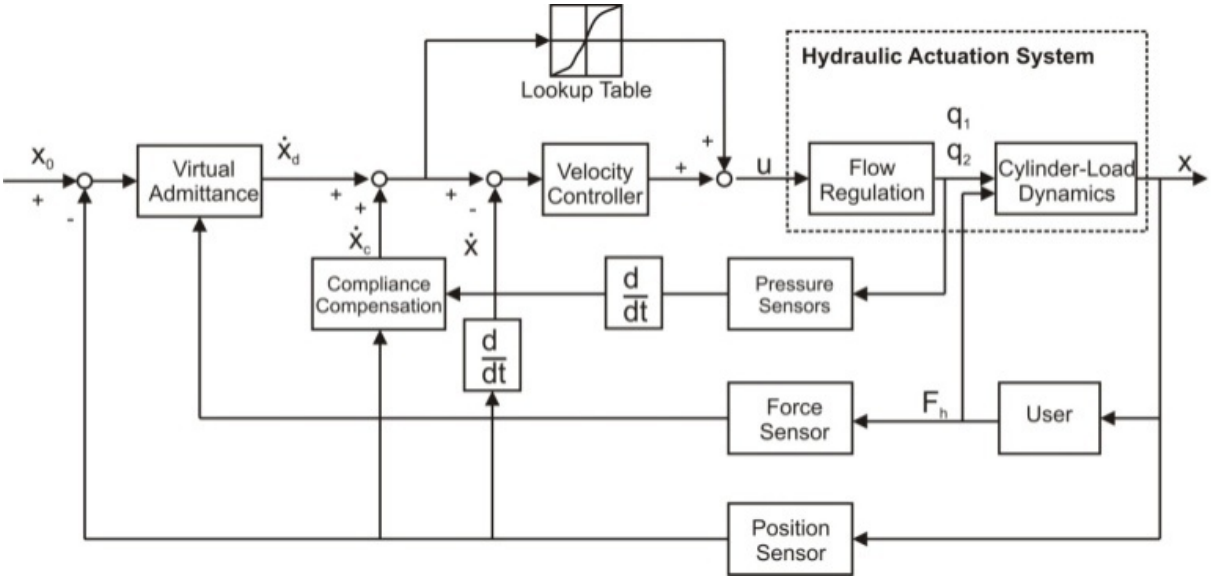

Figure III-23 Admittance controller for the hydrodynamic system. The virtual spring can be achieved by setting the virtual admittance to be $\dot{x}_d = F_h / K_v - K_x / K_V (x - x_0)$.

It is not possible to realize impedance control on the hydrodynamic system, because it is not naturally back-drivable due to the incompressibility of oil. However, the virtual spring for user active movements can be simulated by the following admittance control law (Fig. 23):

$$\dot{x} = \frac{1}{K_v}\left[F_h - K_x (x - x_0)\right] \quad (5)$$

Since the manipulandum moves in a low speed range, we can set K_v to be a small value such that the viscous term $K_v \dot{x}$ is relatively insignificant in the admittance relationship. Then

$$F_h - K_x (x - x_0) = K_v \dot{x} \approx 0 \quad (6)$$

and the hydrodynamic system behaves like a virtual spring with stiffness K_x. Here K_v was experimentally defined to be 1 N/(cm/s), and K_x can vary from 1 to 10 N/cm. If K_x was set to be very small to simulate a soft spring, the term $K_x (x - x_0)$ goes close to $K_v \dot{x}$, and the viscous effect becomes obvious. With these parameters the system remained stable.

Pneumatic Controller Design

Since the pressure sensor measures the cylinder pressure relative to the environmental pressure, we also use relative pressure. The force by the pneumatic cylinder is

$$F_c = P_1 A_1 - P_2 A_2 \quad (7)$$

Here, we regulate the pressures P_1 and P_2 in two cylinder chambers by two independent valves (Fig. 21), and thus regulate the force produced by the cylinder.

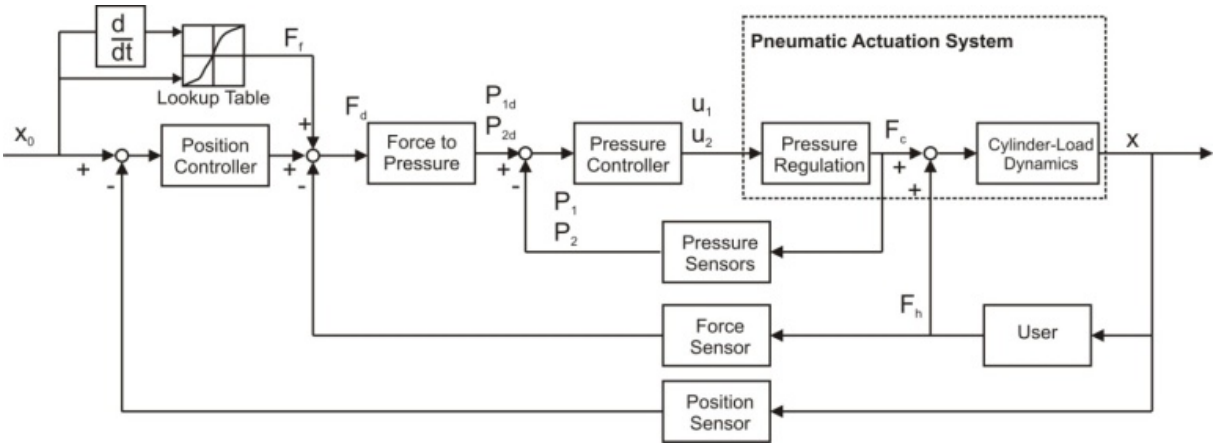

Figure III-24 Position controller for the pneumatic system

Given the desired force F_d, the desired pressures P_{1d} and P_{2d} are calculated. If $F_d \geq 0$, then

$$\begin{cases} P_{1d} = \dfrac{1}{A_1}(F_d + P_{20} A_2) \\ P_{2d} = P_{20} \end{cases} \quad (8)$$

and if $F_d < 0$, then

$$\begin{cases} P_{1d} = P_{10} \\ P_{2d} = -\dfrac{1}{A_2}(F_d - P_{10} A_1) \end{cases} \quad (9)$$

where $P_{10} = P_{20} = 1$ bar. A first order controller was designed for pressure control:

$$u_{1,2} = \frac{2}{1/2\pi \times 25)s+1}(P_{1,2d} - P_{1,2}) \quad (10)$$

The pressure control loop is the innermost loop of the pneumatic system for both position and impedance control. We close the force control loop for force and impedance control, and then close the position loop for position control (Fig 25).

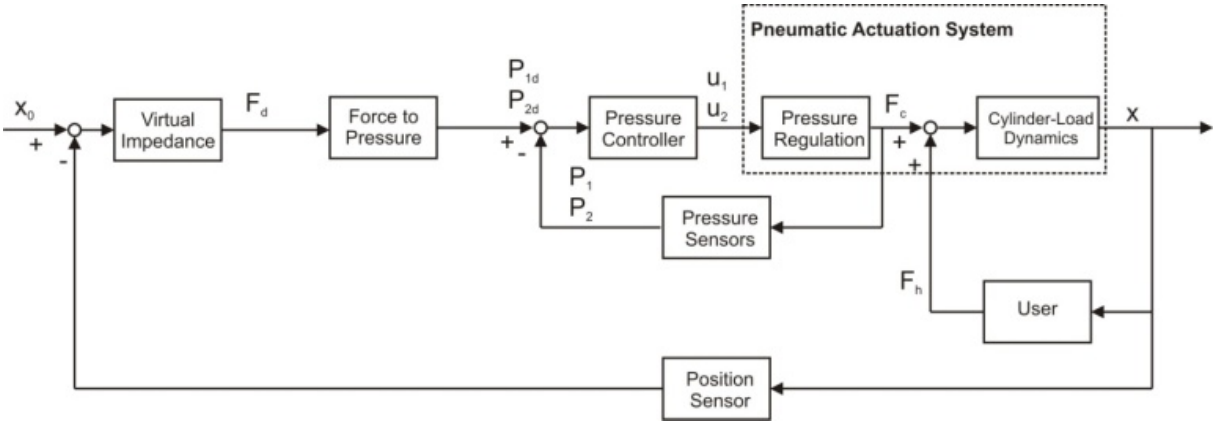

Figure III-25 Impedance controller for the pneumatic system. The virtual spring can be achieved by setting the virtual impedance to be $F_d = -K_x(x - x_0)$.

A position controller with friction compensation worked in cascade with the force-pressure regulator to obtain user passive movement. Due to manufacture and material properties, the friction depends not only on velocity, but also on position. The friction was modeled by a 2-D lookup table of the reference position signal, and then compensated by force -pressure control. The user force was measured by the optical force sensor and got corrected afterwards. The position controller is also of PD form.

Both admittance control and impedance control can be implemented on the pneumatic system (Richardson, et al. 2003; Yong and Barth 2005) for virtual spring simulation. Admittance control requires a good position/velocity controller that is robust against force disturbances, as the velocity controller in our hydrodynamic system. Here the position controller depends on the nested force-pressure regulator and suffers from the long distance between the valves, pressure sensors and the cylinder. Thus, admittance control is not the optimal option. On the other hand, pneumatic systems are natural impedances due to the compressibility of air, and impedance control can be realized directly by pressure regulation.

The impedance control law is quite straightforward

$$F_d = -K_x(x - x_0) \quad (11)$$

It calculates the desired force from the measured position and the specified stiffness, and then feed this signal to force-pressure regulation to achieve the desired force (Fig. 25).

Results and Discussion

Hydrodynamic System Control Performance

To analyze the influence of working pressure on the dynamic performance, we tested the hydrodynamic system at two supply pressures of 15 bar and 25 bar, respectively. Here, 15 bar is the minimal working pressure for the hydrodynamic system to fulfill the defined velocity requirement, while 25 bar is the limit pressure for the hydrodynamic system to work safely.

The position control performance was first examined for step responses (Fig. 26). The reference step curve jumped twice from 5 cm to 15 cm and back, and then jumped twice from 5cm to 10 cm and back. When the hydrodynamic system worked at 15 bar, the steady position error was smaller than 0.06 cm, overshoot was smaller than 0.02 cm, and rise time was about 3.14 s. When the system worked at 25 bar, the steady position error was still smaller than 0.06 cm, but the overshoot went up to 0.27 cm and the rise time decreased to 0.86 s.

We then checked the position controlled hydrodynamic system for dynamic tracking performance. A so-called “chirp” signal from MATLAB Simulink was taken as the reference trajectory. The signal was of sinusoidal shape, fixed amplitude of 10 cm, and offset 12 cm. The frequency of this signal linearly increased from 0 to 1 Hz as time went from 0 to 100 s. The actual position curve was recorded and compared with the reference “chirp” signal for bandwidth information (Fig. 27). The position bandwidth for the given signal was 0.48 Hz when the hydrodynamic system worked at 15 bar, and went up dramatically to 0.65 Hz for the working pressure of 25 bar.

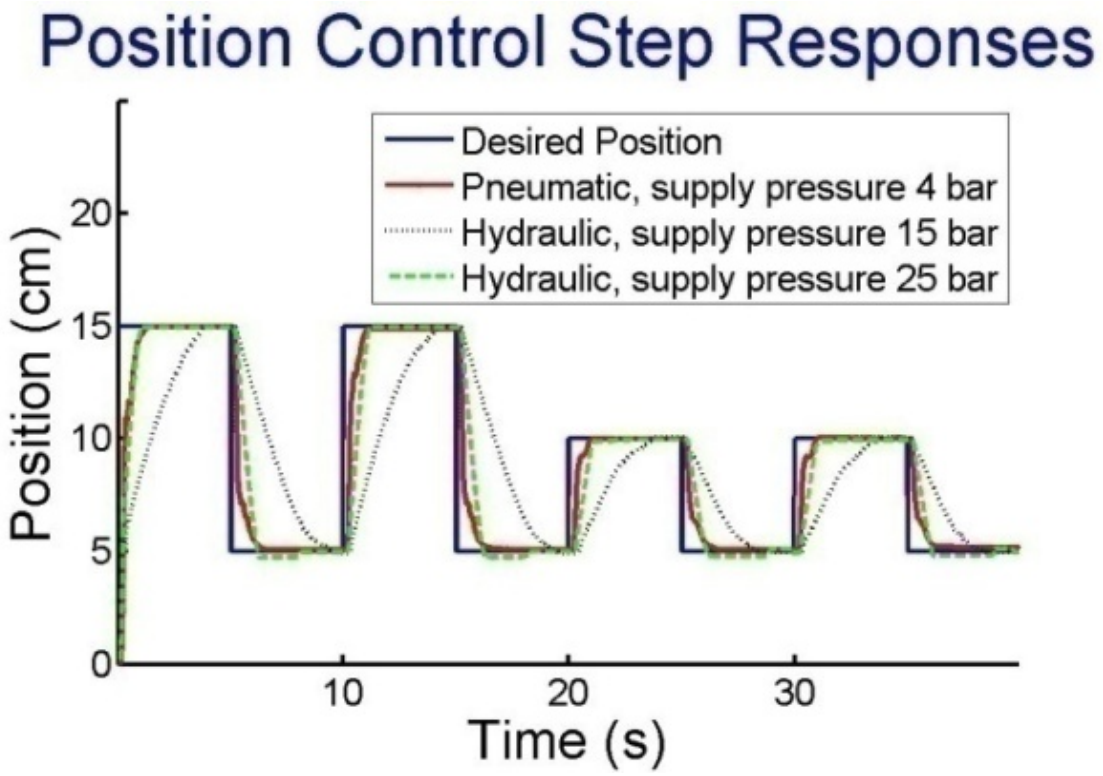

Figure III-26 Step responses of two hydrodynamic systems and the pneumatic system under position control

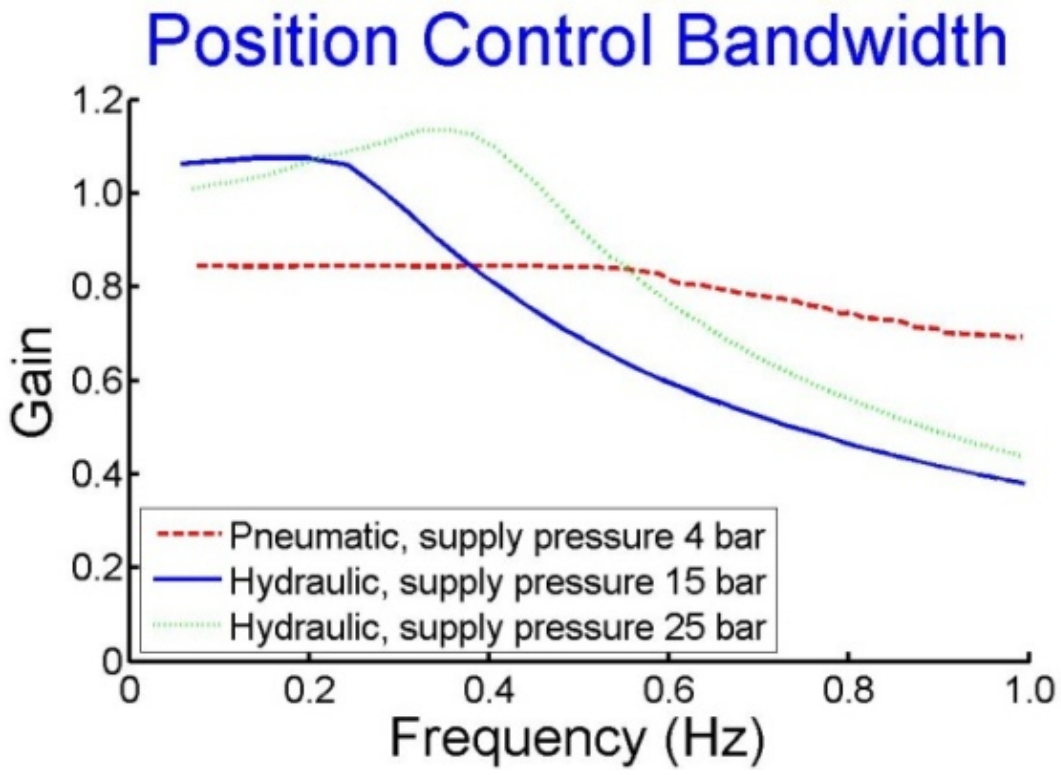

Figure III-27 Position control bandwidth of the hydrodynamic system (at 15 and 25 bar) and the pneumatic system (5 bar)

User active movements were achieved by the simulated virtual spring. Figure 28 shows an example spring of stiffness 5 N/cm when the hydrodynamic system worked at 15 bar and 25 bar of supply pressure. The actual force F is the user force measured by the optical force sensor. This force drives the hand bar from the equilibrium position x_0 to a certain position x. For an ideal spring, there will be a reaction force $K_x(x-x_0)$, which was denoted as the virtual force in the plot. If the hydrodynamic system simulates the virtual spring, there should be $F=K_x(x-x_0)$, and two curves coincide. It can be seen from the plot that the virtual force curve coincided quite well with the actual force curve at 25 bar working pressure, and was slightly postponed at 15 bar working pressure. When the spring constant is small to simulate a soft spring or the device moves fast, the neglected viscous term becomes significant and blurs the spring feeling. This resulted from the admittance control law we used.

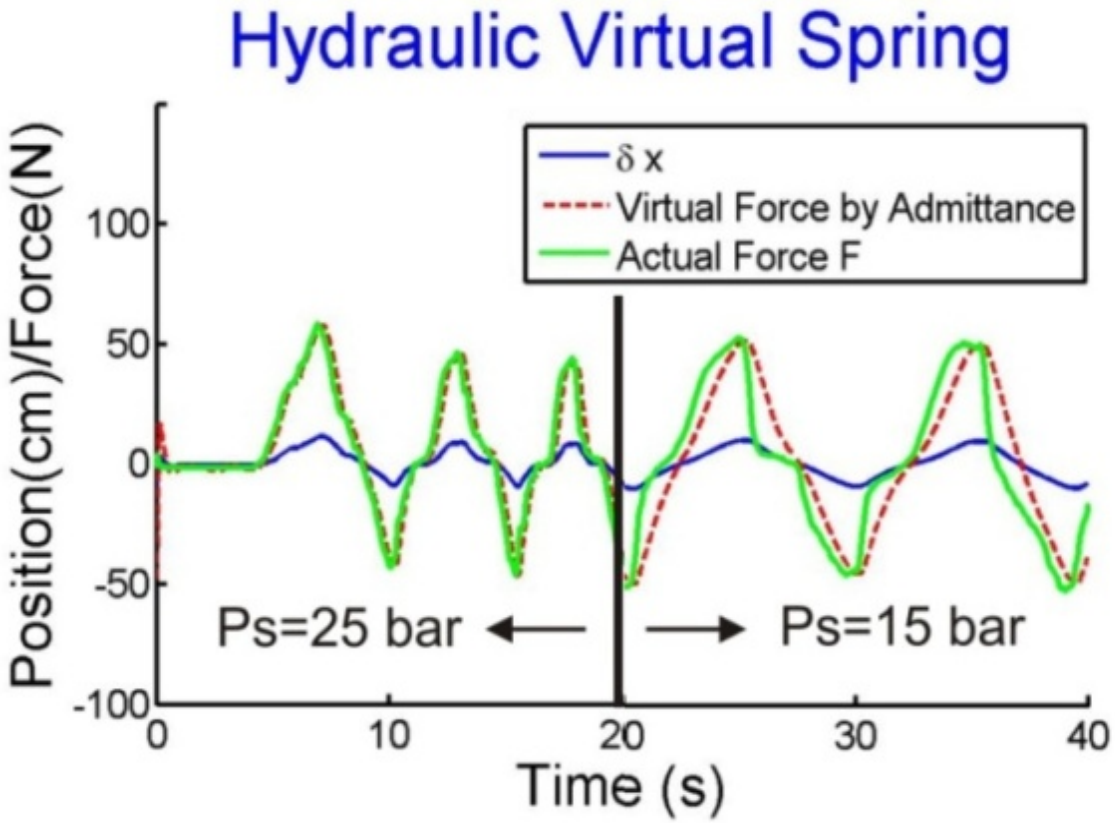

Figure III-28 Results of the hydrodynamic admittance controller at 25 bar (left) and at 15 bar (right) to simulate a virtual spring

Pneumatic System Control Performance

We used exactly the same procedures to analyze the controlled performance of the pneumatic system as we did with the hydrodynamic system. According to the step responses (Fig. 26), the steady position error was smaller than 0.25 cm, overshoot smaller than 0.01 cm, and the

rise time was about 0.86 s. The position bandwidth for the given "chirp" signal was around 0.9 Hz, higher than the bandwidth of the hydrodynamic system working at 15 bar or 25 bar.

An example of the simulated spring was shown in figure 29. The spring constant was also 5 N/cm. The hand bar was driven away from the equilibrium position x_0 to a certain position x by the user. Similar as in the previous section, an ideal spring reaction force is $-K_x(x-x_0)$, which was again denoted as the virtual force in the plot. The cylinder tried to produce this force, and actually generated the force F. It can be seen that the actual force closely followed the desired virtual.

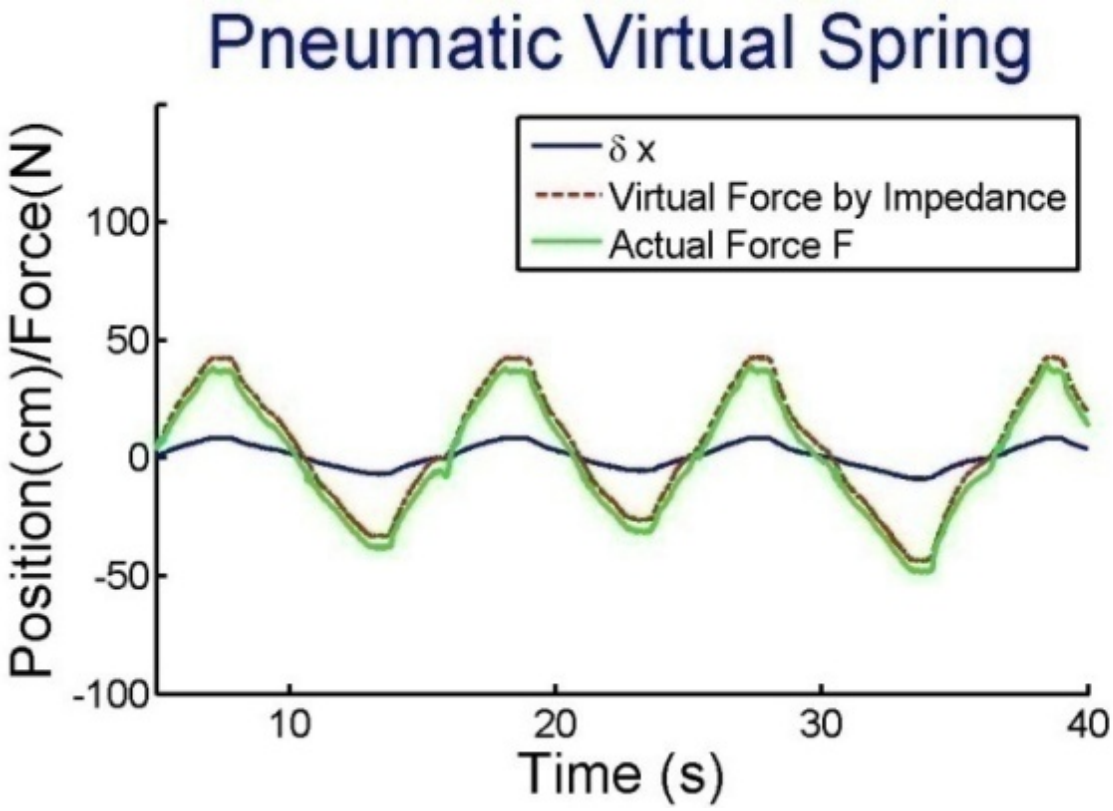

Figure III-29 Results of the pneumatic impedance controller to simulate a virtual spring, supply pressure 4 bar

MRI-Compatibility Evaluation

Both mechatronic systems were tested for MRI compatibility in a 3.0 T MRI system (Philips Medical Systems, Eindhoven, The Netherlands) equipped with an 8 channel SENSE(tm) head coil. For the functional acquisitions, a T2* weighted, single-shot, field echo, EPI sequence of the whole brain (TR = 3000msec, TE = 40msec, flip angle = 82°, FOV = 220mm × 220mm, acquisition matrix = 128 × 128, in plane resolution = 1.7 × 1.7mm. thickness = 3mm, no gap) with a SENSE factor of 2 was applied to collect signals from 39 contiguous slices. Both devices were placed completely inside the scanner bore, but not in the imaging region

(Fig. 30) The imaging object is a mineral oil phantom. For every slice of the phantom, 20 fMRI images were acquired in each of the three experimental conditions.

Figure III-30 fMRI experiment to examine the MRI-compatibility of our devices

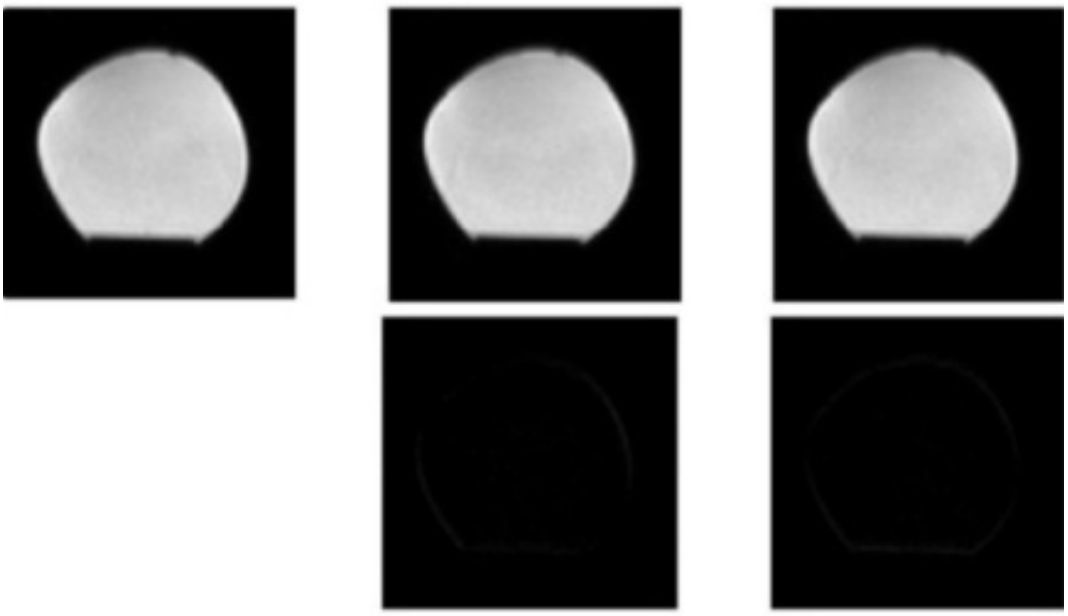

Figure III-31 Phantom scan example images. The left image was obtained when there was no device in the scanner room and used as the control image. The two images at the top of the middle and right columns were obtained from the same location of the phantom as the control image, but in the "silent device" and "functioning device" conditions respectively. These two images were subtracted by the control image and resulted in the two "empty" images below them. No deformations or shifts were observed

Table 17 summarizes the SNR values measured at slice 6 of the phantom for both hydrodynamic and pneumatic fMRI tests. It is shown that high SNR values were obtained in all fMRI experiments. Introduction of the hydrodynamic and pneumatic devices into the MRI environment did not increase the noise level, demonstrating that the construction materials used in the two systems are MRI-compatible. Slight SNR decrease happens to both hydrodynamic and pneumatic systems when they move. As a part of the system, the potentiometer was also proved to be MRI-compatible.

Three example images acquired by the phantom during the hydrodynamic test were presented in figure 31. We took the image obtained when no device was in the scanner as the control image, and subtracted this image from the images of the other two experimental conditions. No deformation, shift, or dark spots were observed.

Table III-17 fMRI test: signal, noise and SNR comparison Values are given as: mean (standard deviation)

Condition	Parameters	Hydraulic*	Pneumatic*
No Device	Image SNR**	427.8 (34.5)	315.7 (23.3)
	Signal level	1338.4 (1.4)	1424.9 (2.3)
	Noise level	2.1 (0.2)	3.0 (0.2)
Silent Device	Image SNR**	432.7 (42.5)	336.3 (28.6)
	Signal level	1346.4 (1.6)	1398.2 (1.7)
	Noise level	2.1 (0.2)	2.8 (0.2)
Functioning Device	Image SNR**	436.4 (23.7)	324.0 (32.1)
	Signal level	1328.4 (1.4)	1377.6 (1.7)
	Noise level	2.0 (0.1)	2.8 (0.3)

*: Two experiments were not done at the same day
**: calculated by 0.66×signal/noise

Under the "functioning device" condition, the devices worked in position control mode, without load. The obtained results were closely similar to the test results obtained in normal environments. Thus, the devices are not affected by the scanner and are compatible with fMRI scanning.

Comparison of the Hydrodynamic & Pneumatic Systems

We summarize the characteristics of hydrodynamic and pneumatic actuation in table 18.

Table III-18 Comparison of hydrodynamic and pneumatic actuation for MRI-compatible applications

Aspects	**Hydrodynamic Actuation**	**Pneumatic Actuation**
MRI-Compatibility and Related Challenges		
Fluid media	Oil and air are both magnetically inert	
Cylinder	MRI-compatible materials such as Bronze, aluminum, plastic, etc.	
Hose length	≥ 5m Active components (e.g., valves) are far from the scanner, which ensures MRI-compatibility This increases compliance of the system Pressure sensors are far away from actuator, causing inaccuracies and time delay	
Fluid Power		
Power generation	Compressor	Compressor
Flow	Laminar	Laminar & turbulent
Working pressure	≥15bar*	≤6bar*
Force	Large	Medium
Working Mode		
Component	Directional valve	Pressure regulation valve
Control target	Flow control, regulate velocity and position	Pressure control, regulate force
Position control	High accuracy Low bandwidth	Medium accuracy Medium bandwidth
Velocity range	Small	Big
Friction or force disturbances	Robust	Sensitive
Back drivability	Not backdrivable when powered off	backdrivable
Others		
Leakage	Rare	Not a problem
Complexity & Cost	High	Medium
Maintenance	Medium	Simple

*: Relative to environment air pressure.

The design requirements have been fulfilled by both the hydrodynamic system and the pneumatic system with different working pressures. With the hydrodynamic system, we were able to achieve smoother movements, higher position control accuracy and improved robustness against force disturbances than with the pneumatic system. In contrast, the pneumatic system is backdrivable and shows better and faster force control performance. Furthermore, it is easier to maintain and has no serious consequences by leakages. In general, pneumatic actuation is more favorable for fast or force-controlled MRI-compatible applications, whereas hydrodynamic actuation can be recommended for applications that require higher position accuracy and slow and smooth movements.

The position bandwidth results shown in figure 27 were obtained in no-load conditions, and they may change when a subject is holding the device.

Conclusion

We have developed two closed-loop MRI-compatible manipulandum interfaces with fluidic actuation, and force as well as position measurement. Both hydrodynamic and pneumatic actuation systems provided satisfactory control performances for defined passive and active fMRI tasks, despite the existing limiting factors such as material choice, long distance between cylinders and valves/pressure sensors, long transmission, and the use of second quality MRI-compatible components. Explicit description and comparison of the controlled hydrodynamic and pneumatic systems were given. This work has resulted to a functional system, which can be the basis for developing different MRI-compatible devices to be used in future fMRI/MRI applications, and can help potential development of devices for specific applications. Due to the different physical properties of oil and air, the performances of hydrodynamic and pneumatic actuation systems differ from each other. The user has to decide, which system better fits the specific applications.

Acknowledgment

The authors would like thank Dr. Tobias Nef, Mr. Joachim von Zitzewitz, Mr. Severin Eisner, Mr. Wolfram Murr and Mr. Andreas Brunschweiler for their support for this work. The authors would also thank Prof. Dr. Peter Bösiger, Dr. Roger Lüchinger and the MR center of ETH and University Zurich for providing the MRI scanner facility

IV. General Discussion

The goal of this thesis has been the implementation of new rehabilitation techniques – namely FES and therapeutic robotics – into an MR-environment. The present results contribute to the debate whether these two both approaches are beneficial to an ongoing recovery process opposed to conventional therapy. The conformance to effectiveness criteria (objectivity, reliability and validity) certainly makes the use of FES and robotics more reasonable – at least for research. Even though the results of the three studies are promising, they only represent the start of verifying suitability in patient treatment. Ultimately, the realization of long-term patient studies will give more revealing answers as to whether FES and robotics are superior to conventional treatment.

The results of the first study demonstrate that FES can be used in the MR-scanner. No reciprocal effects were observed. Images were not affected by FES nor was stimulation influenced by the magnetic field. Two different fMRI paradigms have led to similar brain activations, and repeatability was demonstrated in consecutive measurements.

The second study gives an example how FES-related changes in brain activation patterns as well as motor output can be assessed in a long-term setting. Critical points have been addressed in the above. Relevant patient treatment issues are certainly force gain and functionality of the affected limb. However, the results did not show an increase in maximal force. For this reason, stimulation parameters must be individually adjusted, which might lead to a more difficult fMRI analysis. For the sake of the patient, this must remain the main priority of research. Furthermore, patients being weaker in their limbs compared to healthy controls might even respond to the applied experimental strategy simply because it is challenging enough. And lastly, one factor has been neglected in the study design: the importance of voluntary drive (Lotze, et al. 2003) given that active training is more effective than passive training. Moreover, combining individual effort with FES probably leads to better results as it has been demonstrated in sports training (Gondin, et al. 2006a; Gondin, et al. 2005; Gondin, et al. 2006b; Maffiuletti, et al. 2002a) For rehabilitative treatment, the voluntary cooperation of patients is mandatory for achieving progress. Thus for future studies, the voluntary component has to be implemented in the study designas it seems to play a major role in achieving progress in sports and therapy.

The third study investigated two actuation principles for MR compatible robotics: namely hydrodynamic and pneumatic systems. Both systems can be used for fMRI experiments, depending on the subject of research. Currently, we are testing the hydrodynamic system with healthy subjects (Estevez, et al. 2009). The main reason for the choice of hydrodynamic actuation was the ability to perform slow and smooth movements. Patients with no or little force should be able to move the robot without any disturbances such as rocking motions, and slow movements are less likely to cause head motion artifacts in fMRI images. Even though smooth and slow movements can be generated; head movements could not be totally avoided (Fig. 1).

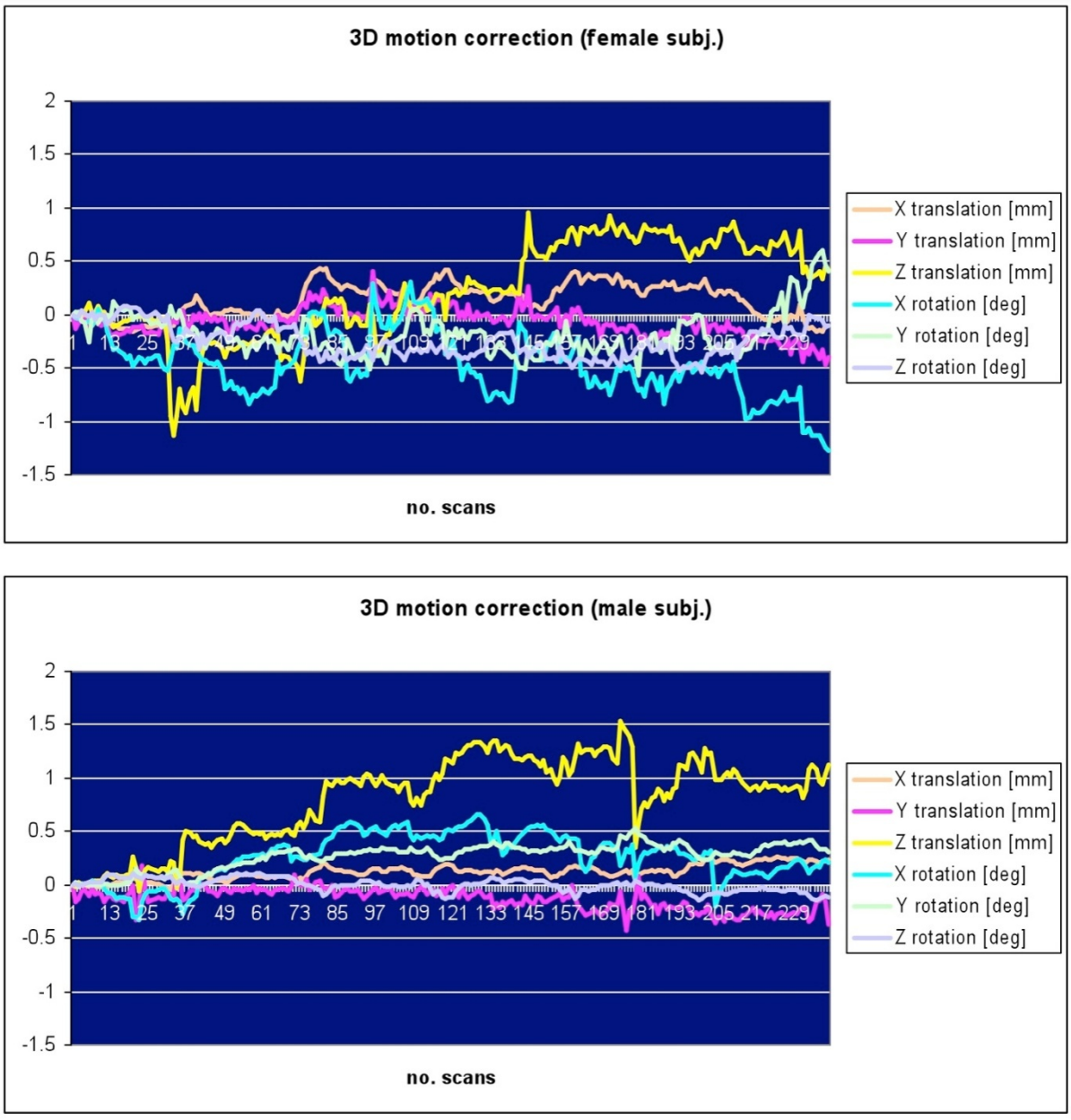

Figure IV-1 Head motions (translations and rotations in each dimension) of two subjects using the fMRI compatible manipulandum

In a test run, 2 subjects (1 female, 1 male) performed push-pull movements at a frequency of apx. 2 Hz. Head motion parameters of the female subject were in the range of apx. -1 to 1mm whereas the male subject was in the range between 0 and 1.5 mm. Nonetheless, resulting preliminary data analysis showed promising images yielding activations within the expected sensorimotor network (Fig. 2 & 3) similar to our results from the FES-studies.

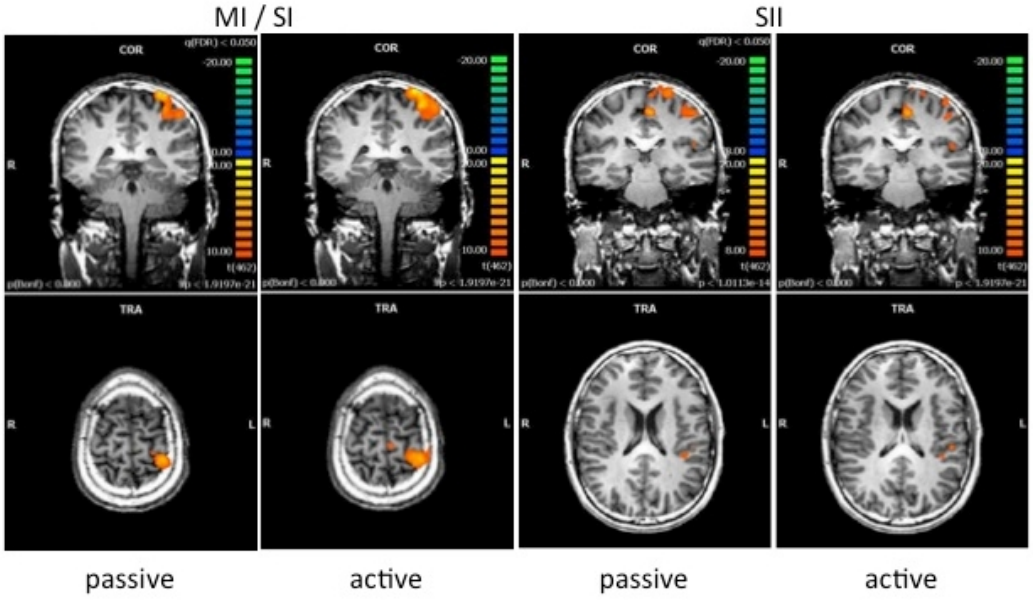

Figure IV-2 fMRI activation maps of two subjects using the fMRI compatible manipulandum. Top row coronar view, bottom row transversal view. MI / SI = primary motory and sensomotory areas. SII secondary senorimotor area. Passive = subjects arms were moved by the device, active = subjects moved voluntarily the device.

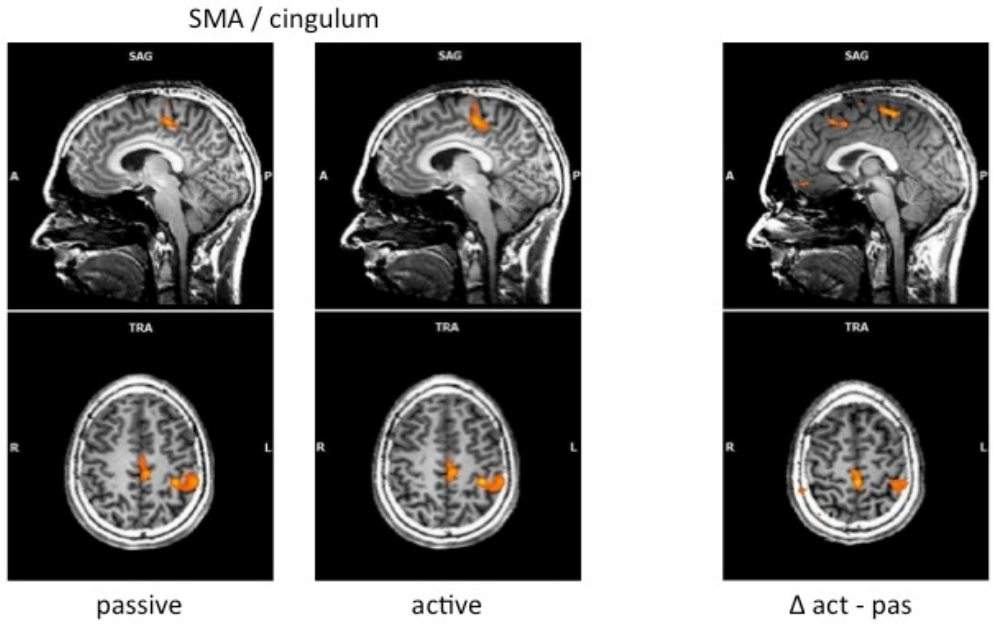

Figure IV-3 MRI activation maps of two subjects using the fMRI compatible manipulandum. Top row sagital view, bottom row transversal view. SMA = supplementary motor area. Passive = subjects arms were moved by the device, active = subjects moved voluntarily the device. Δ act – pas = contrast active vs. passive movement.

Head motion

The problem of head movement in fMRI is well-known (Lund, et al. 2005). One way to correct the data from head motion artifacts is to include movement parameters in the data analysis (Lund, et al. 2005). This approach can lead to increased sensitivity and reduced likelihood of motion-related artifacts. On the other hand, it can also mean that true activation may be removed due to co-activation with stimulus-correlated movement (Lemieux, et al. 2007). An interesting solution addressing large head movements comes from an fMRI study (Lemieux, et al. 2007) investigating epilepsy-related head jerks. They employed two approaches removing motion-related effects: First Friston's Volterra expansion of the six realignment parameters to account for spin excitation history effects across successive scans (Friston, et al. 1996); and an ad-hoc method that attempts to account for effects of large head movements (jerks) by removing the scans from the analysis (Salek-Haddadi, et al. 2006). The results showed that the Volterra component was effective removing small motion artifacts while the scan nulling (removing) of the model was efficient for datasets with higher degrees of motion. Nonetheless, head motion remains an issue in fMRI data analysis; and unfortunately, there is currently not a standard threshold determining the exclusion of data sets. For this reason, it is still mandatory to design fMRI experiments that cause as little movement as possible. Movement preventing aids such as shoulder straps, chest straps, forehead straps, possibly vacuum pillows, might also cause patients to feel more uncomfortable, already lying strapped in a narrow tube. Furthermore, sophisticated restraints such as vacuum pillows can even be less effective reducing smaller head motions (Benar, et al. 2003). Intensifying restraints might even lead to a contrary effect resulting in larger movements of the subject avoiding uncomfortable pressure marks. Thus, it is a tightrope walk between movement restraining and motion-related effects in fMRI data analysis.

Future proceeding

The strength of FES and robotic devices lies in the applications of a passive mode as well as supporting a voluntary action during a rehabilitation program. In other words in the early stage of therapy, FES and robotics provide at least a means to move the affected limb at all. During the ongoing recovery, the patient gains more and more self control to execute the therapeutic tasks, minimizing the effect of FES and robotics to a supporting role. This would be the ideal case. I am aware that there might be no progress at all and a permanent disability may persist. However, several studies report on the beneficial effect of FES in a combined motor therapy (Chae & Yu, 1999; Barbeau, et al. 2002; Rushton, 2003). The initial FES-

therapy starts with a strengthening program followed by the functional training (Popovic, et al. 2001). These training related behavioral gains can be compared with corresponding processes of cerebral reorganization. So far there have been only few studies relating changes within sensorimotor regions over the course of a specific therapy to rehabilitation (Liepert, et al. 2000; Binkofski, et al 2001; Johansen-Berg, et al. 2002; Dobkin, et al. 2004; Winchester et al., 2005; Hamzei, et al. 2006). A well-defined rehabilitation strategy that emphasizes the practice of functional movements is required to accomplish this goal. (Dobkin, et al. 2004). Hence an activation paradigm during neuroimaging that incorporates relevant movements being practiced during rehabilitation is essential to follow the recovery related changes in regions of interest. And finally, behavioral outcome measures must be available that monitor the progress of the patient with adequate sensitivity (Dobkin, 2003).

Here we have demonstrated the use of FES and a robotic arm-device within the MR-scanner. The employed FES-device has already been used in improving grasping and walking functions in patients after stroke or spinal cord injury (Mangold & Keller, 2003 & 2004; Mangold ,et al. 2005; Popovic, et al 2006). In line with Dobkin's above mentioned proposal regarding a well-defined rehabilitation strategy (Dobkin, et al., 2004), the two devices offer an opportunity to produce movements in the scanner, that are a part of the ongoing rehabilitation program. Possible approaches could be generation of isometric strength (Keller & Dewald, 2004), grasping tasks (Mangold, et al. 2005) or stimulation of the ankle (only FES). Dobkin, et al. (2004) and MacIntosh, et al., (2004) demonstrated the feasibility of an ankle dorsiflexion paradigm within the MR-Scanner and its potential value of evaluating gains in gait function. Recently, new MR-compatible robots have been developed (Newton, et al. 2008; Takahashi, et al. 2008). One of them has already been used in an fMRI study investigating its effect on stroke patients (Takahashi, et al. 2008). Patients received 3 weeks therapy that emphasized intense active movement repetition, attention, speed, force, precision, timing and participation in virtual reality games. The employed Hand Wrist Assistive Rehabilitative Device (HWARD) was used in every therapeutic intervention. This is beneficial in terms of data interpretation since no other devices were used (one for fMRI and one for treatment). The main result was that patients with chronic stroke showed significant gains in distal arm behavioral measurements that persisted at least 1 month after the end of treatment. The fMRI findings showed changes within the sensorimotor network that were task related (Takahashi, et al. 2008). This is an exemplary study showing the direction in which our work is going to. In agreement with Takahashi, et al. (2008) the debate whether FES- or robot-assisted therapy is better than conventional therapy has to be continued. This line of

work – especially when behavioral gains are generated – points in the right direction and needs more substantial investigations for instance in multi-center studies.

Implication for therapy

The present study shows that the therapy assisting approaches such as FES and robotics can be used for assessing plastic changes within the cortical areas related to rehabilitative therapy. As a design in patients we would propose to use a block design. Duration of the block design is considerably shorter than in an event-related approach, which makes it fare more tolerable for patients. Furthermore, does an event-related design provide lower statistical power compared to block design due to a smaller ratio of task period to baseline period (MacIntosh et al., 2004). Within rehabilitative training, the duration of a task is designed to regaining strength and, in a later stage, achieving the best functional recovery as possible. Thus, the actual therapeutic session is resembled more by the on-off procedure within a block design. This is one of the critical points addressed by Dobkin, et al. (2004). Event-related designs are more accurate in fast tasks and allow a depiction of the corresponding time courses within different regions of the brain. However, this is not essential in the line of recovering from motor deficits elicited by spinal cord injury or stroke.

V. References

Aagaard P, Simonsen EB, Andersen JL, Magnusson P, Dyhre-Poulsen P. (2002): Neural adaptation to resistance training: changes in evoked V-wave and H-reflex responses. J Appl Physiol 92(6):2309-18.

Adams GR, Harris RT, Woodard D, Dudley GA. (1993): Mapping of electrical muscle stimulation using MRI. J Appl Physiol 74(2):532-537.

Adrian ED, Bronk DW. (1929): The discharge of impulses in motor nerve fibres: Part II. The frequency of discharge in reflex and voluntary contractions. J Physiol 67(2):119-151.

Aisen ML, Krebs HI, Hogan N, McDowell F, Volpe BT. (1997): The effect of robot-assisted therapy and rehabilitative training on motor recovery following stroke. Archives of neurology 54(4):443-6.

Alkadhi H, Crelier GR, Boendermaker SH, Golay X, Hepp-Reymond MC, Kollias SS. (2002a): Reproducibility of primary motor cortex somatotopy under controlled conditions. Ajnr 23(9):1524-32.

Alkadhi H, Crelier GR, Boendermaker SH, Hepp-Reymond MC, Kollias SS. (2002b): Somatotopy in the ipsilateral primary motor cortex. Neuroreport 13(16):2065-70.

Arienzo D, Babiloni C, Ferretti A, Caulo M, Del Gratta C, Tartaro A, Rossini PM, Romani GL. (2006): Somatotopy of anterior cingulate cortex (ACC) and supplementary motor area (SMA) for electric stimulation of the median and tibial nerves: an fMRI study. NeuroImage 33(2):700-5.

Arthurs OJ, Boniface S. (2002): How well do we understand the neural origins of the fMRI BOLD signal? Trends in neurosciences 25(1):27-31.

Baker LL, McNeal DR, Benton LA, Bowman BR, Waters RL. (1993): Neuromuscular Electrical Stimulation: A practical Guide. Downey: Los Amigos Research & Education Institue, Inc. Rancho Los Amigos National Rehabilitation Center.

Beekhuizen KS, Field-Fote EC. (2005): Massed practice versus massed practice with stimulation: effects on upper extremity function and cortical plasticity in individuals with incomplete cervical spinal cord injury. Neurorehabilitation and neural repair 19(1):33-45.

Benar C, Aghakhani Y, Wang Y, Izenberg A, Al-Asmi A, Dubeau F, Gotman J. (2003): Quality of EEG in simultaneous EEG-fMRI for epilepsy. Clin Neurophysiol 114(3):569-80.

Bishop J, Poole G, Leitch M, Plewes DB. (1998): Magnetic resonance imaging of shear wave propagation in excised tissue. J Magn Reson Imaging 8(6):1257-65.

Blickenstorfer A, Kleiser R, Keller T, Keisker B, Meyer M, Riener R, Kollias S. (2008): Cortical and subcortical correlates of functional electrical stimulation of wrist extensor and flexor muscles revealed by fMRI. Hum Brain Mapp.

Briggs RW, Dy-Liacco I, Malcolm MP, Lee H, Peck KK, Gopinath KS, Himes NC, Soltysik DA, Browne P, Tran-Son-Tay R. (2004): A pneumatic vibrotactile stimulation device for fMRI. Magnetic Resonance in Medicine. p 640-643.

Buccino G, Binkofski F, Fink GR, Fadiga L, Fogassi L, Gallese V, Seitz RJ, Zilles K, Rizzolatti G, Freund HJ. (2001): Action observation activates premotor and parietal areas in a somatotopic manner: an fMRI study. The European journal of neuroscience 13(2):400-4.

Burgar CG, Lum PS, Shor PC, Machiel Van der Loos HF. (2000): Development of robots for rehabilitation therapy: the Palo Alto VA/Stanford experience. Journal of rehabilitation research and development 37(6):663-73.

Bushara KO, Wheat JM, Khan A, Mock BJ, Turski PA, Sorenson J, Brooks BR. (2001): Multiple tactile maps in the human cerebellum. Neuroreport 12(11):2483-6.

Butefisch CM, Khurana V, Kopylev L, Cohen LG. (2004): Enhancing encoding of a motor memory in the primary motor cortex by cortical stimulation. Journal of neurophysiology 91(5):2110-6.

Cannon RJ, Cafarelli E. (1987): Neuromuscular adaptations to training. J Appl Physiol 63(6):2396-402.

Carel C, Loubinoux I, Boulanouar K, Manelfe C, Rascol O, Celsis P, Chollet F. (2000): Neural substrate for the effects of passive training on sensorimotor cortical representation: a study with functional magnetic resonance imaging in healthy subjects. J Cereb Blood Flow Metab 20(3):478-84.

Chainay H, Krainik A, Tanguy ML, Gerardin E, Le Bihan D, Lehericy S. (2004): Foot, face and hand representation in the human supplementary motor area. Neuroreport 15(5):765-9.

Chaljub G, Kramer LA, Johnson RF, 3rd, Johnson RF, Jr., Singh H, Crow WN. (2001): Projectile cylinder accidents resulting from the presence of ferromagnetic nitrous oxide or oxygen tanks in the MR suite. Ajr 177(1):27-30.

Chapuis D, Gassert R, Sache L, Burdet E, Bleuler H. (2004): Design of a Simple MRI/fMRI Compatible Force/Torque Sensor. Proc. IEEE International Conference on Robotics and Intelligent Systems.

Chinzei K, Hata N, Jolesz FA, Kikinis R. (2000a): MR compatible surgical assist robot: System integration and preliminary feasibility study. In: Delp S, DiGioia AM, Jaramaz B, editors. Medical Image Computing and Computer-Assisted Intervention - Miccai 2000. Berlin: Springer-Verlag Berlin. p 921-930.

Chinzei K, Hata N, Jolesz FA, Kikinis R. (2000b): MR compatible surgical assist robot: System integration and preliminary feasibility study. Medical Image Computing and Computer-Assisted Intervention - Miccai 2000 1935:921-930.

Ciccarelli O, Toosy AT, Marsden JF, Wheeler-Kingshott CM, Sahyoun C, Matthews PM, Miller DH, Thompson AJ. (2005): Identifying brain regions for integrative sensorimotor processing with ankle movements. Experimental brain research. Experimentelle Hirnforschung 166(1):31-42.

Classen J, Liepert J, Wise SP, Hallett M, Cohen LG. (1998): Rapid plasticity of human cortical movement representation induced by practice. Journal of neurophysiology 79(2):1117-23.

Collins DF, Burke D, Gandevia SC. (2001): Large Involuntary Forces Consistent with Plateau-Like Behavior of Human Motoneurons. J. Neurosci. 21(11):4059-4065.

Conforto AB, Cohen LG, dos Santos RL, Scaff M, Marie SK. (2007): Effects of somatosensory stimulation on motor function in chronic cortico-subcortical strokes. Journal of neurology 254(3):333-9.

Conforto AB, Kaelin-Lang A, Cohen LG. (2002): Increase in hand muscle strength of stroke patients after somatosensory stimulation. Annals of neurology 51(1):122-5.

Cramer SC, Lastra L, Lacourse MG, Cohen MJ. (2005): Brain motor system function after chronic, complete spinal cord injury. Brain 128(Pt 12):2941-50.

Cruz VT, Nunes B, Reis AM, Pereira JR. (2003): Cortical remapping in amputees and dysmelic patients: a functional MRI study. NeuroRehabilitation 18(4):299-305.

Culham J. (2008): Basics of fMRI and the BOLD Response. fMRI 4 Newbies. London: University of Western Ontario. p Tutorial.

Curt A, Alkadhi H, Crelier GR, Boendermaker SH, Hepp-Reymond MC, Kollias SS. (2002): Changes of non-affected upper limb cortical representation in paraplegic patients as assessed by fMRI. Brain 125(Pt 11):2567-78.

Dai TH, Liu JZ, Sahgal V, Brown RW, Yue GH. (2001): Relationship between muscle output and functional MRI-measured brain activation. Experimental brain research. Experimentelle Hirnforschung 140(3):290-300.

Debaere F, Wenderoth N, Sunaert S, Van Hecke P, Swinnen SP. (2004): Changes in brain activation during the acquisition of a new bimanual coodination task. Neuropsychologia 42(7):855-67.

Del Gratta C, Della Penna S, Tartaro A, Ferretti A, Torquati K, Bonomo L, Romani GL, Rossini PM. (2000): Topographic organization of the human primary and secondary somatosensory areas: an fMRI study. Neuroreport 11(9):2035-43.

DeSantana JM, Walsh DM, Vance C, Rakel BA, Sluka KA. (2008): Effectiveness of transcutaneous electrical nerve stimulation for treatment of hyperalgesia and pain. Current rheumatology reports 10(6):492-9.

Diedrichsen J, Yasmin H, Tushar R, Reza S. (2005): Neural Correlates of Reach Errors. Journal of Neuroscience. p 9919 –9931.

Dietz V. (2002): Schwerpunkt aktueller Forschung: die Mobilitätsverbesserung Querschnittgelähmter. Swiss Medical Weekly 130:829 - 839.

Dobkin BH. (2004): Strategies for stroke rehabilitation. Lancet neurology 3(9):528-36.

Dobkin BH, Firestine A, West M, Saremi K, Woods R. (2004): Ankle dorsiflexion as an fMRI paradigm to assay motor control for walking during rehabilitation. NeuroImage 23(1):370-81.

Doyon J, Penhune V, Ungerleider LG. (2003): Distinct contribution of the cortico-striatal and cortico-cerebellar systems to motor skill learning. Neuropsychologia 41(3):252-262.

Doyon J, Song AW, Karni A, Lalonde F, Adams MM, Ungerleider LG. (2002): Experience-dependent changes in cerebellar contributions to motor sequence learning. Proceedings of the National Academy of Sciences of the United States of America 99(2):1017-22.

Durmus D, Alayli G, Canturk F. (2007): Effects of quadriceps electrical stimulation program on clinical parameters in the patients with knee osteoarthritis. Clinical rheumatology 26(5):674-8.

Duzel E, Habib R, Rotte M, Guderian S, Tulving E, Heinze HJ. (2003): Human hippocampal and parahippocampal activity during visual associative recognition memory for spatial and nonspatial stimulus configurations. J Neurosci 23(28):9439-44.

Eickhoff SB, Grefkes C, Zilles K, Fink GR. (2007): The somatotopic organization of cytoarchitectonic areas on the human parietal operculum. Cereb Cortex 17(8):1800-11.

Elbert T, Pantev C, Wienbruch C, Rockstroh B, Taub E. (1995): Increased cortical representation of the fingers of the left hand in string players. Science (New York, N.Y 270(5234):305-7.

Elbert T, Sterr A, Flor H, Rockstroh B, Knecht S, Pantev C, Wienbruch C, Taub E. (1997): Input-increase and input-decrease types of cortical reorganization after upper extremity amputation in humans. Experimental brain research. Experimentelle Hirnforschung 117(1):161-4.

Elhawary H, Zivanovic A, Davies B, Lamperth M. (2006): A review of magnetic resonance imaging compatible manipulators in surgery. Proceedings of the Institution of Mechanical Engineers 220(3):413-24.

Eliassen JC, Souza T, Sanes JN. (2001): Human brain activation accompanying explicitly directed movement sequence learning. Experimental brain research. Experimentelle Hirnforschung 141(3):269-80.

Elsinger CL, Harrington DL, Rao SM. (2006): From preparation to online control: reappraisal of neural circuitry mediating internally generated and externally guided actions. NeuroImage 31(3):1177-87.

Emmiler M, Solak O, Kocogullari C, Dundar U, Ayva E, Ela Y, Cekirdekci A, Kavuncu V. (2008): Control of acute postoperative pain by transcutaneous electrical nerve stimulation after open cardiac operations: a randomized placebo-controlled prospective study. The heart surgery forum 11(5):E300-3.

Enzinger C, Johansen-Berg H, Dawes H, Bogdanovic M, Collett J, Guy C, Ropele S, Kischka U, Wade D, Fazekas F, Matthews PM. (2008): Functional MRI Correlates of Lower Limb Function in Stroke Victims With Gait Impairment. Stroke; a journal of cerebral circulation 39(5):1507-1513.

Estevez N, Blickenstorfer A, Yu N, Hollnagel C, Kollias S, Riener R. (2009): Preliminary fMRI results of the MR compatible arm-robot. NCCR Neural Plasticity and Repair Symposium. Berlingen, Switzerland.

Fasoli SE, Krebs HI, Stein J, Frontera WR, Hughes R, Hogan N. (2004): Robotic therapy for chronic motor impairments after stroke: Follow-up results. Archives of physical medicine and rehabilitation 85(7):1106-11.

Ferretti A, Babiloni C, Gratta CD, Caulo M, Tartaro A, Bonomo L, Rossini PM, Romani GL. (2003): Functional topography of the secondary somatosensory cortex for nonpainful and painful stimuli: an fMRI study. NeuroImage 20(3):1625-38.

Ferretti A, Del Gratta C, Babiloni C, Caulo M, Arienzo D, Tartaro A, Rossini PM, Romani GL. (2004): Functional topography of the secondary somatosensory cortex for nonpainful and painful stimulation of median and tibial nerve: an fMRI study. NeuroImage 23(3):1217-25.

Floyer-Lea A, Matthews PM. (2005): Distinguishable brain activation networks for short- and long-term motor skill learning. Journal of neurophysiology 94(1):512-8.

Flueckiger M, Bullo M, Chapuis D, Gassert RAGR, Perriard YAPY. (2005): fMRI compatible haptic interface actuated with traveling wave ultrasonic motor. In: Bullo M, editor. Industry Applications Conference, 2005. Fourtieth IAS Annual Meeting. Conference Record of the 2005. p 2075-2082 Vol. 3.

Fong PW, Ng GY. (2001): Effect of wrist positioning on the repeatability and strength of power grip. Am J Occup Ther 55(2):212-6.

Friston KJ, Holmes AP, Worsley KJ, Poline JP, Frith CD, Frackowiak RSJ. (1994): Statistical parametric maps in functional imaging: A general linear approach. Human Brain Mapping 2(4):189-210.

Friston KJ, Williams S, Howard R, Frackowiak RS, Turner R. (1996): Movement-related effects in fMRI time-series. Magn Reson Med 35(3):346-55.

Gassert R, Dovat L, Ganesh G, Burdet E, Imamizu H, Milner T, Bleuler H. (2005): Multi-joint arm movements to investigate motor control with FMRI. Conf Proc IEEE Eng Med Biol Soc 5:4488-91.

Gassert R, Moser R, Burdet E, Bleuler H. (2006): MRI/fMRI-compatible robotic system with force feedback for interaction with human motion. IEEE-ASME Transactions on Mechatronics 11(2):216-224.

Gazzaniga MS, Ivry RB, Mangun GR. (2002): Cognitive Neuroscience: The Biology of Mind. New York, London: W.W. Norton & Co.

Gerardin E, Lehericy S, Pochon JB, Tezenas du Montcel S, Mangin JF, Poupon F, Agid Y, Le Bihan D, Marsault C. (2003): Foot, hand, face and eye representation in the human striatum. Cereb Cortex 13(2):162-9.

Golaszewski SM, Siedentopf CM, Baldauf E, Koppelstaetter F, Eisner W, Unterrainer J, Guendisch GM, Mottaghy FM, Felber SR. (2002): Functional Magnetic Resonance

Imaging of the Human Sensorimotor Cortex Using a Novel Vibrotactile Stimulator. NeuroImage 17(1):421-430.

Golaszewski SM, Siedentopf CM, Koppelstaetter F, Rhomberg P, Guendisch GM, Schlager A, Gallasch E, Eisner W, Felber SR, Mottaghy FM. (2004): Modulatory effects on human sensorimotor cortex by whole-hand afferent electrical stimulation. Neurology 62(12):2262-9.

Gondin J, Duclay J, Martin A. (2006a): Neural drive preservation after detraining following neuromuscular electrical stimulation training. Neuroscience letters 409(3):210-4.

Gondin J, Guette M, Ballay Y, Martin A. (2005): Electromyostimulation training effects on neural drive and muscle architecture. Medicine and science in sports and exercise 37(8):1291-9.

Gondin J, Guette M, Ballay Y, Martin A. (2006b): Neural and muscular changes to detraining after electrostimulation training. European journal of applied physiology 97(2):165-73.

Gordon T, Mao J. (1994): Muscle atrophy and procedures for training after spinal cord injury. Physical therapy 74(1):50-60.

Grodd W, Hulsmann E, Lotze M, Wildgruber D, Erb M. (2001): Sensorimotor mapping of the human cerebellum: fMRI evidence of somatotopic organization. Human brain mapping 13(2):55-73.

Guyton AC. (1991): Textbook of Medical Physiology. Philadelphia: Saunders.

Halder P, Curt A, Brem S, Lang-Dullenkopf A, Bucher K, Kollias S, Brandeis D. (2006): Preserved aspects of cortical foot control in paraplegia. NeuroImage 31(2):692-8.

Hallett M. (2001): Plasticity of the human motor cortex and recovery from stroke. Brain Res Brain Res Rev 36(2-3):169-74.

Halsband U, Lange RK. (2006): Motor learning in man: a review of functional and clinical studies. Journal of physiology, Paris 99(4-6):414-24.

Harrington GS, Wright CT, Downs JH, 3rd. (2000): A new vibrotactile stimulator for functional MRI. Human brain mapping 10(3):140-5.

Hawkins RD, Lalevic N, Clark GA, Kandel ER. (1989): Classical conditioning of the Aplysia siphon-withdrawal reflex exhibits response specificity. Proceedings of the National Academy of Sciences of the United States of America 86(19):7620-4.

Hazeltine E, Grafton ST, Ivry R. (1997): Attention and stimulus characteristics determine the locus of motor-sequence encoding. A PET study. Brain 120 (Pt 1):123-40.

Hempel E, Fischer H, Gumb L, Hohn T, Krause H, Voges U, Breitwieser H, Gutmann B, Durke J, Bock M, Melzer A. (2003): An MRI-compatible surgical robot for precise radiological interventions. Comput Aided Surg 8(4):180-91.

Hogan N, Krebs HI, Sharon A, J. C. (1995): Interactive robotic therapist. In: Massachusetts Insti. Technol. C, editor. USA.

Hollerbach JM, Hunter IW, Ballantyne J. (1992a): A comparative analysis of actuator technologies for robotics. The robotics review 2: MIT Press. p 299-342.

Hollerbach JM, Hunter IW, Ballantyne J. (1992b): A comperative analysis of actuator technologies for robotics. In: Khatib O, Craig JJ, Tomas L-P, editors. The Robotics Review 2. Cambridge: MIT Press. p 299-342.

Hortobagyi T, Scott K, Lambert J, Hamilton G, Tracy J. (1999): Cross-education of muscle strength is greater with stimulated than voluntary contractions. Motor control 3(2):205-19.

Hotz-Boendermaker S, Funk M, Summers P, Brugger P, Hepp-Reymond MC, Curt A, Kollias SS. (2008): Preservation of motor programs in paraplegics as demonstrated by attempted and imagined foot movements. NeuroImage 39(1):383-94.

Jacobs KM, Donoghue JP. (1991): Reshaping the cortical motor map by unmasking latent intracortical connections. Science (New York, N.Y 251(4996):944-7.

Jancke L. (2005): Methoden der Bildgebung in der Psychologie und den kognitiven Neurowissenschaften. Stuttgart: Kohlhammer.

Jancke L, Baumann S, Koeneke S, Meyer M, Laeng B, Peters M, Lutz K. (2006): Neural control of playing a reversed piano: empirical evidence for an unusual cortical organization of musical functions. Neuroreport 17(4):447-51.

Jancke L, Shah NJ, Peters M. (2000): Cortical activations in primary and secondary motor areas for complex bimanual movements in professional pianists. Brain Res Cogn Brain Res 10(1-2):177-83.

Johansen-Berg H, Dawes H, Guy C, Smith SM, Wade DT, Matthews PM. (2002): Correlation between motor improvements and altered fMRI activity after rehabilitative therapy. Brain 125(Pt 12):2731-42.

Kaelin-Lang A, Luft AR, Sawaki L, Burstein AH, Sohn YH, Cohen LG. (2002): Modulation of human corticomotor excitability by somatosensory input. J Physiol 540(Pt 2):623-33.

Kaelin-Lang A, Sawaki L, Cohen LG. (2005): Role of voluntary drive in encoding an elementary motor memory. Journal of neurophysiology 93(2):1099-103.

Kahn LE, Lum PS, Rymer WZ, Reinkensmeyer DJ. (2006): Robot-assisted movement training for the stroke-impaired arm: Does it matter what the robot does? Journal of rehabilitation research and development 43(5):619-30.

Kampe KK, Jones RA, Auer DP. (2000): Frequency dependence of the functional MRI response after electrical median nerve stimulation. Hum Brain Mapp 9(2):106-14.

Kandel ER, Schwartz JH, Jessel TM. (1996): Neurowissenschaften: eine Einführung. Heidelberg, Berlin, Oxford: Spektrum Akademischer Verlag.

Karni A, Meyer G, Jezzard P, Adams MM, Turner R, Ungerleider LG. (1995): Functional MRI evidence for adult motor cortex plasticity during motor skill learning. Nature 377(6545):155-8.

Katrin Amunts GSLJHSASADKZ. (1997): Motor cortex and hand motor skills: Structural compliance in the human brain. Human brain mapping 5(3):206-215.

Keisker B, Hepp-Reymond M, Blickenstorfer A, Meyer M, Kollias S. (2008): Differential force scaling of fine-graded grip force in the sensorimotor network. Hum Brain Mapp.

Keller T, Popovic MR, Pappas IP, Muller PY. (2002): Transcutaneous functional electrical stimulator "Compex Motion". Artificial organs 26(3):219-23.

Khanicheh A, Muto A, Triantafyllou C, Weinberg B, Astrakas L, Tzika A, Mavroidis C. (2006): fMRI-compatible rehabilitation hand device. Journal of neuroengineering and rehabilitation 3:24.

Kim D, Kobayashi E, Dohi T, Sakuma I. (2002): A new, compact MR-compatible surgical manipulator for minimally invasive liver surgery. Medical Image Computing and Computer-Assisted Intervention-Miccai 2002, Pt 1 2488:99-106.

Kimberley TJ, Lewis SM, Auerbach EJ, Dorsey LL, Lojovich JM, Carey JR. (2004): Electrical stimulation driving functional improvements and cortical changes in subjects with stroke. Experimental brain research. Experimentelle Hirnforschung 154(4):450-60.

Kleim JA, Vij K, Ballard DH, Greenough WT. (1997): Learning-dependent synaptic modifications in the cerebellar cortex of the adult rat persist for at least four weeks. J Neurosci 17(2):717-21.

Koeneke S, Lutz K, Herwig U, Ziemann U, Jancke L. (2006): Extensive training of elementary finger tapping movements changes the pattern of motor cortex excitability. Experimental brain research. Experimentelle Hirnforschung 174(2):199-209.

Koeneke S, Lutz K, Wustenberg T, Jancke L. (2004): Long-term training affects cerebellar processing in skilled keyboard players. Neuroreport 15(8):1279-82.

Korvenoja A, Huttunen J, Salli E, Pohjonen H, Martinkauppi S, Palva JM, Lauronen L, Virtanen J, Ilmoniemi RJ, Aronen HJ. (1999): Activation of multiple cortical areas in response to somatosensory stimulation: combined magnetoencephalographic and functional magnetic resonance imaging. Hum Brain Mapp 8(1):13-27.

Kowalczewski J, Gritsenko V, Ashworth N, Ellaway P, Prochazka A. (2007): Upper-extremity functional electric stimulation-assisted exercises on a workstation in the subacute phase of stroke recovery. Archives of physical medicine and rehabilitation 88(7):833-9.

Krebs HI, Hogan N, Aisen ML, Volpe BT. (1998): Robot-aided neurorehabilitation. IEEE Trans Rehabil Eng 6(1):75-87.

Krieger A, Susil RC, Menard C, Coleman JAACJA, Fichtinger GAFG, Atalar EAAE, Whitcomb LLAWLL. (2005): Design of a novel MRI compatible manipulator for image guided prostate interventions. Biomedical Engineering, IEEE Transactions on 52(2):306-313.

Lang M. (2008): 4 weekly TES sessions improve muscle fatigue resistance and reliability of stimulation force. Department of Biology. Zurich: ETH. p 40.

Larson BT, Erdman AG, Tsekos NV, Yacoub E, Tsekos PV, Koutlas IG. (2004): Design of an MRI-Compatible Robotic Stereotactic Device for Minimally Invasive Interventions in the Breast. Trans. ASME. p 458-465.

Lawrence M, Gross GP, Lang M, Kuhn A, Keller T, Morari M. (2008): Assessment of finger forces and wrist torques for functional grasp using new multichannel textile neuroprostheses. Artificial organs 32(8):634-8.

Lehericy S, Benali H, Van de Moortele PF, Pelegrini-Issac M, Waechter T, Ugurbil K, Doyon J. (2005): Distinct basal ganglia territories are engaged in early and advanced motor sequence learning. Proceedings of the National Academy of Sciences of the United States of America 102(35):12566-71.

Lehericy S, van de Moortele PF, Lobel E, Paradis AL, Vidailhet M, Frouin V, Neveu P, Agid Y, Marsault C, Le Bihan D. (1998): Somatotopical organization of striatal activation during finger and toe movement: a 3-T functional magnetic resonance imaging study. Annals of neurology 44(3):398-404.

Lemieux L, Salek-Haddadi A, Lund TE, Laufs H, Carmichael D. (2007): Modelling large motion events in fMRI studies of patients with epilepsy. Magnetic resonance imaging 25(6):894-901.

Liepert J, Bauder H, Wolfgang HR, Miltner WH, Taub E, Weiller C. (2000): Treatment-induced cortical reorganization after stroke in humans. Stroke; a journal of cerebral circulation 31(6):1210-6.

Liepert J, Miltner WH, Bauder H, Sommer M, Dettmers C, Taub E, Weiller C. (1998): Motor cortex plasticity during constraint-induced movement therapy in stroke patients. Neuroscience letters 250(1):5-8.

Logothetis NK. (2008): What we can do and what we cannot do with fMRI. Nature 453(7197):869-78.

Logothetis NK, Pauls J, Augath M, Trinath T, Oeltermann A. (2001): Neurophysiological investigation of the basis of the fMRI signal. Nature 412(6843):150-7.

Lotze M, Braun C, Birbaumer N, Anders S, Cohen LG. (2003): Motor learning elicited by voluntary drive. Brain 126(Pt 4):866-72.

Lotze M, Laubis-Herrmann U, Topka H. (2006): Combination of TMS and fMRI reveals a specific pattern of reorganization in M1 in patients after complete spinal cord injury. Restorative neurology and neuroscience 24(2):97-107.

Lotze M, Laubis-Herrmann U, Topka H, Erb M, Grodd W. (1999): Reorganization in the primary motor cortex after spinal cord injury - A functional Magnetic Resonance (fMRI) study. Restorative neurology and neuroscience 14(2-3):183-187.

Loubinoux I, Carel C, Alary F, Boulanouar K, Viallard G, Manelfe C, Rascol O, Celsis P, Chollet F. (2001): Within-session and between-session reproducibility of cerebral sensorimotor activation: a test--retest effect evidenced with functional magnetic resonance imaging. J Cereb Blood Flow Metab 21(5):592-607.

Lum PS, Burgar CG, Shor PC, Majmundar M, Van der Loos M. (2002): Robot-assisted movement training compared with conventional therapy techniques for the rehabilitation of upper-limb motor function after stroke. Archives of physical medicine and rehabilitation 83(7):952-959.

Lund TE, Nørgaard MD, Rostrup E, Rowe JB, Paulson OB. (2005): Motion or activity: their role in intra- and inter-subject variation in fMRI. NeuroImage 26(3):960-964.

Maffiuletti NA, Cometti G, Amiridis IG, Martin A, Pousson M, Chatard JC. (2000): The effects of electromyostimulation training and basketball practice on muscle strength and jumping ability. International journal of sports medicine 21(6):437-43.

Maffiuletti NA, Dugnani S, Folz M, Di Pierno E, Mauro F. (2002a): Effect of combined electrostimulation and plyometric training on vertical jump height. Medicine and science in sports and exercise 34(10):1638-44.

Maffiuletti NA, Pensini M, Martin A. (2002b): Activation of human plantar flexor muscles increases after electromyostimulation training. J Appl Physiol 92(4):1383-92.

Maillard L, Ishii K, Bushara K, Waldvogel D, Schulman AE, Hallett M. (2000): Mapping the basal ganglia: fMRI evidence for somatotopic representation of face, hand, and foot. Neurology 55(3):377-83.

Mangold S, Keller T. (2003): Greifen mit Hilfe von Neuroprothesen - Prinzip und Voraussetzungen für den Gebrauch. Ergotherapien & Rehabilitation 42(8):22 - 26.

Mangold S, Keller T. (2004): Greifen mit Hilfe von Neuroprothesen - implantierbare und nicht-invasive Systeme. Ergotherapien & Rehabilitation 43(2):5 - 12.

Marqueste T, Hug F, Decherchi P, Jammes Y. (2003): Changes in neuromuscular function after training by functional electrical stimulation. Muscle & nerve 28(2):181-8.

Masamune K, Kobayashi E, Masutani Y, Suzuki M, Dohi T, Iseki H, Takakura K. (1995): Development of an MRI-compatible needle insertion manipulator for stereotactic neurosurgery. Journal of image guided surgery 1(4):242-8.

Mayer AR, Zimbelman JL, Watanabe Y, Rao SM. (2001): Somatotopic organization of the medial wall of the cerebral hemispheres: a 3 Tesla fMRI study. Neuroreport 12(17):3811-4.

McRobbie DW. (2003): MRI from picture to proton. Cambridge: Cambridge University Press. 359 p.

Meister I, Krings T, Foltys H, Boroojerdi B, Muller M, Topper R, Thron A. (2005): Effects of long-term practice and task complexity in musicians and nonmusicians performing simple and complex motor tasks: implications for cortical motor organization. Hum Brain Mapp 25(3):345-52.

Merzenich MM, Kaas JH, Wall J, Nelson RJ, Sur M, Felleman D. (1983a): Topographic reorganization of somatosensory cortical areas 3b and 1 in adult monkeys following restricted deafferentation. Neuroscience 8(1):33-55.

Merzenich MM, Kaas JH, Wall JT, Sur M, Nelson RJ, Felleman DJ. (1983b): Progression of change following median nerve section in the cortical representation of the hand in areas 3b and 1 in adult owl and squirrel monkeys. Neuroscience 10(3):639-65.

Morgen K, Kadom N, Sawaki L, Tessitore A, Ohayon J, Frank J, McFarland H, Martin R, Cohen LG. (2004): Kinematic specificity of cortical reorganization associated with motor training. NeuroImage 21(3):1182-7.

Muellbacher W, Ziemann U, Boroojerdi B, Cohen L, Hallett M. (2001): Role of the human motor cortex in rapid motor learning. Experimental brain research. Experimentelle Hirnforschung 136(4):431-8.

Muller RA, Kleinhans N, Pierce K, Kemmotsu N, Courchesne E. (2002): Functional MRI of motor sequence acquisition: effects of learning stage and performance. Brain Res Cogn Brain Res 14(2):277-93.

Munte TF, Altenmuller E, Jancke L. (2002): The musician's brain as a model of neuroplasticity. Nature reviews 3(6):473-8.

Naito E, Kochiyama T, Kitada R, Nakamura S, Matsumura M, Yonekura Y, Sadato N. (2002): Internally simulated movement sensations during motor imagery activate cortical motor areas and the cerebellum. J Neurosci 22(9):3683-91.

Nef T, Mihelj M, Riener R. (2007): ARMin: a robot for patient-cooperative arm therapy. Medical and Biological Engineering and Computing 45(9):887-900.

Nelles G, Jentzen W, Jueptner M, Muller S, Diener HC. (2001): Arm training induced brain plasticity in stroke studied with serial positron emission tomography. NeuroImage 13(6 Pt 1):1146-54.

Nelles G, Spiekramann G, Jueptner M, Leonhardt G, Muller S, Gerhard H, Diener HC. (1999): Evolution of functional reorganization in hemiplegic stroke: a serial positron emission tomographic activation study. Annals of neurology 46(6):901-9.

Newton JM, Dong Y, Hidler J, Plummer-D'Amato P, Marehbian J, Albistegui-Dubois RM, Woods RP, Dobkin BH. (2008): Reliable assessment of lower limb motor representations with fMRI: use of a novel MR compatible device for real-time monitoring of ankle, knee and hip torques. NeuroImage 43(1):136-46.

Nudo RJ, Milliken GW, Jenkins WM, Merzenich MM. (1996): Use-dependent alterations of movement representations in primary motor cortex of adult squirrel monkeys. J Neurosci 16(2):785-807.

Oldfield RC. (1971): The assessment and analysis of handedness: the Edinburgh inventory. Neuropsychologia 9(1):97-113.

Pascual-Leone A, Grafman J, Hallett M. (1994): Modulation of cortical motor output maps during development of implicit and explicit knowledge. Science (New York, N.Y 263(5151):1287-9.

Pascual-Leone A, Nguyet D, Cohen LG, Brasil-Neto JP, Cammarota A, Hallett M. (1995): Modulation of muscle responses evoked by transcranial magnetic stimulation during the acquisition of new fine motor skills. Journal of neurophysiology 74(3):1037-45.

Pearce AJ, Thickbroom GW, Byrnes ML, Mastaglia FL. (2000): Functional reorganisation of the corticomotor projection to the hand in skilled racquet players. Experimental brain research. Experimentelle Hirnforschung 130(2):238-43.

Peckham PH, Knutson JS. (2005a): Functional electrical stimulation for neuromuscular applications. Annual Review of Biomedical Engineering 7(1):327-360.

Peckham PH, Knutson JS. (2005b): Functional electrical stimulation for neuromuscular applications. Annual review of biomedical engineering 7:327-60.

Penfield W, Jasper H. (1954): Epilepsy and the Functional Anatomy of the Human Brain. Boston: Little Brown & Co.

Petersen SE, van Mier H, Fiez JA, Raichle ME. (1998): The effects of practice on the functional anatomy of task performance. Proceedings of the National Academy of Sciences of the United States of America 95(3):853-60.

Petrofsky JS, Stacy R, Laymon M. (2000): The relationship between exercise work intervals and duration of exercise on lower extremity training induced by electrical stimulation in humans with spinal cord injuries. European journal of applied physiology 82(5-6):504-9.

Peyron R, Garcia-Larrea L, Gregoire MC, Costes N, Convers P, Lavenne F, Mauguiere F, Michel D, Laurent B. (1999): Haemodynamic brain responses to acute pain in humans: sensory and attentional networks. Brain 122 (Pt 9):1765-80.

Philips. (2007): Technical Description: Intera 1.5T Release 2.5 series, Achieva 1.5T / 3.0T / XR Release 2.5, Panorama HFO Release 2.5 series. Magnetic Resonance 4522 132 68821.

Picard N, Strick PL. (1996): Motor areas of the medial wall: a review of their location and functional activation. Cereb Cortex 6(3):342-53.

Plautz EJ, Milliken GW, Nudo RJ. (2000): Effects of repetitive motor training on movement representations in adult squirrel monkeys: role of use versus learning. Neurobiology of learning and memory 74(1):27-55.

Poldrack RA. (2000): Imaging brain plasticity: conceptual and methodological issues--a theoretical review. NeuroImage 12(1):1-13.

Poldrack RA, Sabb FW, Foerde K, Tom SM, Asarnow RF, Bookheimer SY, Knowlton BJ. (2005): The Neural Correlates of Motor Skill Automaticity. J. Neurosci. 25(22):5356-5364.

Poline JB, Worsley KJ, Evans AC, Friston KJ. (1997): Combining spatial extent and peak intensity to test for activations in functional imaging. NeuroImage 5(2):83-96.

Popovic MR, Curt A, Keller T, Dietz V. (2001a): Functional electrical stimulation for grasping and walking: indications and limitations. Spinal Cord 39(8):403-12.

Popovic MR, Keller T, Papas IPI, Dietz V, Morari M. (2001b): Surface-stimulation technology for grasping and walking neuroprostheses. Engineering in Medicine and Biology Magazine, IEEE 20(1):82-93.

Prange GB, Jannink MJ, Groothuis-Oudshoorn CG, Hermens HJ, Ijzerman MJ. (2006): Systematic review of the effect of robot-aided therapy on recovery of the hemiparetic arm after stroke. Journal of rehabilitation research and development 43(2):171-84.

Pruessmann KP, Weiger M, Scheidegger MB, Boesiger P. (1999): SENSE: sensitivity encoding for fast MRI. Magn Reson Med 42(5):952-62.

Reinkensmeyer DJ, Dewald JP, Rymer WZ. (1999): Guidance-based quantification of arm impairment following brain injury: a pilot study. IEEE Trans Rehabil Eng 7(1):1-11.

Reinkensmeyer DJ, Emken JL, Cramer SC. (2004): ROBOTICS, MOTOR LEARNING, AND NEUROLOGIC RECOVERY. Annual Review of Biomedical Engineering 6(1):497-525.

Reinkensmeyer DJ, Kahn LE, Averbuch M, McKenna-Cole A, Schmit BD, Rymer WZ. (2000): Understanding and treating arm movement impairment after chronic brain injury: Progress with the ARM guide. Journal of rehabilitation research and development 37(6):653-662.

Richardson R, Brown M, Bhakta B, Levesley MC. (2003): Design and control of a three degree of freedom pneumatic physiotherapy robot. Robotica 21(6):589-604.

Ridding MC, Brouwer B, Miles TS, Pitcher JB, Thompson PD. (2000): Changes in muscle responses to stimulation of the motor cortex induced by peripheral nerve stimulation in human subjects. Exp Brain Res 131(1):135-43.

Ridding MC, McKay DR, Thompson PD, Miles TS. (2001): Changes in corticomotor representations induced by prolonged peripheral nerve stimulation in humans. Clin Neurophysiol 112(8):1461-9.

Riener R, Nef T, Colombo G. (2005a): Robot-aided neurorehabilitation of the upper extremities. Medical and Biological Engineering and Computing 43(1):2-10.

Riener R, Nef T, Colombo G. (2005b): Robot-aided neurorehabilitation of the upper extremities. Medical & biological engineering & computing 43(1):2-10.

Riener R, Villgrattner T, Kleiser R, Nef R, Kollias S. (2005c): fMRI-Compatible Electromagnetic Haptic Interface. Proc. IEEE/EMBS Annual International Conference.

Robertson VJ, Ward AR. (2002): Vastus medialis electrical stimulation to improve lower extremity function following a lateral patellar retinacular release. The Journal of orthopaedic and sports physical therapy 32(9):437-43; discussion 443-6.

Rossini PM, Altamura C, Ferreri F, Melgari JM, Tecchio F, Tombini M, Pasqualetti P, Vernieri F. (2007): Neuroimaging experimental studies on brain plasticity in recovery from stroke. Europa medicophysica 43(2):241-54.

Rossini PM, Calautti C, Pauri F, Baron JC. (2003): Post-stroke plastic reorganisation in the adult brain. Lancet neurology 2(8):493-502.

Rushton DN. (2003): Functional electrical stimulation and rehabilitation--an hypothesis. Medical engineering & physics 25(1):75-8.

Salek-Haddadi A, Diehl B, Hamandi K, Merschhemke M, Liston A, Friston K, Duncan JS, Fish DR, Lemieux L. (2006): Hemodynamic correlates of epileptiform discharges: an EEG-fMRI study of 63 patients with focal epilepsy. Brain research 1088(1):148-66.

Schenck JF. (1996): The role of magnetic susceptibility in magnetic resonance imaging: MRI magnetic compatibility of the first and second kinds. Medical Physics.

Schmahmann JD, Doyon J, McDonald D, Holmes C, Lavoie K, Hurwitz AS, Kabani N, Toga A, Evans A, Petrides M. (1999): Three-dimensional MRI atlas of the human cerebellum in proportional stereotaxic space. NeuroImage 10(3 Pt 1):233-60.

Scholz VH, Flaherty AW, Kraft E, Keltner JR, Kwong KK, Chen YI, Rosen BR, Jenkins BG. (2000): Laterality, somatotopy and reproducibility of the basal ganglia and motor cortex during motor tasks. Brain Res 879(1-2):204-15.

Shannon BJ, Buckner RL. (2004): Functional-anatomic correlates of memory retrieval that suggest nontraditional processing roles for multiple distinct regions within posterior parietal cortex. J Neurosci 24(45):10084-92.

Sheffler LR, Chae J. (2007): Neuromuscular electrical stimulation in neurorehabilitation. Muscle & nerve 35(5):562-90.

Shibuya S, Ohki Y. (2004): Cutaneous inputs can activate the ipsilateral primary motor cortex during bimanual sensory-driven movements in humans. Journal of neurophysiology 92(6):3200-9.

Shimada Y, Chida S, Matsunaga T, Misawa A, Ito H, Sakuraba T, Sato M, Hatakeyama K, Itoi E. (2003): Grasping power by means of functional electrical stimulation in a case of C6 complete tetraplegia. The Tohoku journal of experimental medicine 201(2):91-6.

Shimada Y, Sato K, Kagaya H, Konishi N, Miyamoto S, Matsunaga T. (1996): Clinical use of percutaneous intramuscular electrodes for functional electrical stimulation. Archives of physical medicine and rehabilitation 77(10):1014-8.

Slavin KV. (2008): Peripheral nerve stimulation for neuropathic pain. Neurotherapeutics 5(1):100-6.

Smith GV, Alon G, Roys SR, Gullapalli RP. (2003): Functional MRI determination of a dose-response relationship to lower extremity neuromuscular electrical stimulation in healthy subjects. Experimental brain research. Experimentelle Hirnforschung 150(1):33-9.

Sohl GA, Bobrow JE. (1999): Experiments and simulations on the nonlinear control of a hydraulic servosystem. Control Systems Technology, IEEE Transactions on 7(2):238-247.

Sonde L, Gip C, Fernaeus SE, Nilsson CG, Viitanen M. (1998): Stimulation with low frequency (1.7 Hz) transcutaneous electric nerve stimulation (low-tens) increases motor function of the post-stroke paretic arm. Scandinavian journal of rehabilitation medicine 30(2):95-9.

Stefan K, Kunesch E, Cohen LG, Benecke R, Classen J. (2000): Induction of plasticity in the human motor cortex by paired associative stimulation. Brain 123(3):572-584.

Sterr A, Elbert T, Berthold I, Kolbel S, Rockstroh B, Taub E. (2002): Longer versus shorter daily constraint-induced movement therapy of chronic hemiparesis: an exploratory study. Archives of physical medicine and rehabilitation 83(10):1374-7.

Sutherland MT, Tang AC. (2006): Reliable detection of bilateral activation in human primary somatosensory cortex by unilateral median nerve stimulation. NeuroImage 33(4):1042-54.

Takahashi CD, Der-Yeghiaian L, Le V, Motiwala RR, Cramer SC. (2008): Robot-based hand motor therapy after stroke. Brain 131(2):425-437.

Talairach J, Tournoux P. (1988): Co-planar stereotaxic atlas of the human brain. New York: Thieme.

Taub E, Miller NE, Novack TA, Cook EW, 3rd, Fleming WC, Nepomuceno CS, Connell JS, Crago JE. (1993): Technique to improve chronic motor deficit after stroke. Archives of physical medicine and rehabilitation 74(4):347-54.

Toga AW, Mazziotta JC. (1996): Brain Mapping the Methods. Amsterdam, Boston, London, New York, Oxford, Paris, San Diego, San Francisco, Singapore, Sydney, Tokyo: Academic Press. 877 p.

Toga AW, Mazziotta JC. (2002): Brain Mapping the Methods. Amsterdam, Boston, London, New York, Oxford, Paris, San Diego, San Francisco, Singapore, Sydney, Tokyo: Academic Press. 877 p.

Trepel M. (1999): Neuroanatomie: Struktur und Funktion. München, Stuttgart, Jena, Lübeck, Ulm: Urban & Fischer.

Tsekos NV, Khanicheh A, Christoforou E, Mavroidis C. (2007): Magnetic resonance-compatible robotic and mechatronics systems for image-guided interventions and rehabilitation: a review study. Annu Rev Biomed Eng 9:351-87.

Tunik E, Rice NJ, Hamilton A, Grafton ST. (2007): Beyond grasping: representation of action in human anterior intraparietal sulcus. NeuroImage 36 Suppl 2:T77-86.

Tyc F, Boyadjian A, Devanne H. (2005): Motor cortex plasticity induced by extensive training revealed by transcranial magnetic stimulation in human. The European journal of neuroscience 21(1):259-66.

Uy J, Ridding MC, Hillier S, Thompson PD, Miles TS. (2003): Does induction of plastic change in motor cortex improve leg function after stroke? Neurology 61(7):982-4.

Vaillancourt DE, Thulborn KR, Corcos DM. (2003): Neural basis for the processes that underlie visually guided and internally guided force control in humans. Journal of neurophysiology 90(5):3330-40.

van der Lee JH, Wagenaar RC, Lankhorst GJ, Vogelaar TW, Deville WL, Bouter LM. (1999): Forced use of the upper extremity in chronic stroke patients: results from a single-blind randomized clinical trial. Stroke; a journal of cerebral circulation 30(11):2369-75.

Viswanathan A, Freeman RD. (2007): Neurometabolic coupling in cerebral cortex reflects synaptic more than spiking activity. Nature neuroscience 10(10):1308-12.

Volpe BT, Krebs HI, Hogan N, Edelstein OL, Diels C, Aisen M. (2000): A novel approach to stroke rehabilitation: robot-aided sensorimotor stimulation. Neurology 54(10):1938-44.

Wang R, Foniok T, Wamsteeker JI, Qiao M, Tomanek B, Vivanco RA, Tuor UI. (2006): Transient blood pressure changes affect the functional magnetic resonance imaging detection of cerebral activation. NeuroImage 31(1):1-11.

Ward NS, Brown MM, Thompson AJ, Frackowiak RS. (2003): Neural correlates of outcome after stroke: a cross-sectional fMRI study. Brain 126(Pt 6):1430-48.

Weiller C, Juptner M, Fellows S, Rijntjes M, Leonhardt G, Kiebel S, Muller S, Diener HC, Thilmann AF. (1996): Brain representation of active and passive movements. NeuroImage 4(2):105-10.

Weiner DK, Perera S, Rudy TE, Glick RM, Shenoy S, Delitto A. (2008): Efficacy of percutaneous electrical nerve stimulation and therapeutic exercise for older adults with chronic low back pain: A randomized controlled trial. Pain.

Wolf SL, Lecraw DE, Barton LA, Jann BB. (1989): Forced use of hemiplegic upper extremities to reverse the effect of learned nonuse among chronic stroke and head-injured patients. Experimental neurology 104(2):125-32.

Worsley KJ, Marrett S, Neelin P, Vandal AC, Friston KJ, Evans AC. (1996): A unified statistical approach for determining significant signals in images of cerebral activation. Human Brain Mapping 4(1):58-73.

Wu T, Chan P, Hallett M. (2008): Modifications of the interactions in the motor networks when a movement becomes automatic. J Physiol 586(17):4295-4304.

Yong Z, Barth EJ. (2005): Impedance Control of a Pneumatic Actuator for Contact Tasks. Robotics and Automation, 2005. ICRA 2005. Proceedings of the 2005 IEEE International Conference on. p 987-992.

Yu N, Murr W, Blickenstorfer A, Kollias S, Riener R. (2007): An fMRI compatible haptic interface with pneumatic actuation International Conference on Rehabilitation Robotics Nordwijk, The Netherlands.

Yu N, Riener R. (2006): Review on MR-Compatible Robotic Systems. Biomedical Robotics and Biomechatronics, 2006. BioRob 2006. The First IEEE/RAS-EMBS International Conference on. p 661-665.

Zappe AC, Maucher T, Meier K, Scheiber C. (2004): Evaluation of a pneumatically driven tactile stimulator device for vision substitution during fMRI studies. Magnetic Resonance in Medicine. p 828-834.

VI. Curriculum Vitae

Armin Blickenstorfer

Personal data

Date of birth:	September 2 1975
Place of birth:	Zurich, Switzerland
From:	Stallikon, Switzerland
Marital status:	married, 2 sons (May 2005, May 2009)

Career & Education

05/2011	Dr. phil, University of Zurich. Thesis: Effects of new Rehabilitation Techniques on the Human Brain using functional Resonance Imaging
02/2009 – to date	Psychotherapist in education (cognitive behavioral therapy) at the Psychiatric Clinic Königsfelden in Brugg, Switzerland
09/2008 – 01/2009	Post-Doc at the Sensory Motor Systems Lab of the Federal Institute of Technology (ETH) Zurich, Switzerland
09/2005 – 09/2008	PhD student at the Institute of Neuroradiology University Hospital Zurich, Switzerland
10/2002 – 06/2005	MSc Psychology, University of Zurich, Switzerland Major: Neuropsychology 1st Minor: Psychopathology of the adulthood 2nd Minor: Criminology (Faculty of Law)
10/1998 – 09/2002	Bachelor in Psychology, University of Zurich, Switzerland
10/1996 – 03/1998	Biology student at University of Zurich, Switzerland
1991 – 1996	Mittelschule in Zürich-Oerlikon

Publications

Blickenstorfer A., Lutz K., Lang M., Keller T., Meyer M., Keisker B., Riener R., Hepp-Reymond M.-C., Kollias S. 2011. Effects of a 4-week FES-Training applied to the dominant forearmon brain plasticity and muscle strength. In prep.

Blickenstorfer A., Kleiser R., Keller T., Keisker B., Meyer M., Riener R., Kollias S. 2008. Cortical and subcortical correlates of functional electrical stimulation of wrist extensor and flexor muscles revealed by fMRI. Hum Brain Mapp 30(3):963-75.

Keisker B., Hepp-Reymond M-C., Blickenstorfer A., Kollias S. 2010. Differential representation of dynamic and static power grip force in the sensorimotor network. Eur J Neurosci. Volume 31 (8):1483 - 1491.

Keisker B., Hepp-Reymond M-C., Blickenstorfer A., Meyer M., Kollias S.S., 2009. Differential force scaling of fine- graded power grip force in the sensorimotor network. Hum Brain Mapp. 30(8):2453-65.

Yu N., Hollnagel C., Blickenstorfer A., Kollias S., Riener R., 2008. Comparisons of MRI-compatible mechatronic systems with hydronamic and pneumatic actuation. IEEE/ASME Trans. Mechatronics 13(3): 268-277.

Poster Presentations

6th FENS Forum of European Neuroscience, July 12 – 16, 2008, Geneva, Switzerland: Effects of a 4-week FES-Training applied to the dominant forearm on brain plasticity, muscle strength and fatigue. A. Blickenstorfer, K. Lutz, M. Lang, T. Keller, M. Meyer, R. Riener, S. Kollias

Joint Meeting of Swiss Society of Neuroscience, NCCR "Neural Plasticity and Repair", Swiss Multiple Sclerosis Society. March 9 -10, 2007, Berne, Switzerland: Cerebral representations of active and passive ankle movements elicited by functional electrical stimulation (FES) in healthy subjects and paraplegic patients – Preliminary fMRI results. A. Blickenstorfer, F. Taut, T. Keller, B. Keisker, M. Meyer R. Riener, S. Kollias

Zentrum für Neurowissenschaften Zürich (ZNZ) Symposium, October 20, 2006, Zurich, Switzerland: Cortical correlates of functional electrical stimulation (FES) of wrist extensors and flexors: an fMRI feasibility study. A. Blickenstorfer, R. Kleiser, T. Keller, B. Keisker, R. Riener, S. Kollias

Meeting of International Neuropsychological Society, the Swiss Neuropsychological Society (SVNP), and the German Neuropsychological Society (GNP), July 26 – 30, 2006, Zurich, Switzerland: Cortical Correlates of Functional Electrical Stimulation (FES) of Wrist Extensors and Flexors: A fMRI Feasibility Study. A. Blickenstorfer, R. Kleiser, T. Keller, B. Keisker, R. Riener, S. Kollias

12th Annual Meeting of the Organization for Human Brain Mapping, June 11 – 15, 2006, Florence, Italy: Electrical Stimulation of Wrist Extensors and Flexors in a MR-Environment. A. Blickenstorfer, R. Kleiser, T. Keller, B. Keisker, R. Riener, S. Kollias

5th Day of Clinical Research, University of Zurich, Medical Faculty, March 23 – 24, 2006, Zurich, Switzerland: Electrical Stimulation of Wrist Extensors and flexors in a MR-Environment. A. Blickenstorfer, R. Kleiser, T. Keller, B. Keisker, R. Riener, S. Kollias

NCCR Neural Plasticity and Repair Symposium, March 3 – 4, 2006, Kartause Ittingen, Warth, Switzerland:Electrical Stimulation of Wrist Extensors and flexors in a MR-Environment. A. Blickenstorfer, R. Kleiser, T. Keller, B. Keisker, R. Riener, S. Kollias

Joint Meeting of Swiss Society of Neuroscience and Swiss Society for Neuroradiology, January 28, 2006, Basel, Switzerland: Electrical Stimulation of Wrist Extensors and flexors in a MR-Environment. A. Blickenstorfer, R. Kleiser, T. Keller, B. Keisker, R. Riener, S. Kollias

Oral presentations:

Clinical Neuroscience Symposium, 12.12.2008, Zurich, Switzerland: Monitoring the effects of Functional Electrical Stimulation (FES) in the sensorimotor system using fMRI.

19. Jahrestagung der Schweizerischen Gesellschaft für Neuroradiologie (SGNR), 27.10.2007, Aarau, Switzerland: Effekte neuer Rehabilitations-techniken auf das menschliche Gehirn erhoben mit fMR.

Neuroradiologisches Kolloquium über funktionelle Magnetresonanz, 13.12.2006, Zurich, Switzerland: Cortical Representation of functional electrical stimulation (FES) in healthy subjects and paraplegic patients investigated with fMRI.

NCCR Neural Plasticity and Repair Symposium, March 3 – 4, 2006, Kartause Ittingen, Warth, Switzerland: Electrical Stimulation of Wrist Extensors and flexors in a MR-Environment.

Neuroradiologisches Kolloquium über funktionelle Magnetresonanz, 02.11.2005, Zurich, Switzerland: Assessment of Rehabilitation Approaches in a MR-Environment.